

**An- Najah National University
Faculty of Graduate Studies**

**Solar Energy Refrigeration by Liquid-Solid
Adsorption Technique**

**By
Watheq Khalil Said Hussein**

**Supervisor
Dr. Abdelrahim Abusafa
Co-Supervisor
Dr. Imad Ibrik**

**Submitted in Partial Fulfillment of the Requirements for the Degree of
Master of Science in Clean Energy and Energy Conservation
Engineering, Faculty of Graduate Studies, An-Najah University,
Nablus – Palestine.**

2008

Solar Energy Refrigeration by Liquid-Solid Adsorption Technique

By
Watheq Khalil Said Hussein

This thesis was defended successfully on 14/12/2008, and approved by:

Committee Members

| | Signature |
|---|---|
| 1. Dr. Abdelrahim Abusafa (Supervisor) | (..... ) |
| 2. Dr. Imad Ibrik (Co-Supervisor) | (..... ) |
| 3. Dr. Afif Hasan (External Examiner) | (..... ) |
| 4. Dr. Hosni Audeh (Internal Examiner) | (..... ) |

TO MY HOLLY LAND

Acknowledgment

I would like to express my sincerest gratitude to my supervisor Dr. Abdelrahim Abusafa who has always been providing kindest support, encouragement, and guidance throughout the accomplishment of this dissertation. I would like also to thank Dr. Imad Ibrik, whom I can refer to as my second supervisor; he has given me an opportunity to learn more in this work. I also like to thank my wife, my parents and my family for their encouragement. Lastly, I would like to thank my friends and colleagues in clean energy and conservation engineering program for their encouragement.

الإقرار

أنا الموقع أدناه مقدم الرسالة التي تحمل العنوان:

Solar Energy Refrigeration by Liquid-Solid Adsorption Technique

التبريد بواسطة الطاقة الشمسية باستخدام تقنية الادمصاص

أقر بأن ما اشتملت عليه هذه الرسالة إنما هي نتاج جهدي الخاص، باستثناء ما تمت الإشارة إليه حيثما ورد، وان هذه الرسالة ككل، أو أي جزء منها لم يقدم من قبل لنيل أية درجة علمية أو بحث علمي أو بحثي لدى أية مؤسسة تعليمية أو بحثية أخرى.

Declaration

The work provided in this thesis, unless otherwise referenced, is the researcher's own work, and has not been submitted elsewhere for any other degree or qualification.

Student's name:

اسم الطالب:

Signature:

التوقيع:

Date:

التاريخ:

TABLE OF CONTENTS

| No. | Contents | Page |
|---|--|-----------|
| | Acknowledgment | iv |
| | Declaration | v |
| | TABLE OF CONTENTS | vi |
| | LIST OF TABLES | viii |
| | LIST OF FIGURES | ix |
| | Abstract | xi |
| | Introduction | 1 |
| Chapter One : Solar Cooling | | 3 |
| 1.1 | Refrigeration Definition | 3 |
| 1.2 | Solar Cooling Options and Technologies | 4 |
| 1.3 | Solar Cooling Path | 4 |
| 1.4 | Cycle Efficiency | 7 |
| 1.5 | Solar Collector Efficiency | 8 |
| 1.6 | Photovoltaic Efficiency | 12 |
| 1.7 | System Efficiency | 13 |
| 1.8 | Solar Cooling Technologies | 14 |
| 1.8.1 | Thermal – Driven system | 15 |
| 1.8.1.1 | Absorption Refrigeration Cycle | 15 |
| 1.8.1.2 | Adsorption Refrigeration Cycle | 19 |
| 1.8.1.3 | Chemical reaction (solid-sorption) refrigeration cycle | 21 |
| 1.8.1.4 | Desiccant Refrigeration System | 23 |
| 1.8.1.5 | Ejector Refrigeration Cycle | 26 |
| 1.8.1.6 | Rankin-Driven Refrigeration Cycle | 28 |
| 1.8.2 | Electricity (Photovoltaic) driven system | 30 |
| Chapter Two : Solar Adsorption Refrigeration | | 33 |
| 2.1 | History and Advantages | 33 |
| 2.2 | System Description | 35 |
| 2.3 | Principle of Adsorption | 37 |
| 2.4 | Selection of Adsorbent / Adsorbate Pair | 39 |
| 2.5 | Operation and Analysis of the Adsorption Cycle | 48 |
| 2.6 | Coefficient of Performance (COP) | 51 |
| 2.7 | The Effects of Collector and Environment Parameters on the Performance of a Solar Powered Adsorption Refrigeration | 54 |
| 2.7.1 | Parametric Effects | 54 |
| 2.7.2 | Environmental Effects | 57 |
| 2.8 | Solar Adsorption Cooling Technologies | 60 |
| 2.8.1 | Heat Recovery Adsorption Refrigeration Cycle | 60 |

| No. | Contents | page |
|--|--|------------|
| 2.8.2 | Mass Recovery Adsorption Refrigeration Cycle | 62 |
| 2.8.3 | Thermal Wave Cycle | 64 |
| 2.8.4 | Multi-Stage and Cascading Cycle | 66 |
| 2.8.5 | A combined Solar Adsorption Heating and Cooling System | 68 |
| 2.8.6 | Solar House | 72 |
| 2.8.7 | Solar-Driven Combined Ejector and Adsorption Refrigeration Systems | 74 |
| Chapter three: Potential of Solar Energy in Palestine | | 75 |
| 3.1 | Solar Energy | 75 |
| 3.1.1 | Solar Radiation Components | 76 |
| 3.1.2 | Measurement of Solar Radiation - Pyranometer | 77 |
| 3.2 | Climate and Potential of Solar Radiation in Palestine | 78 |
| 3.2.1 | Climate in Palestine | 78 |
| 3.2.2 | Potential of Solar Energy in Palestine | 79 |
| 3.3 | Solar Energy Conversion System Design | 82 |
| 3.3.1 | Solar Collectors | 82 |
| 3.3.2 | Collector Performance | 83 |
| Chapter four: Experimental Work, Results and Discussion | | 88 |
| 4.1 | Working principle of the No Valve Solar Cooler | 88 |
| 4.2 | Construction of No Valve Solar Cooler | 90 |
| 4.2.1 | Adsorbent Bed | 90 |
| 4.2.2 | Condenser and Evaporator | 92 |
| 4.2.3 | Integration of the Subsystems | 93 |
| 4.3 | The experimental Method | 94 |
| 4.3.1 | Methanol Charging and Heating Process | 95 |
| 4.3.2 | Lab Scale Experiments | 101 |
| 4.3.3 | Conclusions | 107 |
| 4.3.4 | Experimental Work on the Modified Solar Pilot Setup | 109 |
| 4.3.5 | Experiment on the Optimized Pilot Scale Setup | 118 |
| 4.3.5.1 | Effect of Generator Temperature | 118 |
| 4.3.5.2 | Effect of Heating Behavior | 119 |
| 4.3.5.3 | Effect of Fixed Flux Heating | 120 |
| 4.3.5.4 | Effect of Heating Time | 121 |
| 4.3.6 | Experimental Data Summary | 122 |
| Chapter Five : Conclusions and Recommendations | | 123 |
| 5.1 | Conclusions | 123 |
| 5.2 | Recommendations | 125 |
| References | | 126 |
| Appendix | | 133 |
| الملخص | | ب |

LIST OF TABLES

| No. | Tables | Page |
|--------------------|---|------|
| Table (1.1) | The Value of $F_R(\tau\alpha)_e$ and F_{RU_L} for Some Type of Solar Collector | 12 |
| Table (1.2) | Advantages and Disadvantages of the Absorption Refrigeration System | 18 |
| Table (1.3) | Advantages and Disadvantages of the Adsorption Refrigeration System | 21 |
| Table (1.4) | Comparisons between Physical and Chemical Adsorption Refrigeration Cycles | 22 |
| Table (1.5) | Advantages and Disadvantages of Chemical Reaction Refrigeration System | 23 |
| Table (1.6) | Advantages and Disadvantages of the Desiccant Refrigeration System | 25 |
| Table (1.7) | Advantages and Disadvantages of the Ejector Refrigeration System | 28 |
| Table (1.8) | Advantages and Disadvantages of the Rankine's Driven Refrigeration System | 30 |
| Table (1.9) | Advantages and Disadvantages for the Solar Vapor Compression Refrigerator | 32 |
| Table (2.1) | Differential Heats of Adsorption for Some Adsorbent/Adsorbate Pairs | 44 |
| Table (2.2) | Parameters of Activated Carbon | 47 |
| Table (3.1) | The Average Total Solar Radiation per day for each month during 2006 at Jenin | 80 |
| Table (4.1) | Results of 7 hours Heating by Electrical Heater at 770 W with 2 L of Methanol and 30kPa Starting Pressure | 98 |
| Table (4.2) | Results of 770 W Heating and 92.5 kPa Starting Pressure with 2L of Methanol | 98 |
| Table (4.3) | Results of Heating and Charging with 4L of Methanol | 99 |
| Table (4.4) | Result of Solar Heating with 6L of Methanol | 100 |
| Table (4.5) | Experimental Results of Pilot Setup Charged with 8L of Methanol, and Heated by Solar Energy at 26kPa. | 102 |
| Table (4.6) | Results of Solar Heating of Pilot System at 26kPa | 104 |
| Table (4.7) | Results of Heating and Evacuations Process of the Modified System | 111 |
| Table (4.8) | Preliminary Results of Evacuated Pilot Solar Setup Charged with 2L of Methanol | 112 |
| Table (4.9) | Effect of Rapid Cooling | 112 |
| Table(4.10) | Successive Heating, Evacuation, and Heating for Several Days | 114 |
| Table(4.11) | Results of Charging the Pilot Scale Setup Charges with 6.75 L of Methanol | 116 |
| Table(4.12) | Results Pilot Scale Setup Charged with Optimum Volume of Methanol(7.4L) | 117 |

LIST OF FIGURES

| No. | FIGURES | Page |
|---------------------|--|------|
| Figure (1.1) | Solar Cooling Paths | 5 |
| Figure (1.2) | Heat Balance for a Refrigeration Cycle | 8 |
| Figure (1.3) | Characteristic Curve of a Solar Collector | 11 |
| Figure (1.4) | Definition of System Carnot Efficiency | 13 |
| Figure (1.5) | Simple Diagram of the Absorption Refrigeration System. | 16 |
| Figure (1.6) | The Solar-Operating Platen-Munters Refrigeration system. | 18 |
| Figure (1.7) | (a)The adsorption (Refrigeration) Process and (b) The desorption (Regeneration) Process | 20 |
| Figure (1.8) | The Solid Desiccant Cooling Machine | 24 |
| Figure (1.9) | Desiccant Cooling Process | 25 |
| Figure(1.10) | Ejector Refrigeration Cycle | 27 |
| Figure(1.11) | Solar Driven Rankine Cycle | 29 |
| Figure(1.12) | Solar-Driven Vapor Compression Refrigeration Cycle | 31 |
| Figure(1.13) | T- s Diagram of the Vapor Compression Refrigeration Cycle | 31 |
| Figure (2.1) | Typical Set of Isosters for Different Absorbent/Adsorbate Pairs and their Refrigeration Cycle. | 46 |
| Figure (2.2) | Comparison Between Zeolite–Water and Charcoal–Methanol Adsorption System. | 46 |
| Figure (2.3) | Operation Principle of Solid Adsorption Refrigeration System Utilizing Solar Heat. | 49 |
| Figure (2.4) | Clapeyron Diagram ($\ln P$ versus $-1/T$) of Ideal Adsorption Cycle. | 50 |
| Figure (2.5) | Variation of COP with Solar Radiation Energy. | 57 |
| Figure (2.6) | COP _{Solar} for Different Collector Radiation Values | 58 |
| Figure (2.7) | Clapeyron Diagram ($\ln P$ vs. $-1/T$) of Ideal Adsorption Cycle. | 61 |
| Figure (2.8) | Schematics of Heat Recovery Two-Beds Adsorption Refrigeration System. | 62 |
| Figure (2.9) | Diagram of Heat and Mass Recovery Cycle. | 63 |
| Figure(2.10) | Thermal Wave Cycle | 65 |
| Figure(2.11) | n-Adsorber Cascading Cycle. | 67 |
| Figure(2.12) | Schematic of the Solar Hybrid System. | 69 |
| Figure(2.13) | Clapeyron Diagram ($\ln P$ Vs $-1/T$) of Ideal Adsorption Cycle. | 71 |
| Figure(2.14) | Section of the Adsorbent Bed. | 72 |
| Figure(2.15) | Solar House with Enhanced Natural Ventilation Driven by Solar Chimney and Adsorption Cooling Cavity. | 73 |

| No. | FIGURES | Page |
|---------------------|--|-------------|
| Figure(2.16) | Solar Driven Ejector-Adsorption System and an Concentrating Adsorber | 74 |
| Figure (3.1) | Areas of the World with High Insulation | 76 |
| Figure (3.2) | Sketches of the Solar Radiation Through the Atmosphere | 77 |
| Figure (3.3) | Pyranometers Used for Measuring the Global Radiation and Diffuse Radiation | 78 |
| Figure (3.4) | The Average Total Solar Radiation per day for each month during 2006 at Jenin | 80 |
| Figure (3.5) | Meteorological Station Used by The Energy Research Centre At An- Najah National University | 81 |
| Figure (3.6) | Yearly Average Solar Radiation in Different Cities in Palestine | 81 |
| Figure (3.7) | Energy Balance on a Solar Collector Absorber / Receiver | 85 |
| Figure (3.8) | Typical Solar Collector Efficiency Curves | 87 |
| Figure (4.1) | The Sketch Structure of the No Valve Cooler | 89 |
| Figure (4.2) | Cross Section of the Adsorbent Bed | 92 |
| Figure (4.3) | Sketch of the Evaporator (mm.) | 93 |
| Figure (4.4) | The Photograph of the Pilot Scale Setup System | 94 |
| Figure (4.5) | Lab Scale Setup | 101 |
| Figure (4.6) | Sketch of the Suggested Coaxial Pipes Generator/Collector | 109 |
| Figure (4.7) | The Schematic Diagram of the Modified Solar System | 110 |
| Figure (4.8) | Continuous Data from the Pilot Scale Setup Using Variable Heat Flux. | 119 |
| Figure (4.9) | The temperature Variations with Time Under the Average Daily Solar Radiation at Palestine (5.4 kWh/m ² / day) | 120 |
| Figure(4.10) | The Temperature Variations with Time Under the Heat Flux 7.25kWh/m ² /day. | 121 |
| Figure(4.11) | The Temperature Variations with Time Under Partially Solar Heating, at Low Generation Temperature | 121 |

**Solar Energy Refrigeration by Liquid-Solid
Adsorption Technique**

By

Watheq Khalil Said Hussein

Supervisor

Dr. Abdelrahim Abusafa

Co-Supervisor

Dr. Imad Ibrik

Abstract

The design, construction and operation of a solid adsorption solar cooler are presented in this work. Granular activated carbon-methanol as the adsorbent /adsorbate pair was used. The System has three important components: collector/adsorber, condenser and evaporator.

A flat plate type collector made of stainless steel with effective exposed area of 0.95m² was used. Two types of condensers were tested, the first one was a helical copper tube immersed in water tank and the other one was a finned stainless steel tube.

Solar radiation was simulated using an electrical heater regulated by a solid state relay and potentiometer. The experimental work was focused on optimizing the suitable amount of activated carbon/methanol pairs, the influence of regenerator temperature, and the influence of solar flux on the performance of the system.

It was found that regenerator temperature greater than 100 °C was necessary to release methanol from the activated carbon.

The operating pressure was also found to be an important parameter to achieve cooling effect; the system pressure must be less than 20kPa absolute.

As the adsorbent bed is the heart of such system, and its characteristics directly affected the performance of the system, the experimental work showed that the adsorbent bed which was used in this study didn't achieve the best results expected, therefore another adsorbent bed with hollow tubes generator was suggested, it was found that in this type of generator is easier to control the leakage and the pressure inside the system.

The type of the condenser and its length was found to be important parameters that affect the performance of the used system. The condenser length should be as short as possible, however, the condenser tube should be straight pipe with fins and without any curvatures to prevent pressure drop in the system.

In most cases, the water temperature of 10 °C was obtained using the system for air-conditioning, food and vaccines preservation, and for producing chilled water. The obtained temperature was effected directly by the heat flux applied and the heating period. The optimum heating period was found to be at least 5 hours, while the cooling period was more than 10 hours.

In a Lab scale setup solar cooler, it was found that the evaporator volume has a significant effect on the performance of such system; the evaporator volume should not be much larger than the maximum methanol volume charged in the system. The maximum methanol adsorption capacity of the used activated carbon was found to be 0.26 kg methanol / kg activated carbon.

Introduction

Everywhere in our world, refrigeration is a major energy user. In poor areas, “off grid” refrigeration is a critically important need. Both of these considerations point the way toward refrigeration using renewable energy, as part of a sustainable way of life. Solar-powered refrigeration is a real and exciting possibility.

Due to the increasing concentration of greenhouse gases and climate changes, the need for renewable energy sources is greater than ever. This has now attracted attention from the countries that has set up targets to increase the share of renewable energy supply in the world in order to reduce greenhouse gas emissions.

Today about 82% of the world’s primary-energy requirements are covered by coal, natural gas, oil and uranium. Approximately 12% comes from biomass and 6% from hydroelectric power. A reduction of greenhouse gases throughout the world of about 50 % is required in the next 50-100 years, according to many experts. In order to achieve this, a reduction of greenhouse gas emissions of approximately 90% per capita in the industrial countries, will be necessary. If we shall be able to change our energy supply system and reduce greenhouse gases, we need to use renewable energy sources, and solar energy is one of the most environmentally safe energy sources.

Energy supply to refrigeration and air-conditioning systems constitutes a significant role in the world. The International Institute of Refrigeration (IIR) has estimated that approximately 15% of all electricity

produced worldwide is used for refrigeration and air-conditioning processes of various kinds [1].

The cooling load is generally high when solar radiation is high. Together with existing technologies, solar energy can be converted to both electricity and heat; either of which can be used to power refrigeration systems. Being provided with a good electricity grid worldwide, people are, however, more likely to choose a vapor compression air-conditioning system.

Palestine climate has an attractive potential for solar energy application. The overall aim of this study is to develop a solar powered solid adsorption cooler using locally available technologies. Many experiments were done to optimize the best design, the suitable conditions, and the influence of temperature levels and different power fluxes on the solar cooler performance. Despite the greatest effort needed to make the system sealed, the system was very simple, needs no maintenance and has no moving parts consequently it is noiseless.

Chapter One

Solar Cooling

1.1 Refrigeration Definition

In general, refrigeration is defined as any process of heat removal. More specifically, Refrigeration is defined as the branch of science that deals with the process of reducing and maintaining the temperature of a space or material below the temperature of the surroundings.

To accomplish this, heat must be removed from the body being refrigerated and transferred to another body whose temperature is below that of the refrigerated body. Removing heat from inside a refrigerator is somewhat like removing water from a leaking canoe. A sponge may be used to soak up the water. The sponge is held over the side, squeezed, and the water is released over board. The operation may be repeated as often as necessary to transfer the water from the canoe into the lake. In a refrigerator, heat instead of water is transferred[2].

Since the heat removed from the refrigerated body is transferred to another body, it is evident that refrigerating and heating are actually opposite ends of the same process. Often only, the desired result distinguishes one from the other. Therefore, solar energy may be used for cooling. This is usually done by using absorption or adsorption system refrigeration. These systems require a heat source. The heat is used to drive the refrigerant out of another substance which has the opportunity to release it when they are heated and to adsorb it when be cooled. The sun can supply the heat required to operate adsorption or absorption cycles.

1.2 Solar Cooling Options and Technologies

The concept of ‘solar cooling path’ from the energy source to the cooling service, is introduced in this chapter. Before going into detail for each solar-driven refrigeration system, definitions, suitable efficiency terms, and thermodynamic limitations of solar cooling are described. Subsequently, an overview of possible solar-driven refrigeration and air-conditioning options are presented, including some possible and existing cooling cycles. The advantages and disadvantages of each solar cooling system are also compared.

1.3 Solar Cooling Path

The solar cooling system is generally comprised of three subsystems: the solar energy conversion system, refrigeration system, and the cooling load. The appropriate cycle in each application depends on cooling demand, power, and the temperature levels of the refrigerated object, as well as the environment. A number of possible “paths” from solar energy to “cooling services” are shown in Figure 1-1. Starting from the inflow of solar energy there are obviously two significant paths to follow; solar thermal collectors to heat or PV cells to electricity [3].

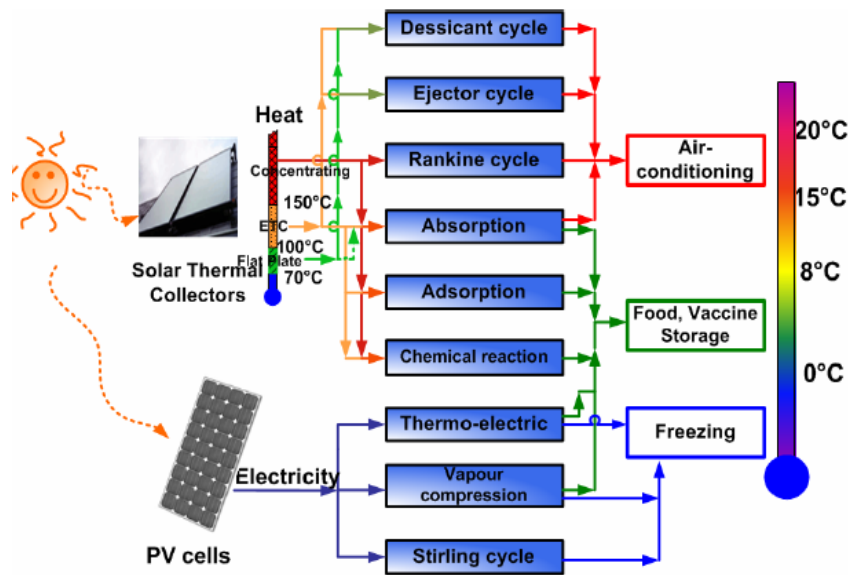


Figure (1-1): Solar Cooling Paths [3].

For solar thermal collectors, different collector types produce different temperature levels. This indicates that the temperature level can be matched to various cycle demands. For example, the Rankine cycle, requires a rather high driving temperature whereas the desiccant cycle manages at a lower temperature level of heat supply. The same type of temperature matching is important for the cold side of the solar cooling path, i.e. in the cold object. Since several cycles typically operates with water as a working fluid, it is impossible to achieve temperatures below 0°C for some cycles. The solar thermal-driven air conditioning cycles can be based on absorption cycles, adsorption cycles, duplex Rankine, desiccant cooling cycles, or ejector refrigeration cycles. When using low temperature applications for food storage at 0 to -8°C, various cycles can be applied, i.e. the vapor compression cycle, thermoelectric cycle (Peltier), absorption cycle, adsorption cycle or a chemical reaction cycle. Applications requiring temperatures below 0°C generally require small

storage volumes e.g., freezing boxes. A suitable cycle for this application has proved to be the PV-driven vapor compression cycle, or a PV-driven Sterling cycle. The double effect absorption cycle, adsorption cycle and chemical reaction cycle can also be used, especially for larger storage volumes, i.e. ice production [1] .

Typically for the cycles in Figure 1-1 are that, the efficiency of the electricity-driven refrigeration cycles is quite high but they require photovoltaic panels and batteries, which are expensive. Heat driven cycles on the other hand, are less efficient, but the thermal solar collectors may reach much higher conversion efficiencies than the PV's, even though the output is heat, not electricity. Therefore, the question is: which path provides the highest overall efficiency? One example: System 1, a heat driven cycle with a cycle COP of 0.7 receives its heat from a solar collector with 80% efficiency, System 2, a vapor compression refrigeration cycle with a COP of 4 receives its electricity from a PV array with an efficiency of 15%. Which one gives the highest overall efficiency?

$$\text{COP}_{\text{solar}} = \eta_{\text{collector, th}} \times \text{COP}_{\text{cycle}} = 0.7 \times 0.8 = 0.56$$

$$\text{COP}_{\text{solar}} = \eta_{\text{collector, pv}} \times \text{COP}_{\text{cycle}} = 0.15 \times 4.0 = 0.6$$

The solar energy collection efficiency, $\eta_{\text{collector}}$ of both thermal collectors and photovoltaic collectors is defined as the ratio of the rate of useful thermal energy leaving the collector, to the useable solar irradiance falling on the aperture area. Simply stated, collector efficiency is:

$$\eta_{\text{coll}} = Q_{\text{useful}} / A_a I_a \quad (1-1)$$

where:

Q_{useful} = rate of (useful) energy output (W)

A_a = aperture area of the collector (m^2)

I_a = solar irradiance falling on collector aperture (W/m^2)

The $\text{COP}_{\text{solar}}$ (coefficient of performance) is the ratio of the refrigeration effect to the solar energy input (I), while the $\text{COP}_{\text{cycle}}$ is the ratio of the refrigeration effect to the required input work to drive the refrigerator.

1.4 Cycle Efficiency

The performance of a refrigeration cycles is generally presented in terms of a coefficient of performance, COP, illustrating how much energy that heat can be removed from a cold space (Q_e) for each unit of energy expended (W or Q_g) as in figure 1-2. The COP can be written differently, depending on the type of drive energy. The frequently used definitions for COP of an electricity/ work-driven system and thermally driven system are shown in equation 1-2 and 1-3, respectively [4].

$$\text{COP}_{\text{el}} = Q_e / W \quad (1-2)$$

$$\text{COP}_{\text{thermal}} = Q_e / Q_g \quad (1-3)$$

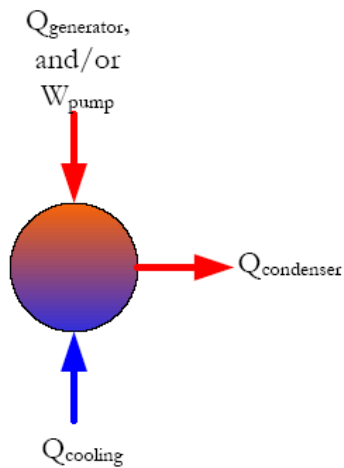


Figure (1-2): Heat Balance for a Refrigeration Cycle

Where:

Q_e = Cooling effect (Desired output)

W = Work input (Desired electrical input)

Q_g = Work input (Desired thermal input)

1.5 Solar Collector Efficiency

The major energy gains in the absorber in a solar collector are from the direct absorption of visible light from the sun and, additionally, the absorption of infrared radiation from the warm glass. Important energy losses are infrared radiation emission, convective heat due to natural convection between the absorber and glass, as well as conduction of heat through the rear and sides of the collector. Therefore, the efficiency of the solar collector depends on all of these factors. The efficiency of the solar collector sub-system can be defined as the ratio of useful heat output to the total incident solar radiation (insolation).

In the following efficiency definition, it is assumed that radiation is in the hemispherical region, all rays reach the absorber, and the multiple reflections between the cover and absorber are neglected. The solar collector efficiency can be written as in equation 1-4 [5]:

$$\eta = F_m \left\{ \eta_{\text{opt}} - \frac{U_L(T_{\text{abs,avg}} - T_a)}{I} \right\} \quad (1-4)$$

Where:

F_m : is called the collector efficiency factor or a heat transfer factor.

η_{opt} : is the optical efficiency which is defined as the rate of optical (short wavelength) energy reaching the absorber or receiver, divided by the appropriate solar resource[5].

U_L is overall heat loss coefficient, (W/m²K).

$T_{\text{abs,avg}}$ is the average temperature of the absorber surface

T_a is the ambient temperature

The value of F_m depends on the type of the collector and operating conditions. Typical values of F_m is in the range of 0.8-0.9 for non-evacuated air collectors, 0.9-0.95 for non-evacuated liquid collectors, and 0.95-1 for evacuated collectors [6]. In essence, it is easier to measure the temperature of the heat transfer fluid than to measure the temperature of the absorber surface temperature. Therefore, the solar collector efficiency is often written in terms of the temperature of the inlet (T_i) and outlet (T_o) temperature of the heat transfer fluid.

The average temperature of the absorber surface can be assumed to be:

$$T_{abs,avg} = \frac{T_i + T_o}{2} \quad (1-5)$$

The efficiency of the solar collector can be defined as

$$\eta = F_m \left\{ \eta_{opt} - \frac{U_L(T_i - T_a)}{I} \right\} \quad (1-6)$$

Or

$$\eta = F_R (\tau\alpha)_e - F_R U_L \frac{(T_i - T_a)}{I} \quad (1-7)$$

Where:

F_R is the collector heat removal factor.

(τ) is the transmissivity of the glass cover

(α) is the absorptivity of absorber,

The later equation is based on the ‘Hottel-Whillier-Bliss’ Equation [3]. The value of factors $F_R (\tau\alpha)_e$ and $F_R U_L$ depend on the type of the collectors, layer of the cover glass and selective material. Typical values of these factors are shown in Table1-1. The efficiency of the solar collector (η) and the value of $(T_i - T_a) I^{-1}$ can be plotted in Figure (1-3), as shown below [3].

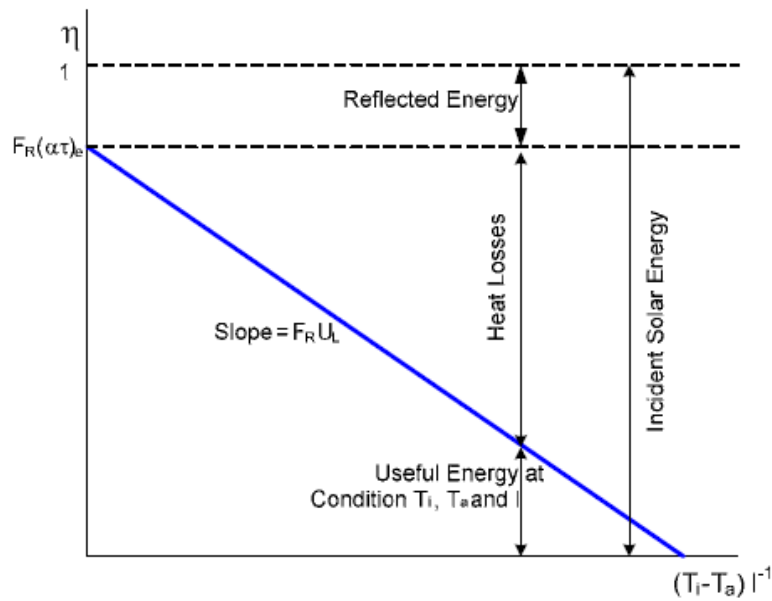


Figure (1.3): Characteristic Curve of a Solar Collector

Occasionally, the efficiency of a solar collector is written in quadratic form as shown in equation 1-8. This equation is commonly used in simulation to the solar collectors [1].

$$\eta = k(\Theta) \cdot C_0 - C_1 \frac{(T_{abs,avg} - T_a)}{I} - C_2 \frac{(T_{abs,avg} - T_a)^2}{I} \quad (1-8)$$

Where: $k(\Theta)$ = incident angle modifier, which accounts for the influence of non perpendicular incident radiation at the incident angle, Θ , in relation to the normal incidence radiation of $\Theta=0$

c_0 = optical efficiency

c_1 = linear heat loss coefficient

c_2 = quadratic heat loss coefficient

Table (1.1): The Value of $F_R(\tau\alpha)_e$ and F_RU_L for Some Type of Solar Collector

| Solar Collector Type | $F_R(\tau\alpha)_e$ | F_RU_L ($W\ m^{-2}\ K^{-1}$) |
|---|---------------------|-------------------------------------|
| Flat-Plate, Selective-Surface, Single-Glass Cover | 0.80 | 5.00 |
| Flat-Plate, Selective-Surface, Double-Glass Cover | 0.80 | 3.50 |
| Evacuated Tubular Collectors | 0.80 | Range 1-2 |
| Parabolic-Through Concentrating solar collector (PTC) | 0.70 | 2.50 |

The optical efficiency of a flat plate solar collector can be written as a product of the transmissivity (τ) of the glass cover and absorptivity (α) of the absorber,

$$\eta_{opt} = \tau \alpha \quad (1 - 9)$$

1.6 Photovoltaic Efficiency

The efficiency of a photovoltaic cell can be written as

$$\eta_{pv} = \eta_R [1 - \beta (T_C - T_R)] \quad (1-10)$$

Where:

η_R = Reference efficiency at $0^\circ C$ (about 0.12 for single crystalline cells)

β = Coefficient of variation of the solar cell efficiency (about $0.04\ K^{-1}$ for single crystalline cells)

T_c = Cell Temperature ($^\circ C$)

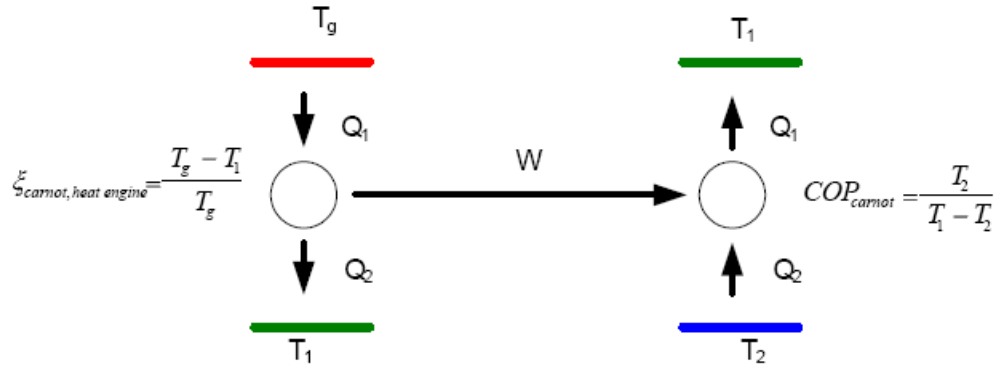
T_{ref} = Reference Temperature ($^\circ C$)

Normally, one cell produces a potential difference of 0.5 volt and a current density of $200\ Amp\ m^{-2}$ at $1\ kW\ m^{-2}$ of solar radiation. The efficiency of available commercial photovoltaic cells is about 10-17% and

they can produce 1-1.5 kWh m⁻² per day. The current is proportional to the light exposure area [7].

1.7 System Efficiency

In the case of an ideal heat engine and refrigerator, here referred to as Carnot cycles, the performance of the Carnot Heat Engine Cycle driving the Carnot Refrigeration Cycle can be written in terms of the Carnot efficiency and the Carnot Coefficient of Performance (COP_{Carnot}), as shown in Figure 1-4. T₂, T₁, and T_g are the thermodynamic temperature of the refrigerated space, the environment, and the heat source, respectively.



Carnot Heat Engine Carnot Refrigeration System

Figure (1-4): Definition of System Carnot Efficiency

$$\xi_{\text{carnot heat engine}} = \frac{T_g - T_1}{T_g} \quad (1-11)$$

$$\text{COP}_{\text{carnot}} = \frac{T_2}{T_1 - T_2} \quad (1-12)$$

$$\eta_{\text{carnot}} = \xi_{\text{carnot heat engine}} \cdot \text{COP}_{\text{carnot}} \quad (1-13)$$

$$\eta_{\text{carnot}} = \left\{ \frac{T_g - T_1}{T_g} \right\} \cdot \left\{ \frac{T_2}{T_1 - T_2} \right\} \quad (1-14)$$

For a PV-driven system, the simple Carnot Engine Efficiency (ξ) becomes the efficiency of the PV-array.

$$\eta_{\text{system,el}} = \text{COP}_{\text{el}} \times \eta_{\text{pv}} \quad (1-15)$$

Since the main energy source is free for solar cooling systems, the term 'solar fraction' is better suited for demonstrating the overall effectiveness of the system. Solar fraction is defined as the ratio of the total solar energy used to the total energy used in the system.

Solar Fraction = Solar Energy Used in the System / Total Energy Used in the System.

1.8 SOLAR COOLING TECHNOLOGIES

The solar-driven refrigeration system, as mentioned previously, is mainly classified into two main groups depending on the energy supply: thermal/work driven system and electricity (Photovoltaic) driven system, each group can be classified as the following,

1. Thermal/work driven systems

- Absorption refrigeration cycle
- Adsorption refrigeration cycle
- Chemical reaction refrigeration cycle
- Desiccant cooling cycle
- Ejector refrigeration cycle
- Expansion refrigeration cycle

2. Electricity (Photovoltaic) driven system

- Sterling refrigeration cycle
- Thermo-electric refrigeration cycle
- Vapor compression refrigeration cycle

1.8.1 Thermal – driven systems

1.8.1.1 Absorption Refrigeration Cycle

The main components of the absorption refrigeration system are an absorber, generator, a condenser, an expansion valve, a heat exchanger and a pump. The Simple diagram of the absorption refrigeration system shown in Fig. 1.5. Two kinds of working medium are used at the same time in refrigeration and absorption processes. The refrigerant vapor flows to the condenser passing through a vapor-trap and condensed. Liquid refrigerant from the condenser goes through an expansion valve while the pressure is decreased to an evaporation pressure. At the evaporator, cooling effect is achieved by the vaporization of the refrigerant at a low temperature. Refrigerant vapor from the evaporator continues to an absorber and dissolves in a weak refrigerant solution, and it becomes a stronger refrigerant solution, which is called “rich solution”. A pump is the only moving part in this system. The “rich solution” is pumped to a generator. At the generator, the rich solution is heated up; the refrigerant is separated from the solution. The refrigerant is vaporized and goes to the condenser while the weak solution is passed through a heat exchanger and returned to the absorber to absorb the refrigerant vapor. The refrigeration process and the regeneration process operate at the same time as the continuous

process, producing a continuous cooling effect. A flat plate solar collector can maintain the operating condition at the generation temperature about 75-100°C but very efficient heat exchangers are required [3] .

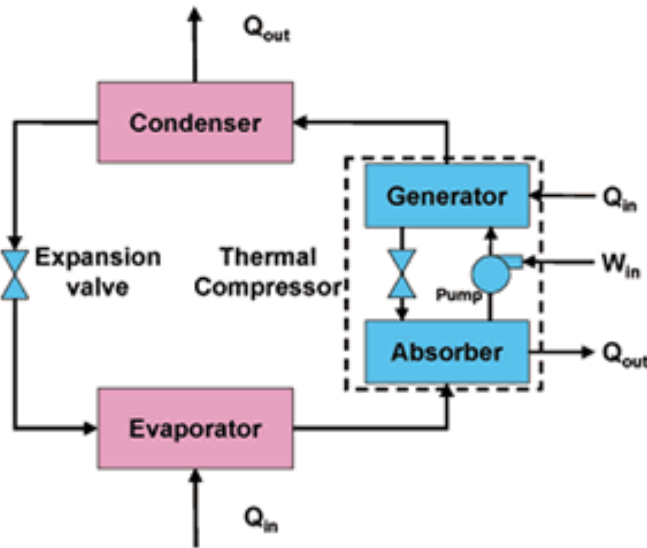


Figure (1.5): Simple diagram of the absorption refrigeration system [8].

Working Media:

Several pairs of working media have been used for absorption refrigeration system e.g. a pair of ammonia-water (ammonia is the refrigerant and water, is the absorption medium), a pair of water-lithium bromide (water is the refrigerant and lithium bromide is the absorbent) and a pair of water-lithium chloride. (Water being the refrigerant and lithium chloride is the absorbent). Both ammonia and water have good heat transfer characteristic. In addition, water separator (rectifier) is needed to be installed in order to prevent water from passing to the condenser with pure ammonia.

Platen-Munters Cycle:

This system is a special case of the absorption system, and well known as the Electrolux refrigerator and principally was invented from the division of applied thermodynamics and refrigeration, KTH, Sweden[3]. It is developed from the Carré absorption cycle but operating without pump. It can be called no-moving part and no-auxiliary energy supply system, Fig1.6. Hydrogen is used to maintain the total pressure in the whole system to be constant. The refrigerant partial pressure is allowed to be low at the evaporator, achieving the refrigeration effect. Ammonia is conventionally used as the refrigerant, water is used as the absorption media and hydrogen is used as the inert gas. The principle of the cycle is similar to absorption cycle; however, total pressure in the whole system is constant. Hydrogen is circulated between the evaporator and the absorber, compensating the pressure difference between the high and low-pressure side. Ammonia vapor evaporates in the generator and then condenses in the condenser before flowing to the evaporator. The ammonia poor aqueous solution is then back to the absorber by the gravitational flow. At the evaporator, the liquid-ammonia is exposed into the hydrogen atmosphere, and evaporates due to a low partial pressure (of ammonia). The ammonia hydrogen mixture continues to the absorber (passing through the heat exchanger), in which ammonia is absorbed in the water solution. The hydrogen returns to the evaporator through the heat exchanger while aqueous ammonia solution forwards to the generator by a thermosyphon pump. The generator temperature is typically varied between 120 to 180°C, depending on the operating temperature. The conventional energy sources are natural gas, kerosene or electricity. The practical COP varies between 0.2 and 0.3 at 25

and 100 W of cooling capacity [9]. Large capacity system is difficult to be achieved. Table 1.2 shows the Advantages and disadvantages of the absorption refrigeration system.

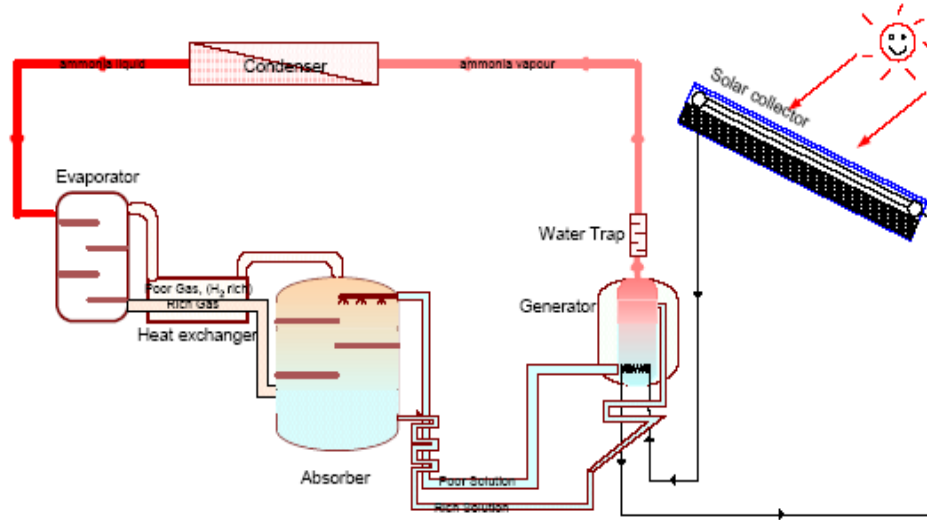


Figure (1.6): The solar-operating Platen-Munters refrigeration system [3].

Table (1.2): Advantages and disadvantages of the absorption refrigeration system

| Advantages | Disadvantages |
|--|---|
| 1. Require little maintenance. | 1. Low COPs. |
| 2. Only one moving part (pump) and might be no moving part for a small system. | 2. It cannot be applied for a very low evaporating temperature (when water LiBr are used). |
| 3. No auxiliary energy for operation of the small system. | 3. High heat release to the ambient. |
| 4. Solar thermal collector is used, that is cheaper than Photovoltaic cells. | 4. A continuous and big system need pump which is not solar thermal energy dependent. |
| 5. Low energy cost (for pump only). A small system might not require pump. | 5. Quite complicated system and require advanced knowledge for maintenance. |
| 6. Low-temperature heat supply. | 6. For the big system such as an air conditioning unit, it requires a large area of solar collector, which means a very high installation cost and a large installation area. |

1.8.1.2. Adsorption Refrigeration Cycle

An adsorption, also called a solid-sorption cycle, is a preferential partitioning of substances from a gaseous or liquid phase onto a surface of a solid substrate. This process involves the separation of a substance from one phase to accumulate or concentrate on a surface of another substance. An adsorbing phase is called an 'adsorbent'. Material, which is accumulated, concentrated or adsorbed in another surface, is called an 'adsorbate'. The sticking process should not change any macroscopic form of the adsorbent except the changing in adsorbent's mass.

Both adsorption and absorption can be expressed in term of sorption process. The adsorption process is caused by the Van der Waals force between adsorbate and atoms or molecules at the adsorbent surface. The adsorbent is characterized by the surface and porosity. In the adsorption refrigeration cycle, refrigerant vapor is not be compressed to a higher temperature and pressure by the compressor but it is adsorbed by a solid with a very high microscopic porosity. This process requires only thermal energy, no mechanical energy requirement. The principles of the adsorption process provide two main processes, adsorption or refrigeration and desorption or regeneration. In case zeolite and water, as an example, the refrigerant (water) is vaporized by, the heat from cooling space and the generator (adsorbent tank) is cooled by ambient air. The vapor from the cooling space is leaded to the generator tank and absorbed by adsorbent (zeolite). The rest of the water is cooled or frozen. In the regeneration process, the zeolite is heated at a high temperature until the water vapor in the zeolite is desorbed out, goes back and condenses in the water tank,

which is now acting as the condenser. For a discontinuous process, the desorption process can be operated during daytime by solar energy, and the adsorption or the refrigeration process can be operated during night-time, figure 1.7. The solar energy can be integrated with a generator. The single adsorber is required for a basic cycle. The number of adsorbers can be increased to enhance the efficiency, which depends on the cycle. This process can also be adapted to the continuous process. Table 1.3 shows Advantages and disadvantages of the adsorption refrigeration system.

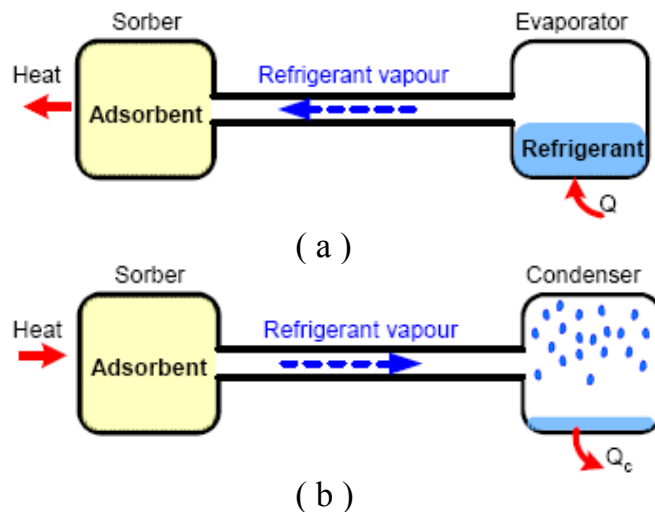


Figure (1.7): (a) The adsorption (Refrigeration) process and (b) The desorption (Regeneration) process

Working Media:

Typical and commercial adsorbents are made from silica gels, zeolite and activated carbons. The adsorbate (refrigerant fluid) could be water, ammonia or methanol. The famous pairs that have been used commercially are zeolite '13x' / H₂O for the temperature above 0°C and activated carbon 35 / methanol for the temperature below 0°C. The others are ammonia / SrCl₂, water / silica gel or air / silica gel in the open cycle [1].

Table (1.3): Advantages and disadvantages of the adsorption refrigeration system.

| Advantages | Disadvantages |
|--|--|
| Require little maintenance | High heat release to the ambient. |
| No moving part | The high weight of absorbent, not suitable to build in the high capacity. |
| Thermal COP is not so low (~0.4 at T_e 0°C, T_c 40°C, T_{ad} 35°C and T_{des} 100°C) | Poor thermal conductivity of the solid adsorbent, which cause the long-term problems. |
| Solar thermal collector is used, that is cheaper than photovoltaic cells. | Low operating pressure requirement, which is difficult to achieve air-tightness. For Activated carb35/Methanol, the operating pressure is around 50 mbar and around 6 mbar for zeolite/water. |
| Low operating temperature can be achieved. | Low energy density. The quantity of the cycled gas (kg gas/kg solid) is very low, around 0.13 for activated carbon/methanol pair and the quantities of ice recovered per1 kg per activated carbon 35 is 0.26 kg. |
| | Very sensitive to low temperature especially the decreasing temperature during night-time. |
| | It is an intermittent system. |

1.8.1.3. Chemical Reaction (solid-sorption) Refrigeration Cycle

A chemical reaction refrigeration cycle is a solid-gas adsorption process with a chemical reaction. It is an intermittent system. The principle of chemical reaction solid-sorption process is similar to the adsorption process. The same analogies of these two systems are:

- They are intermittent processes since the cold cycle is not continuously produced.

- They are heat-driven refrigeration cycles (The mechanical work is required in some cases to blow out the vapor). The sorption latent heat from the gas phase is the driving energy.

The differences between adsorption and chemical reaction solid-sorption refrigeration cycle, and the advantages and the disadvantages of chemical reaction refrigeration system are shown in table 1.4, and table 1.5, respectively.

Table(1-4): Comparisons between Physical and Chemical Adsorption Refrigeration Cycles.

| The main different properties | Physical Adsorption | Chemical Adsorption |
|--|--|---|
| Forces Causing the Adsorption Process | The physical adsorption process occurs due to the Van der Waals force. This force binds the adsorbing molecules to the solid phase. This adsorption process on the surface of the adsorbent does not cause deformation or changes any macroscopic structure of the adsorbent (or solid). The binding molecules can be released by applying heat. | The chemical adsorption process occurs due to covalent or ionic bonds. The adsorbent and the adsorbate share electrons between each other and form a complex surface compound. The forces of these bonds are much stronger than the Van der Waal force. |
| The Thermodynamic Operation of the Cycle | The physical adsorption is a reversible process. To complete the adsorption and desorption cycle, heat supply is required to the adsorber to increase the temperature of the adsorbent. Heat of adsorption is usual not exceed 80 kJ/ mole. | The chemical adsorption process is very difficult to reverse. To complete the cycle, more heat supply to the adsorption cycle is required to achieve high kinetics of reaction. Heat of adsorption is up to 800 kJ/mole. The volume of the sorbent is also changed significant |
| The Working Media | Several pairs can be used e. g . - Activated carbon / ammonia - Activated carbon / methanol - Silicagel / water | There are two main groups of working pairs Ammonia salts with alkaline compounds e.g . BaCl ₂ , MnCl ₂ , SrCl ₂ , et c. Hydrogen and Methalhydrides with low-hysterisintermetallic or meshed metal compounds e .g . LaNi ₅ , LaNi ₄ . 5Al ₀ . 5 or LaNi ₄ . 6Al ₀ . 4 . |

Table (1.5): Advantages and disadvantages of chemical reaction refrigeration system

| Advantages | Disadvantages |
|---|---|
| Require little maintenance | High heat release to the ambient. |
| No moving part, it is a static system | Low COPs. |
| Low operating temperature can be Achieved. | Poor thermal conductivity of the solid adsorbent, which cause the long-term problems. |
| Solar thermal collector is used, that is cheaper than Photovoltaic cells. | The high weight of adsorbent, not suitable to build in a high capacity. |
| Large energy density. | |
| | Low operating pressure at the lower temperature, difficult to achieve air tightness. |

1.8.1.4. Desiccant Refrigeration System

A desiccant cooling system is based on an open-cycle dehumidification process. Heat and water are needed to operate this system. Water is commonly used as a refrigerant since it is cheap and environmentally friendly. A desiccant material can be either liquid or solid. This cycle consists of one drying process, one heat exchanging process and one humidifying process. There are three major components, operating in an atmospheric pressure. These components are a dehumidifier, an evaporative cooler and a regenerator. Heat exchangers are also used as the additional components to increase the system efficiency. A drying process can be performed in a desiccant wheel when solid desiccant (such as silica gel or zeolite) is used, or it can be performed in an absorption tank when liquid desiccant is used. A heat exchanging process occurs in a heat exchanger and the humidifying process is performed in a saturated pad or humidifier. The rotor wheel is widely used as the heat exchanger wheel and the drying wheel. A simple diagram is shown in figure 1.8. Outdoor air is

dehumidified with a solid or liquid desiccant where some of the moisture is removed, resulting in rising of the air temperature and decreasing of the humidity. The air is then cooled by exchanging sensible heat to the returned air in the heat exchanger and humidified to the desired humidity before supplied to the cooling space. The temperature of the supply air is further lowered by the humidifier or the evaporative cooler before entering the cooling space. The returned air from the cooling space is returned to the evaporative humidifier. It is humidified to a lower temperature at the same enthalpy but with a higher humidity. The cooled air enters the energy recovery unit where acting as the cooling medium for the supply air. The air temperature is increased after passing the heat recovery (heat exchanger wheel). It is then passed through a heater, where it is further heated, and then enters the reactivation sector of the desiccant rotor to reactivate the desiccant.

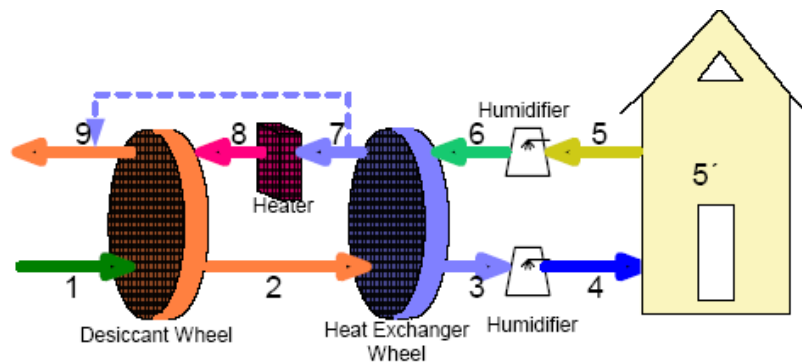


Figure (1.8): Solid Desiccant Cooling Machine

The wet air leaves the rotor as the exhaust air. This process is shown in the Mollier's diagram in figure 1.9. The energy supply to the heater depends on the temperature of the return air entering the desiccant wheel at stage 8. The humidity of the entering air and the effectiveness of the desiccant affect the amount of energy supply.

The low-temperature heat can be supplied to the heater such as solar energy from flat plate solar collector, waste heat from industry or geothermal energy. A small amount of electricity is required for rotating the wheels. The desiccant materials for a solid-desiccant system are usually silica gel or Zeolite. For a liquid desiccant system, the desiccant dehumidifier's hygroscopic aqueous solution can be triethylene glycol (TEG), $\text{CaCl}_2\text{-H}_2\text{O}$, $\text{LiBr-H}_2\text{O}$, $\text{LiCl-H}_2\text{O}$ etc. The advantages and disadvantages of the desiccant refrigeration system are shown in table 1.6.

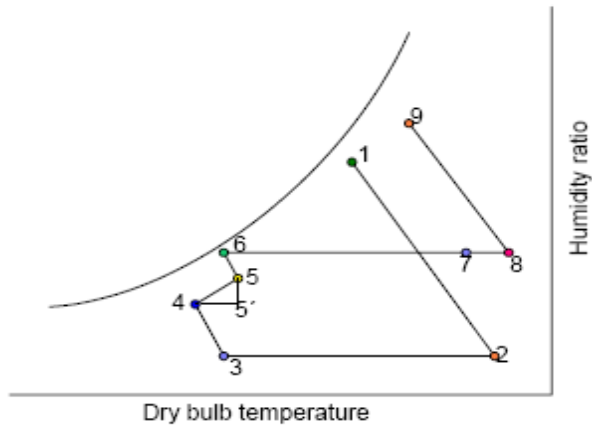


Figure (1.9): Desiccant Cooling Process

Table (1.6): Advantages and disadvantages of the desiccant refrigeration system

| Advantages | disadvantages |
|--|---|
| Environmentally friendly because water is used as the working fluid. | Cannot get the low temperature in the humid region. |
| Can be integrated with a ventilation and heating system. | Required maintenance because of moving part in the rotor wheel of the solid desiccant system. |
| A thermal collector can be used, which is cheaper than PV cells. | Can be contaminated easily. |
| Low heat release to the ambient. | Difficult to design for a small application. Require dehumidifier. |

1.8.1.5. Ejector Refrigeration Cycle

An ejector refrigeration cycle is one of the heat-operating cycles Fig. 1.10. The interesting advantage is as a 'low temperature heat supply' air conditioning system. With this outstanding, the research and development of such a system has been considered increasingly since the energy crisis 1970s. Solar energy (as a renewable source) and waste heat from a heat-operated process such as from truck engines can be integrated with the ejector refrigeration system. The simplicity in installation, design and operation are advantages. The pump is the only moving component in this system. The ejector and the pump are used to maintain the pressure differences in the system. Low efficiency is a drawback of this system, however when the generating temperature is low, the COP of the ejector cycle is higher than the corresponding COP of an absorption system; moreover low-graded heat can be applied.

The major components in the solar-driven refrigeration system are an ejector, a condenser, a generator, an evaporator, an expansion device and a pump. The vapor from the low temperature evaporator is sucked into the high velocity vapor stream in the ejector. The high velocity vapor stream goes through a converging-diverging nozzle in the ejector resulting in the vapor being sucked from the low temperature evaporator. The suction occurs, as the pressure is low at the narrowest section of the ejector. The stream from the evaporator reaches subsonic velocity. A mixing occurs in a mixing zone at the end of the converging section.

Table (1.7): Advantages and disadvantages of the ejector refrigeration system

| Advantages | Disadvantages |
|---|--|
| Low temperature heat source can be supplied. | Low COPs |
| Low operating and installation cost | Difficult to achieve low evaporating temperature |
| Easy to design and install | Superheated is required for some refrigerant such as NH ₃ or water. |
| The system is not complex | Difficult to design an ejector |
| Required less maintenance, less interrupted service. | |
| A large overload capacity can be achieved. | |
| The solar collector can be used to Supply heat, which is cheaper than the Photovoltaic cells. | |
| High reliability. | |

1.8.1.6. Rankin-Driven Refrigeration Cycle

A Carnot heat engine is the most efficient engine to produce work from heat. Heat in the Carnot engine transfers from a higher temperature to a lower temperature.

Generally, the Carnot heat engines cannot be operated since the mechanical problems such as erosion or cavitations of turbine blades, when operating in a two-phase region. The adaptation of the Carnot heat engine in the one-phase region is called "Rankin" cycle. The reversible of the Rankin heat engine is called the 'Rankin refrigeration cycle' or the 'vapor compression cycle'. Work from the turbine of the power cycle drives the compressor of the refrigeration cycle. Any excess energy can be used to produce electricity and reserved as a backup energy when sunshine is lacking or it can be connected to a grid system, figure 1.11[1].

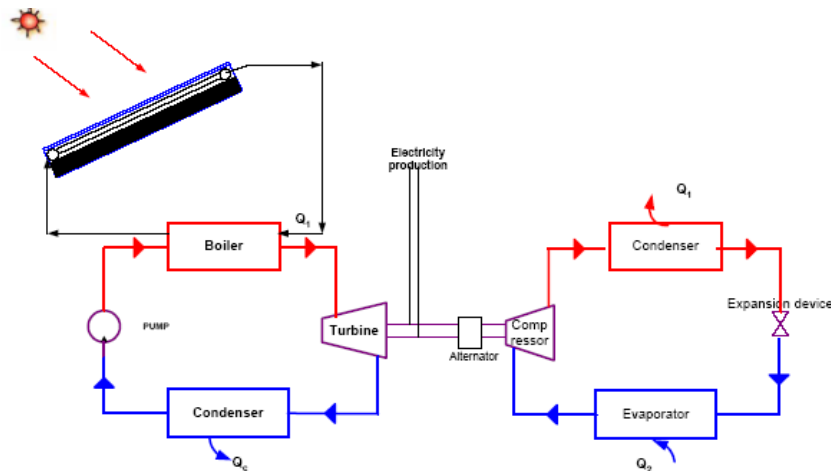


Figure (1.11): Solar Driven Rankine Cycle

A solar-operated Rankine cycle is not much different from a conventional power plant, using water as the working fluid. To increase the efficiency and prevent the erosion of the turbine blades, superheating and extraction processes are used. The working fluid in the Rankine power cycle and the refrigeration cycle can be different. The suitable refrigerant in the solar operating system should be chosen to avoid moisture in a turbine. Superheating is not preferred since the increasing of the collector temperature requirement. The extraction is not economic for a small system. Working fluids such as R114 that give a positive slope of the saturated vapor line on a T-S diagram, the outlet temperature from the turbine is significantly higher than the condensation temperature gives the benefit to preheat the working fluid before it enters the boiler. However R114 is not environmental friendly; it has an ozone depleting potential due to a Chlorine atom.

The speed of the turbine and the compressor should be analogous. The alternator or other equipment that used to adjust the speed should be installed with the system. Table 1.8 illustrate the advantages and disadvantages of the Rankine's driven refrigeration system.

Table (1.8): Advantages and disadvantages of the Rankin's driven refrigeration system

| Advantages | Disadvantages |
|---|---|
| Excess energy can produce electricity. | High installation cost |
| Suitable for high capacity system | Large system |
| The thermal collector can be used as the heat supply, which is cheaper than PV cells. | Required maintenance because of moving parts. |
| | Low capacity |
| | Working fluids are easy to contaminate and are harmful for environment. |

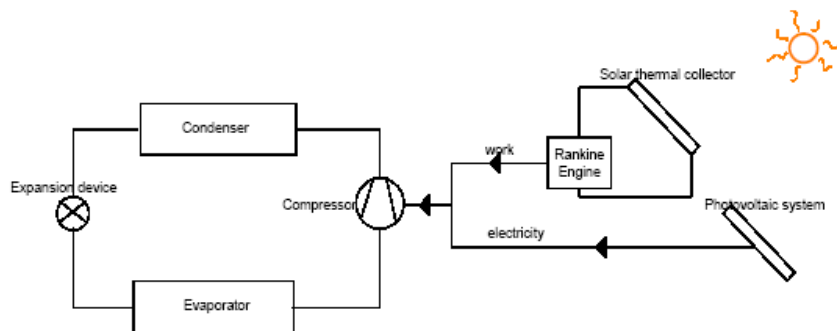
1.8.2 Electricity (Photovoltaic) Driven Systems

Vapor Compression Refrigeration Cycle

A vapor compression refrigeration system is the most widely used cooling system because of high efficiency and reliability. Electricity, as the main energy source, is used as the driven energy for almost vapor compression system. Solar energy can be integrated with vapor compression cooling system by both Photovoltaic cells and solar thermal collectors with the Rankin engines, Figure 1.12 [1].

The main components of the vapor compression refrigeration system are a compressor, a condenser, an expansion device and an evaporator. Refrigerant is circulated in a closed system among these components. In the compressor, the appropriate pressures between high and low pressure are maintained at two temperature levels. At the lower pressure and temperature, in the evaporator, liquid refrigerant is allowed to vaporize when it absorbs heat from the surroundings and creates the refrigeration effect. Vapor is compressed and pumped to the higher temperature and

pressure. The high-pressure vapor from the compressor is then condensed, heat is transferred to the surrounding and vapor becomes the liquid refrigerant. The liquid refrigerant goes to the evaporator passing through the expansion device the refrigerant pressure has falling down to the evaporator pressure. Table 1.9 shows the advantages and disadvantages for the solar vapor compression refrigerator.



Figure(1.12): Solar-driven vapor compression refrigeration cycle

The T-s diagram of the vapor compression refrigeration cycle is illustrated in figure 1.13. The compressor for the solar-driven system usually is a direct current (DC, 12 or 24 volts) compressor since the electricity output from the PV cell is the direct current. Inverter is needed to convert DC electricity to be AC electricity when using AC-compressor[3].

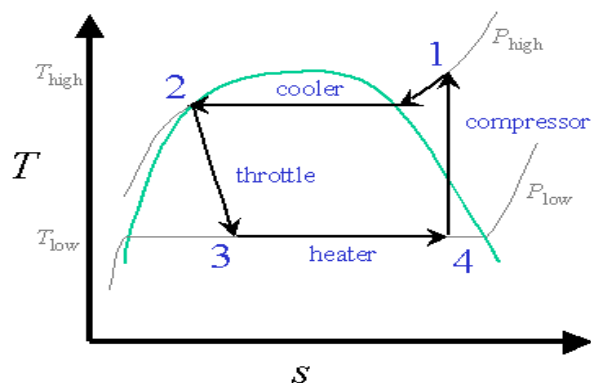


Figure (1.13): T- s Diagram of the Vapor Compression Refrigeration Cycle.

Battery is needed to prolong the cooling period when there is lack of sunlight. Battery's capacity is generally 340 Amp-hour [10]. The size of the PV array depends on the available insolation of each area. The small application such as a vaccine box or a cooling box is more economic than the large one. Other electric equipments can be shared electricity from solar cells such as lighting, radio transmitter, ventilation fan or television; thus make the system more efficient. The power-driven compressor requires Rankin engine to convert heat from the solar thermal collector into a useful work for the compressor. A high technology solar collector is needed since the temperature requirement for the Rankin machine is quite high.

Table(1.9): Advantages and Disadvantages for the solar vapor compression refrigerator

| Advantages | Disadvantages |
|--|---|
| High COPs | For a PV system, installation cost is high and it requires battery for energy backup. |
| Simplicity for the refrigeration system | Noisy from compressor |
| Long term experiences that is easy to maintenance when the problem happens | Required high technical knowledge for PV system |
| Low price | Refrigerant can be leaked. |
| Require little maintenance | |
| Low heat loss | |
| Widely commercial available | |
| Adjustable from a small to a large system | |

Chapter Two

Solar Adsorption Refrigeration

2.1 History and Advantages

In the early years of the previous century, sorption (adsorption) refrigeration was frequently used, later with the development of cheap reliable compressors and electrical motors, the improvement in power station efficiency and the introduction of CFCs in the 1930s, sorption refrigeration became a niche technology [11].

Heat-driven sorption refrigeration cycles have existed in patent literature since at least 1909, and refrigerators were commercially available in the 1920s. In 1929, Miller described several systems, which utilized silica gel and sulfur dioxide as an adsorbent/adsorbate pair [12]. However, recent years have witnessed increasing interest in this technology for many different reasons. The main arguments in favor are that sorption systems are quiet, long lasting, cheap to maintain and environmentally benign.

Refrigeration technology is required to evolve due to the new environmental regulation. The first regulation concerning the depletion of the ozone layer (Montreal protocol, 1988) [13], decided to phase-out chlorofluorocarbons (CFCs) and then hydro chlorofluorocarbons (HCFCs). More recently adsorptive processes have been proposed for heat pump and refrigeration as consistent alternative to vapor compression systems. Ecological problems concerning the emission of CFCs from refrigerating units have stimulated several theoretical and experimental studies on adsorption cooling systems. The environmental impact of fluorocarbon

traces in the atmosphere has shown that CFC emissions are responsible for about one-third the global greenhouse effect [14].

These trends bring to a strong exigency of new systems for space heating and cooling, with the possibility also to obtain a primary energy diversification. Among the proposed technologies, the solid sorption has a very good perspective, in fact, in addition to the non-polluting refrigerants, they can efficiently use natural gas or solar energy as primary energy and they have no moving parts, which makes the machine silent and with no maintenance needs. Therefore, adsorption heating and cooling can be a good alternative to classical vapor-compression machines. Adsorption cooling units are attractive since they can be operated at temperature levels where liquid absorption systems cannot work.

Adsorption is accompanied by evolution of heat. Also, the heat of adsorption is usually 30–100% higher than that of condensation of the adsorbate. Thus, if a fresh adsorbent and adsorbate in liquid form coexist separately in a closed vessel, transport of adsorbate from the liquid phase to the adsorbent occurs in the form of vapor, since adsorption is stronger than condensation to liquid phase. During this step, the temperature of the liquid phase becomes lower while the adsorbent temperature rises. Air-conditioning and refrigeration utilize this phenomenon [15]. Solid/gas systems present the advantage of being absolutely benign for the environment: zero ODP (ozone depletion potential) as well as zero GWP (global warming potential). However, to become a realistic alternative, those systems must exhibit high enough performances to avoid extra primary energy consumption. The figures of merit which are commonly

used to characterize the performances of such cycles are the COP (coefficient of performance), the SCP (specific cooling power) and the thermodynamic efficiency, which is the ratio between the COP and the Carnot COP. The use of solids for removing substances from either gaseous or liquid solutions has been widely used since biblical times. This process, known as adsorption, involves nothing more than the preferential partitioning of substances from the gaseous or liquid phase onto the surface of a solid substrate. From the early days of using bone char for depolarization of sugar solutions and other foods, to the later implementation of activated carbon (AC) for removing nerve gases from the battlefield, to today's thousands of applications, the adsorption phenomenon has become a useful tool for purification and separation[13].

2.2 System Description

One of the very effective forms of solar refrigeration is the production of ice, since ice accumulates much latent heat in it. The most promising application to produce ice by using solar energy is the solid adsorption refrigeration, due to its simple operation and its ability to utilize low grade thermal energy. Although different adsorption pairs had been studied to build adapted solar ice maker. The activated carbon–methanol pair was found the most suitable for solar-powered refrigeration since it could be driven by heat of relatively low, near ambient temperatures. Also it is less expensive than other pairs [16,17]. The adsorption solar refrigerator in its simplest form is a closed system composed of the container of adsorbents and adsorbate (sorption bed), which serves as a solar collector, a condenser and an evaporator. The cycle of this system is

divided into two periods: First, the adsorbent is heated by solar energy during the day and the desorbed adsorbate is condensed. Then the adsorbent is cooled after sunset, thereby re-adsorbing the adsorbate, the evaporation of which produces the refrigeration effect. As desorption is highly endothermic, the heat input to the adsorber must be large enough to allow for sufficient refrigerant to be desorped. On the other hand, adsorption is highly exothermal, so, cooling down of the adsorber is also a major concern. Although, the alternation of heating and cooling during the cycle perfectly suits the intermittent nature of solar energy, yet efficient operation of the system requires high rates of heat transfer in and out of the adsorbent. Unfortunately, some problems are encountered which affect rates of heat transfer. First, the heat transfer of adsorbent bed is very poor, due to low convective heat transfer to the adsorber and bad thermal conductivity of the adsorbent. Second, the thermal mass of the container presented an unacceptably high thermal load which affected alternation of heating and cooling. Third, the system suffers from the problem of being tightly sealed against air leakage through the joints and valves which results in degrading the cooling performance. In addition, all solar systems usually suffer from the large variations in ambient conditions between winter and summer, which makes these systems inefficient for part of the year. In solar adsorption systems, while good heating is attained during day time in summer, cooling during night by ambient air will be limited. On the other hand, in winter, the system will attain good cooling during the night, but heating will be insufficient. In the last two decades, different approaches have been developed to improve heat transfer rates and enhance heating and cooling of the adsorbent bed. The use of composite adsorbent

blocks and monolithic carbon are useful methods to increase both thermal conductivity and density of the bed [18]. To enhance heating of the beds, flat plate solar collectors with selective surfaces, evacuated tubular collectors and simple concentration non-tracking collectors as compound parabolic concentrator collector have been used. As cooling of the adsorbent is by rejecting heat to the environment, heat loss from the collector to the ambient could be enhanced by means of removable insulation, flaps, or dampers [19]. Some designs combine the collector and finned condenser at one unit since outside fins have been located on the rear surface of the collector [20]. By day the solar collector is a desorber and a condenser. At night, the condenser cools the collector. Therefore the investigations must be focused to improve heat transfer in the adsorbent bed, thereby increasing COP, and to improve external heating and cooling of the bed all year round, thereby realizing good performance of the system for most times of the year.

2.3 Principle of Adsorption

Adsorption is a solid sorption process where the binding forces between fluid molecules and the solid medium come from an electrostatic origin or from dispersion - repulsion forces (Van der Waals forces). It is an exothermic process due to the gas-liquid phase change. The energy liberated in adsorption is called isosteric heat, and it depends on the nature of the adsorbent - adsorbate pair.

To describe the thermodynamic equilibrium of adsorption, several state equations known as isotherms of adsorption are proposed. These functions correlate the temperature **T**, the pressure **P**, and the concentration

of the adsorbed phase \mathbf{a} , so that $f(T, P, \mathbf{a}) = 0$, [21]. The main isotherms of adsorption are: (a) Henry's law, valid for weak concentrations; (b) Langmuir's approach, which considers adsorption in monomolecular layers and that there is a dynamic equilibrium between the phases; (c) Gibbs' theory, based on the perfect gas equation, in which the adsorbate is treated in microscopic and bidimensional form; and (d) Adsorption Potential theory, based on a model originally proposed by Polanyi by the end of the 20s, which is a purely thermodynamic approach, suitable for adsorption in micro porous materials. A detailed analysis of the thermodynamics of adsorption and its different isotherms is given by [22].

All micro porous materials are generally adsorbent media, characterized by high porosity. Their structures have pores with diameters smaller than 20Å. The most commonly utilized adsorbents are silica gel, activated carbon, aluminas and zeolites. Zeolite-water and activated carbon-methanol are the most used adsorbent-adsorbate pairs in refrigeration systems. These two pairs have entirely different physical and chemical properties: methanol is easily desorbed from activated carbon when it is heated, while in zeolite, the water is kept much longer. Thus, the activated carbon-methanol pair is best adapted to operating cycles with small evaporating temperature variation (up to 40 °C), since adsorption cycles with the Zeolite+water pair need a larger evaporating temperature change (70 °C or more) to operate, [23].

For the equilibrium of adsorption in micro porous materials with a polymodal distribution of pore dimensions, such as the activated carbon-methanol pair, Dubinin and Astakhov [24] proposed the following isotherm:

$$a = W_0 \rho_1(T) \exp\{-D[T \ln(p / P_s)]^n\} \quad (2.1)$$

where a , is the adsorbed mass per unit of adsorbent mass, W_0 the maximum adsorption capacity (volume of adsorbate/mass of adsorbent), ρ_1 the specific mass of the adsorbate in the liquid state, D the coefficient of affinity" and n is a characteristic parameter of the adsorbent/adsorbate pair.

This equation has a wide field of application, and it is particularly appropriate strongly for activated carbon with a large pores heterogeneousness. According to [21], a fitted curve obtained from experimental results of methanol adsorption in activated carbon presented a residual error of 2.2%, related to the characteristic function proposed by Dubinin and Astakhov. These experiments were performed within a temperature range between 20 and 100 °C and for an adsorbed mass ranging from 71 to 286 g/kg of adsorbent. For smaller temperatures, the residual error was lower than 2%. These results indicate that this state equation is possibly adequate for many engineering applications of low grade heat, especially those concerning solar energy [21].

2.4 Selection of Adsorbent / Adsorbate Pair

At present, three types of working adsorbate and adsorbent, respectively, are favored for pairing for use in solid adsorption solar refrigeration technology: Ammonia, Methanol and Water for adsorbate and activated carbon, silica-gel and zeolite for the adsorbent. The selection of any pair of adsorbent/adsorbate depends on certain desirable characteristics of their constituents, including the affinity for each other. These characteristics range from their thermodynamic and chemical properties to their physical properties and even to their costs or availability.

For refrigerating applications, "the adsorbent must have high adsorptive capacity at ambient temperature and low pressures and a small capacity of adsorption at high temperatures and pressures". The cooling effect, or the temperature attained in the evaporator, depends on the adsorptive capacity at small pressures. This is the property that allows the adsorbent, at a given temperature, to retain vapors from a fluid at a lower temperature. On the other hand, the more intense this property is, the higher the adsorbent regenerating temperature is. Thus, choosing the adsorbent will depend on two basic factors:

- The temperature at which the evaporator must operate;
- The regenerating temperature that the thermal source can possibly attain.

Another important aspect in choosing the adsorbent is the possible catalysis of the adsorbate's dissociating reactions. For example, the methanol adsorption in zeolite is restricted to 100 °C as its maximum temperature. At higher values, the zeolite is a catalyst for the methanol, water and dimethyl ether reaction, producing a blockage of the adsorption process [11]. For the activated carbon-methanol pair, this catalyst reaction will only occur above 150 °C, which is perfectly suitable for solar refrigeration applications. Thus we can summarize the considerations influencing the choice of a suitable adsorbent as follows :

- Porous materials that should adsorb a large amounts of the adsorbate under low temperature conditions to yield good COP.
- Desorption of most of the adsorbate when exposed to thermal energy.

- Possession of high latent heat of adsorption compared to its sensible heating load.
- No deterioration with age or use, thus it is reversibility of adsorption process for many cycles.
- Non-toxic and non-corrosive.
- Low cost and widely available.
- Wide concentration change in a small temperature range. □ □ □
- Good thermal conductivity.

The choice of the adsorbate, or the working fluid, shall depend on the main conditions:

- The evaporator temperature, according to the application;
- The latent heat of evaporation, which should be high;
- The molecular dimensions, which should be small enough to allow easy adsorption.
- Thermally stable with the adsorbent at the cycle operating temperature ranges.
- Non-toxic, non-corrosive and non-flammable.
- Low saturation pressures (slightly above atmospheric) at normal operating temperature.

A survey of the favored working adsorbates shows that methanol and water operate at subatmospheric saturation pressures at the operating temperatures needed, and an ingress of air immediately results in system malfunction. Ammonia does not have this problem because its outward leak could be tolerated for some time, but its saturation pressure of 13 bar at 35 °C condensing temperature is quite high. In the case of methanol, with a normal boiling point of 65 °C, the low saturation pressures could be exploited advantageously to detect leakages, since it must necessarily result in abnormal increases in system pressure and poor performances.

Ammonia, methanol and water, all have relatively high latent heat values of 1368, 1102 and 2258 kJ/kg, respectively, and their specific volumes are low, on the order of about 10^{-3} m³/kg [25].

Ammonia is toxic and corrosive, while water and methanol are not, but the problem with alcohols is that they are flammable. Water is the most thermally stable with adsorbents, closely followed by methanol and ammonia in that order. However, water cannot be used for freezing purposes because its freezing temperature is 0 °C. This makes methanol a favored adsorbate for pairing with a stable adsorbent.

Various kinds of working pairs for adsorption refrigeration have been already studied, and they include both physical and chemical adsorption working pairs. The main physical adsorbents are activated carbon, zeolite, and silica gel, and accordingly, the physical adsorption working pairs are mainly activated carbon–methanol, activated carbon–ammonia, zeolite–water and silica gel–water. In recent years, the working

pairs activated carbon–HFC-134a, and activated carbon–dimethylether were also investigated [26].

As water is the refrigerant normally used with zeolite or silica gel, the evaporating temperature is never lower than 0°C. Compared to other physical adsorption working pairs, the main advantage of the utilization of activated carbon as adsorbent is the low evaporating temperature that can be reached, as the refrigerants most employed are ammonia or methanol. Due to the low evaporation temperature of these refrigerants, these pairs are more suitable for ice making technology.

Chemical adsorbents mainly include metal chlorides and metal hydrides. The metal chlorides generally use ammonia as refrigerant when designed for ice making purposes. The main advantage of the metal chlorides working pairs is the larger adsorption quantities, which are about 5–6 times of that obtained with the physical adsorption working pairs.

The disadvantages of metal chlorides are the phenomena of swelling and agglomeration when the expansion space for the salt is, respectively, too large or too small. The swelling phenomenon reduces the heat transfer performance, and the agglomeration phenomenon reduces the mass transfer performance. In order to improve the heat and mass transfer of metal chlorides, composite adsorbents using graphite or carbon fiber as porous additives were researched. Various studies have developed detailed models and examined the suitability of various adsorbent/adsorbate pairs for solar cooling applications [26]. Differential heats of adsorption for some adsorbent/adsorbate pairs are given at Table 2.1[13].

Table(2.1): Differential heats of adsorption for some adsorbent/adsorbate pairs.

| Adsorbent | Adsorbate | Heat of adsorption (kJ/kg) | Density of the adsorbate (kg/m³) | Application area |
|-----------------------------------|--|---|--|---|
| Activated alumina | H ₂ O H ₂ O | 2800 3000 | 1000 | Used mostly for desiccant cooling Water is perfect, except for very low operating pressure |
| Zeolite (various grades) | H ₂ O NH ₃ CO ₂ CH ₃ OH | 3300-4200 4000-6000 800-1000 2300-2600 | 681 - 791 | Natural zeolites have lower values than synthetic zeolites |
| Silica gel | Methyl alcohol | 1000-1500 | 703 | Not suitable above 200°C |
| Charcoal(activated carbon) | C ₂ H ₄ NH ₃ H ₂ O CH ₃ OH C ₂ H ₅ OH | 1000-1200 2000-2700 2300-2600 1800-2000 1200-1400 | 789 | Reacts at 100°C. Ammonia and methanol are not compatible with copper at high temperature |
| Calcium chloride | CH ₃ OH | | | Used for cooling |
| Metal hydrides | Hydrogen | | | For air conditioning |
| Complex compounds | Salt and ammonia or water | | | Refrigeration |

The Dubinin–Astakhov (D–A) equation can also be employed to evaluate the desorption/adsorption capacity of the activated carbon, this equation can be written in the form [27]:

$$x = x_0 \exp[-k (T/T_s - 1)^n] \quad (2.2)$$

where x_0 , k , and n are coefficients specific for different activated carbons and refrigerants, T is adsorption temperature (K), T_s is the saturated temperature of refrigerant (K), and x is the adsorption quantity of refrigerant in the activated carbon (kg/kg).

Adsorption properties of activated carbon–methanol were tested [27], and the coefficients of D–A equations are: $x_0 = 0.45$; $k = 13.38$; $n = 1.5$

The adsorption properties of activated carbon–methanol were calculated by Eq. (2.2) at different evaporation temperatures, ranging from -20 to 35 °C, while the adsorption properties of activated carbon–ammonia were $x_0 = 0.29$; $K = 3.57$; $n = 1.38$ [27].

The cooling quantity is the product of latent heat and the adsorption quantity. The values of latent heat for ammonia and methanol are similar. For example, at the evaporating temperature of -30 °C, the latent heat of ammonia is 1365 kJ/(kg °C), which is only 5% larger than the value of methanol that is 1299.1 kJ/(kg °C). The adsorption quantity of activated carbon–methanol is 59% larger than that of activated carbon–ammonia, which means that the adsorption performance of activated carbon–methanol is better than that of activated carbon–ammonia [27].

The temperature lift capabilities of adsorbent/adsorbate pairs [25], which are adsorption– evaporation and generation–condensation temperatures, have been used as the basis for their selection. Meunier,[28] comparing activated carbon/methanol (AC 35/CH₃OH) and zeolite 13X/water (NaX/H₂O) using their isosters and typical refrigeration cycles (see Fig. 2.1), reports that the AC- 35/CH₃OH adsorption evaporation temperature lift has to be limited to 40 °C and low generating temperatures (<150 °C), whereas for NaX/H₂O the corresponding temperature lift may be up to 70 °C, or even more, with very high generating temperatures (250–300 °C).

Activated carbon/ methanol are limited to a maximum generating temperature of 150 °C due to methanol instability at higher temperatures. This feature of the pair makes it possible for low temperature heat sources to be used in the operation of its refrigeration cycle. Fig.2.2 [29] shows the results of another study, based on adsorbent/adsorbate pair thermodynamic performances, for selection of two particular combinations. It is seen that for condenser temperature $T_c = 40^\circ\text{C}$, evaporator temperature $T_e = 0^\circ\text{C}$, adsorption temperatures $T_a = 25$ and 35°C and a maximum generating temperature of 100 °C, the activated carbon/methanol pair gave a COP in the range 0.4–0.5 against 0.3 for zeolite/water.

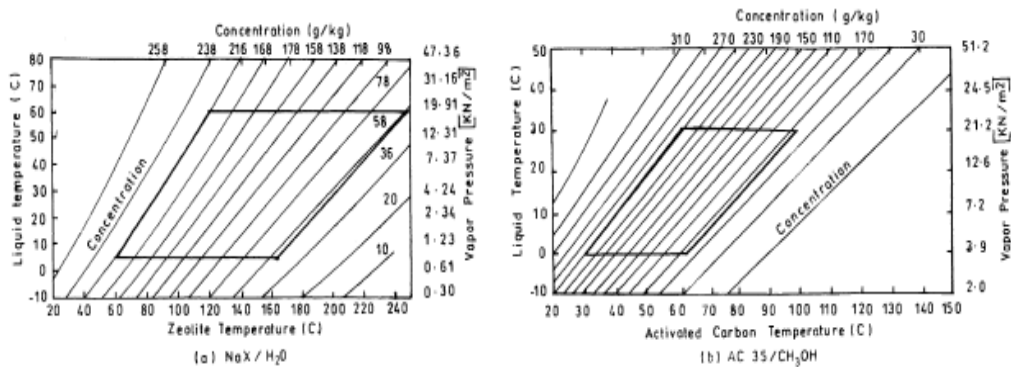


Figure (2.1): Typical set of isosters for different absorbent/adsorbate pairs and their refrigeration cycle[29].

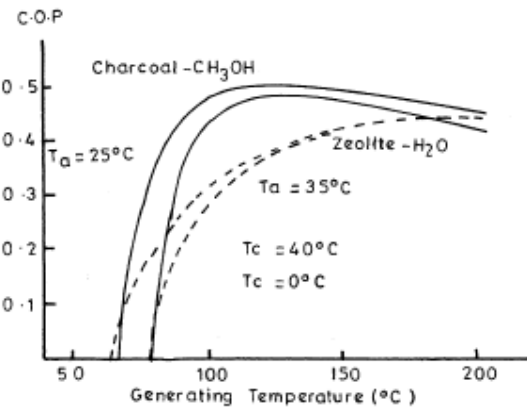


Figure (2.2): Comparison between zeolite–water and charcoal–methanol adsorption system[30].

There are other reasons that make the activated carbon/methanol pair more attractive for use in solar cooling systems. Consolidated activated carbon bed is an effective way to improve the heat transfer performance of granular activated carbon. Activated carbon grains are consolidated by mixing and compressing them with a binder. The thermal conductivity of granular and consolidated activated carbons was measured according to [26], by a transient hot wire method, which had an estimated maximum error of $\pm 8\%$. The density of two kinds of adsorbents was also measured, and results are shown in Table 2.2. When compared to granular carbon, the density of consolidated activated carbon has been improved by 30%, and the thermal conductivity has been 172% higher, [26].

Table (2.2) Parameters of activated carbon[26]

| Physical properties | Granular activated carbon | Consolidated activated carbon |
|------------------------------|--|--|
| Density | 460 kg m ⁻³ | 600kg m ⁻³ |
| Average thermal conductivity | 0.11 W m ⁻¹ K ⁻¹ | 0.30 W m ⁻¹ K ⁻¹ |
| Specific heat capacity | 0.93 kJ kg ⁻¹ K ⁻¹ | 0.93 kJ kg ⁻¹ K ⁻¹ |

After the above arguments and considering the cooling adsorption system purpose, which is ice production, the activated carbon-methanol pair seems to be very adequate. Methanol is a good working fluid because:

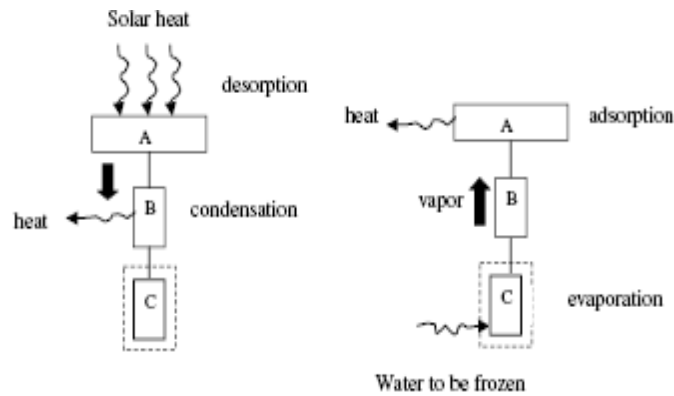
- it can evaporate at a temperature largely below 0 °C (its melting point is -94 °C);
- its enthalpy of vaporization is high (≈ 1200 kJ/kg at -5 °C);
- its molecule is so small (4 Å), it can be easily adsorbed in microspores with a diameter smaller than 20 Å.

- its normal boiling point (65 °C) is much higher than room temperature.
- its working pressure is always lower than atmospheric. This is a safety factor because any abnormal behavior of the machine can be detected before methanol leaks from the system.

Activated carbon has a significant volume of microspores of convenient size for adsorption. The void space in the AC-35 carbon adsorbent bed corresponds to 78% of its total volume, and the microspores volume is about 0.4L/kg[21]. Activated carbon present some additional characteristics such as wide concentration change in a small temperature range; reversibility of adsorption process for many cycles, and low cost.

2.5 Operation and Analysis of the Adsorption Cycle

The operation principle of the solid adsorption refrigeration system utilizing solar heat is shown in Fig. 2.3[18]. The system is composed of a container of adsorbents, which serves as a solar collector, a condenser and an evaporator which acts as a refrigerator. A combination of adsorbent and adsorbate is confined in a closed system where no carrier gas exist. The collector is supplied with activated carbon (A.C) which is adsorbed with methanol. During the day-time the activated carbon along with the methanol is heated in the collector. Methanol evaporates from the activated carbon and then is cooled by the condenser and stored in the evaporator.

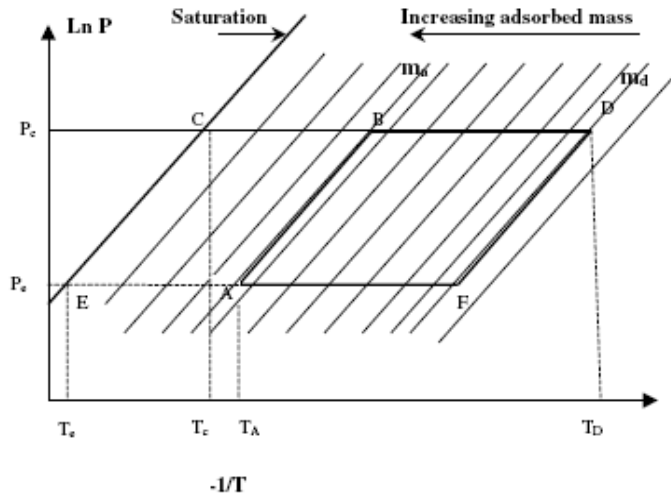


(a) Daytime (heat/desorption) (b) Night-time (evaporation-adsorption)

Figure (2.3): Operation principle of solid adsorption refrigeration system utilizing solar heat A: Sorption bed (solar collector); B: condenser; C: evaporator.

During the night-time, the collector is cooled by ambient air and the temperature of the activated carbon reaches a minimum. In this period, methanol begins to evaporate by absorbing heat from the water to be cooled and is adsorbed by the activated carbon. As the evaporation of the methanol continues, the water temperature decreases until it reaches if possible 0°C , where ice starts to be formed. The principle of the solid-adsorption cooler is explained using a Clapeyron diagram ($\ln P$ versus $-1/T$). Fig.2.4 shows the idealized process undergone by A.C+ methanol in achieving the refrigeration effect. The cycle begins at a point A where the adsorbent is at a low temperature T_A and at low pressure P_e (evaporator pressure). During the daylight, AB represents the heating of A.C along with methanol. The progressive heating of the adsorbent from B to D causes some adsorbate to be desorbed and its vapor to be condensed at the condenser pressure P_c . When the adsorbent reaches its maximum temperature T_D , desorption ceases. Then the liquid methanol is transferred into the evaporator. During night, the decrease in temperature from D to F

induces the decrease in pressure from P_c to P_e . Then the adsorption and evaporation occur while the adsorbent is cooled from F to A . During this cooling period heat is withdrawn both to decrease the temperature of the adsorbent and to withdraw adsorption heat [18].



Figure(2.4): Clapeyron diagram (ln P versus $-1/T$) of ideal adsorption cycle.[18]

From the Clapeyron diagram, the total energy gained by the system during the heating period Q_T will be the sum of the energy Q_{AB} used to raise the temperature of the A.C+ methanol from point A to B and the energy Q_{BD} used for progressive heating of the A.C to point D and desorption of methanol:

$$Q_T = Q_{AB} + Q_{BD} \quad (2.3) \quad Q_{AB} = (m_{A.C} C_{p_{A.C}} +$$

$$C_{p_m} m_{mA})(T_B - T_A) \quad (2.4)$$

$$Q_{BD} = [m_{A.C} C_{p_{A.C}} + C_{p_m} \{(m_{mA} + m_{mD}) / 2\}](T_D - T_B) + (m_{mA} - m_{mD}) H \quad (2.5)$$

Where ; $m_{A.C}$: mass of activated carbon (kg) , $C_{p_{A.C}}$: specific heat of A.C (kJ/kgK)

m_m , C_{p_m} : mass and specific heat of methanol respectively .

H: heat of desorption, kJ/kg.

The gross heat released during the cooling period Q_{e1} will be the energy of vaporization of methanol.

$$Q_{e1} = (m_{mA} - m_{mD}) L \quad (2.6)$$

Where; L is the Latent heat of evaporation of methanol, kJ/kg.

But the net energy actually used to cool water Q_e will be

$$Q_e = Q_{e1} - Q_{e2} \quad (2.7)$$

where Q_{e2} is the energy necessary for cooling the liquid adsorbate from the temperature at which it is condensed to the temperature at which it evaporates.

$$Q_{e2} = (m_{mA} - m_{mD}) C_{p_m} (T_c - T_e) \quad (2.8)$$

If we obtained ice :

Q_{ice} is the energy required to cool water from T_A to 0°C and to produce ice

$$Q_{ice} = M_{ice} (L_{ice} + C_{p_{water}}(T_A - 0)) \quad (2.9)$$

where M_{ice} , and L_{ice} are the mass and latent heat of fusion of ice respectively, [18].

2.6 Coefficient of performance (COP)

The ideal cycle for an adsorption cooling system corresponds to a hypothetical quadrithermal machine. This device consists of two coupled machines operating at two temperature levels without mechanical energy conversion. The Carnot's COP of a quadrithermal machine can be given by:

COP = desired output / required input

$$= Q_e / Q_{gen} \quad (2.10)$$

The maximum COP of an adsorption refrigeration system is determined by assuming that the entire cycle is totally reversible. The refrigeration system would be reversible if the heat from the source (Q_{reg}) were transferred to a Carnot heat engine, and the work output of this heat engine ($W = \eta_{th} Q_{gen}$) is supplied to a Carnot refrigerator to remove heat from the refrigerated space.

Note that $Q_e = W \cdot COP_{R,C} = \eta_{th,C} \cdot Q_{gen} \cdot COP_{R,C}$. Then the overall COP of an adsorption refrigeration system under reversible conditions becomes:

$$COP_{P,rev} = Q_e / Q_{gen} = \eta_{th,c} COP_{R,C} = \left(1 - \frac{T_{con}}{T_{reg}}\right) \left(\frac{T_{ev}}{T_0 - T_{ev}}\right) \quad (2.11)$$

where T_{ev} , T_{con} and T_{reg} are the evaporation, condensation and regeneration temperatures, respectively. T_0 is a reference temperature, above the ambient temperature, considered to be the highest adsorption temperature possible [4,21].

A thermodynamic analysis, given by Leite [22], demonstrates that Carnot's COP can be approximately written as:

$$COP \approx T_{con} / T_{reg} \quad (2.12)$$

Solar COP (COP_{Solar}) is one of the parameters currently used to evaluate the performance of solar ice makers, and defined as the ratio of the total heat extracted by evaporation of the desorbed mass of methanol (kJ) to the total incident global irradiance $\int i(t)dt$ from sunrise to sunset :

$$\text{COP}_{\text{solar}} = (Q_{\text{ref}} - Q_{\text{cc}}) / \int i_{(t)} dt \quad (2.13)$$

Where; $i(t)$: intensity of solar radiation W/m^2

Q_{ref} : refrigeration effect

Q_{cc} : the energy used to cool down the refrigerant liquid from condensing temperature T_c to evaporation temperature T_e .

As it can be deduced from the analysis of the above equation, the $\text{COP}_{\text{solar}}$ depends on both the meteorological conditions and the efficiency of each main component of the system i.e. the solar collector, the condenser and the evaporator.

As the desorbed mass m_{des} is the difference between the concentration of adsorbate in the adsorbent at the beginning and at the end of the desorption phase: $m_{\text{des}} = x_{\text{conc}} - x_{\text{dil}}$.

With a sufficient insolation, the concentration x_{dil} will be in proportion lower if the adsorbent heating and the vapor condensation simultaneously occur efficiently. On the other hand, x_{conc} depends on the initial concentration of the methanol in the adsorbent which, with a favorable ambient temperature, will be in proportion higher if the adsorbent cooling and the liquid evaporation, during the previous cycle, simultaneously occurred efficiently. Then the $\text{COP}_{\text{solar}}$ appears to be an important parameter which has to be taken into account, when comparing different adsorptive solar refrigeration systems. Up to now, the $\text{COP}_{\text{solar}}$ of all experimented adsorption solar refrigerator systems rarely exceeded 0.2, but it is of little importance since solar energy is free [30].

2.7 The Effects of Collector and Environment Parameters on the Performance of a Solar Powered Adsorption Refrigerator

The characteristics of solar cooler are affected by many parameters. Generally speaking, we can divide these parameters into two types. One type is the parametric parameters, such as dimensions, material and characteristics of collector, which decides the physical property of collector. Another type of parameters is environmental parameters, such as radiation intensity, ambient temperature and wind speed, which affect the running quality of system performance.

2.7.1. Parametric Effects

As mentioned above, the characteristics of solar refrigerator are mainly decided by adsorbent bed (collector), so the property of the each collector part determines the behavior of the solar refrigerator in practical application. The solar collector design parameters of interest are the collector plate material and emissivity, the size of housing adsorbent, fins for heat transfer, material, number of glazing, the thermal conductivity, packing density of the adsorbent granules. The performance of solar refrigerator is mainly decided by the total condensed refrigerant, the cooled water, the produced ice mass if possible as well as the useful coefficient of performance (COP). The latter is defined as the total useful cooling divided by the total incident radiation. In the processes of analyzing parametric effects on the solar refrigerator, the environmental conditions assumed remain constant [31].

a- Effect of Heat transfer Fins

Because the thermal conductivity of the adsorbent is low, using fins to improve heat transfer is very important inside the collector adsorbent.

Theoretically speaking, increasing the number of fins will improve heat transfer, but it is obvious that the presence of these fins also has negative effects, because the sensible heat of the fins will be thermodynamically useless. So there is an optimization value about the fin numbers.

b- Effects of the Contact Thermal Resistance

The contact thermal resistance is a key parameter which affects the characteristics of solar refrigerator. The adsorbent is installed usually inside definite shape of metal, the metal accepts the solar radiation energy to heat adsorbent to release refrigerant. Due to the existence of thermal contact resistance between adsorbent and metal surface, this will lead a big temperature gradient and reduce the heat transfer effect from metal surface to adsorbent. Usually, the bigger the contact thermal resistance between metal surface and adsorbent, the inferior is the characteristics of solar refrigerator. Therefore, in order to reduce this contact thermal resistance, a well suited shape of the solid bed with a smooth surface should be taken into consideration carefully.

c- Effects of Adsorbent Thermal Conductivity

Nearly all suitable adsorbents are porous materials that can adsorb a large amount of refrigerant, while the thermal conductivity of the adsorbent is very low, this makes limiting factor to performance of solar cooler. For

flat plate solar refrigerator, activated carbon is usually chosen as adsorbent, and the thermal conductivity values of adsorbent are usually less than $1.0 \text{ W m}^{-1} \text{ K}^{-1}$.

So it is very useful to pay attention to improve the heat transfer in adsorbent bed. In order to improve the adsorbent conductivity, many methods have been adopted [32].

For example, metallic spheres or strips can be incorporated into the bed, or good thermal conductivity material or metallic foam can be used to the adsorbent, and consolidated samples (like bricks) is used. But so far, there are no practical application used in solar refrigerator.

The main reason is the energy density accepted by solar refrigerator is very low, this limits the application of the above mentioned methods.

e- Effect of Number of Glazing and Selective Coating

Besides the above mentioned parameters, there are many other parameters that affect the performance of solar refrigerator and ice mass, such as numbers of glass cover, coating material etc. Among these parameters, two parameters are most important; they are the number of glazing and the selective coating material. Usually, the increase of glazing number is limited by collector structure and dimension; in common practice, not more than two or three glazing. In summary, many parameters affect the characteristics of solar refrigerator. From the view of optimization of design, we should choose the best parameter to build the collector under the suitable cost.

2.7.2 Environmental Effects

When a collector has been built and connected with condenser, charging valve and evaporator, the solar refrigerator device is fabricated. After considering the parametric effects on design of collector, the solar refrigerator properties of COP and water will be cooled are mainly decided by environmental parameters, such as condensing temperature, evaporating temperature and solar radiation intensity. So discussing environmental parameter variation effects on the characteristics of solar refrigerator must be studied.

a- Effects of the Solar Radiation Intensity

Solar refrigerator is powered by solar radiation energy, so the solar radiation intensity decides the water temperature as well as the COP value.

The COP of solar refrigerator increases with the increase of solar radiation intensity first. The COP will reach the maximum value under the region at about 12 MJm^{-2} solar radiation intensity as shown in Fig.2.5[31].

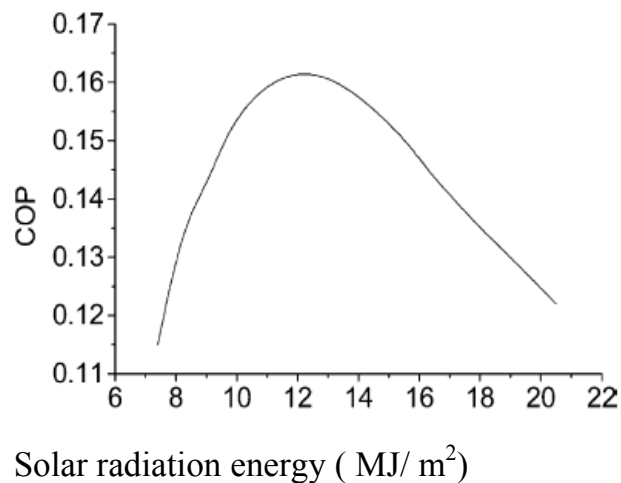


Figure (2.5): Variation of COP with solar radiation energy.

However, with the increase of solar intensity, the value of COP does not increase synchronously, conversely the COP of solar system decreases by some degree. This reason can be explained as follows: solar radiation intensity is used for both adsorbent sensible heat and metallic sensible heat. When solar radiation intensity increases, the adsorbent maximum desorbing temperature T_{g2} increases too. There is an optimum desorbing temperature value T_{g2opt} . When the desorbing temperature T_{g2} is greater than the temperature of T_{g2opt} the ratio of desorbed refrigerant mass will become weaker. This means that most of solar radiation intensity is used for metallic sensible heat; this will cause the COP of solar cooler decrease. The minimum value of solar intensity depends on the variations of the atmospheric temperature during the day and characteristics of solar cooler device, this minimum value is about 11 MJ/ m^2 according to Ref. [33].

The **COP** of solar adsorption refrigerator increases as the solar radiation increased as shown at Fig. 2.6 according to [34].

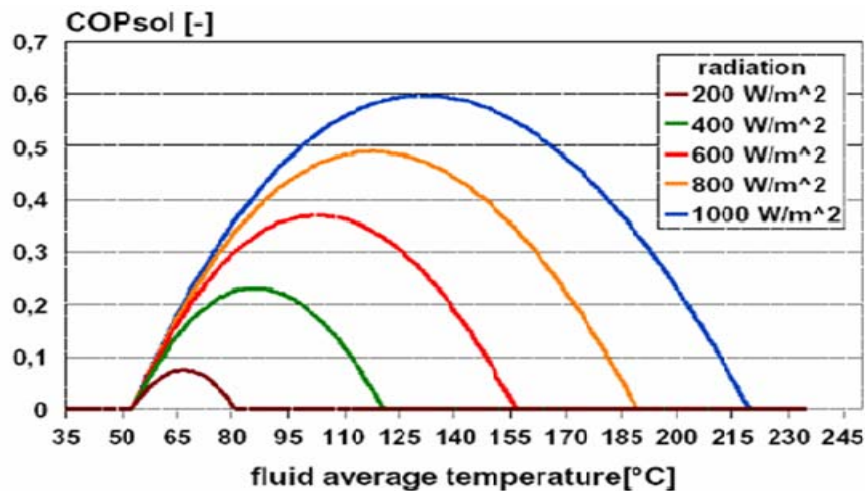


Figure (2.6): COP_{solar} for different collector radiation values

b- Effects of the Condensing Temperature

The performance of solar refrigerator is affected obviously by condensing temperature. In order to keep condensing temperature in a lower level, it is an effective way that adopting water to cool condenser instead of natural convection cooling. With the water cooling method, solar refrigerator can be worked in a suitable environmental condition, and the performance of solar system can be improved efficiently.

c- Effects of the Evaporating Temperature

The use of refrigerant other than water makes it possible that evaporating temperature is below 0°C . Usually, for solar refrigerator, the lower the evaporating temperature is, the poor the performance is. For solar refrigerator, because the energy of solar radiation is limited by weather condition, the evaporating temperature is in the range of $-10^{\circ}\text{C} \leq T_e \leq 0^{\circ}\text{C}$. If evaporating temperature is above 0°C , zeolite–water working pair can be used, this will cause a good refrigeration effect because the latent heat of water is larger than that of methanol.

From the previous discussion, significant improvements in the solar refrigerator performance can be obtained through a careful choice of a number of collector parameters. Generally speaking, enhancing the heat transfer between metallic plate and adsorbent, increasing the thermal conductivity of adsorbent are two obvious methods for improving performance of solar refrigerator. Increasing packing density of adsorbent, adopting double glass covers, using selective coating material as well as using heat transfer fins, all these ways are beneficial to increase properties

of solar refrigerator. Simultaneously, choosing a suitable environmental condition may improve the performance of solar refrigerator.

So long as we choose the optimization parameters on design of solar system, the practical use of solar refrigerator and air conditioning will become more reasonable.

2.8 Solar Adsorption Cooling Technologies

In order to improve the performance and the efficiency of the solar adsorbing cooling cycle, different cycles have been studied in addition to the basic cycle, such as continuous heat recovery cycle, mass recovery cycle, thermal wave cycle, convective thermal wave cycle, cascade multi effect cycle, hybrid heating and cooling cycle etc.

2.8.1 Heat Recovery Adsorption Refrigeration Cycle

As we mentioned already, a basic adsorption cycle consists of , four thermodynamic steps, which can be well represented with the aid of the Clapeyron diagram, as shown in Fig.2.7. The idealized cycle begins at point A where the adsorbent is at low temperature T_A and at low-pressure P_E (evaporating pressure). AB represents the heating of adsorbent, along with adsorbate. The collector is connected with the condenser and the progressive heating of the adsorbent from B to D causes some adsorbate to be desorbed and its vapor to be condensed (point C). When the adsorbent reaches its maximum temperature T_D ; desorption ceases. Then the liquid adsorbate is transferred into the evaporator from C to E and the collector is cooled. The decrease in temperature D to F induces the decrease in pressure from P_C to P_E , and the adsorption and evaporation occur while the

adsorbent is cooled from F to A. During this cooling period heat is withdrawn to decrease the temperature of the adsorbent.

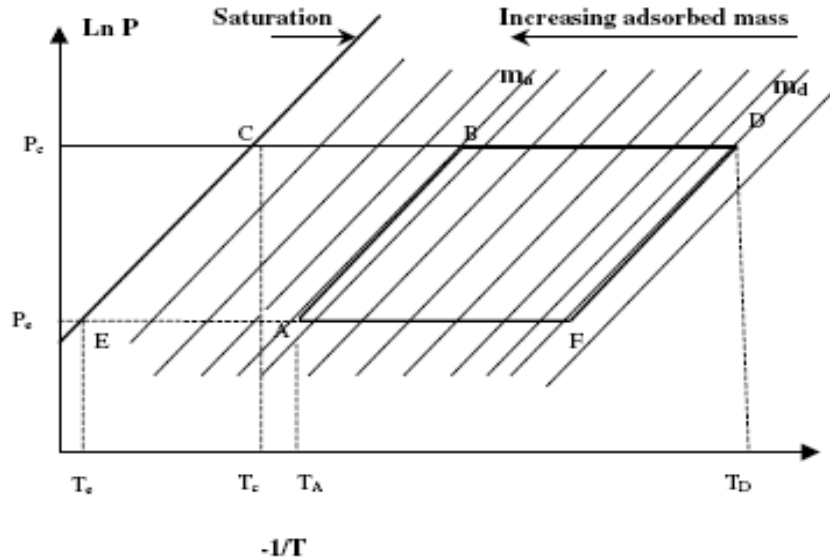


Figure (2.7): Clapeyron diagram ($\ln P$ vs. $-1/T$) of ideal adsorption cycle

The semi-continuous heat recovery cycle is usually operated with two adsorption beds. The adsorber to be cooled will transfer its heat to the adsorber to be heated, which includes sensible heat as well as heat of adsorption. This heat recovery process will lead to a higher system COP. Multi-beds could be also adopted to get more heat recovery and thereby to attain higher COP, but the operation of a practical system will be complicated. A quasi-continuous adsorption refrigeration system with heat recovery was investigated by Wang et al.[35,36] and the flow path is shown in Fig.2.8. While adsorber 1 is cooled and connected to the evaporator to realize adsorption refrigeration in evaporator, the adsorber 2 connected to the condenser is heated to obtain heating-desorption-condensation. The condensed refrigerant liquid flows into evaporator via a flow control valve. The operation phase can be changed, and the go-

between will be a short time heat recovery process. Two pumps are used to drive the thermal fluid in the circuit between two adsorbers (the connection to the heater and cooler are blocked during this process.)

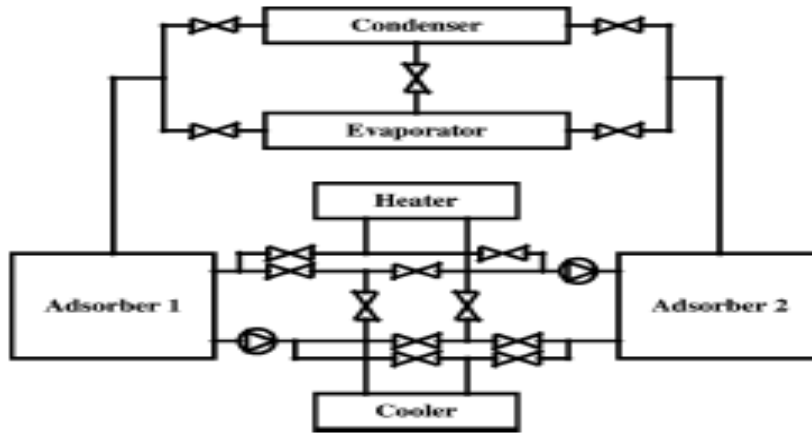


Figure (2.8): Schematics of heat recovery two-bed adsorption refrigeration system

2.8.2 Mass Recovery Adsorption Refrigeration Cycle

Apart from the above discussed heat recovery operation, it had been proved that mass recovery is also very effective for heat recovery adsorption heat pump operation. In this process, at the end of each half cycle, one adsorber is cold and the other one is hot. Meanwhile, the former one which is at low pressure (P_C) must be pressurized up to the condenser pressure, and similarly, the other one which is at high pressure must be depressurized down to the evaporator pressure. With just one tube between the adsorbers and a vapor valve, part of this pressurization–depressurization can be achieved by transferring vapor from the latter adsorber to the former one. This process can also be called as an ‘internal vapor recovery process’, and is reported to enhance the cooling power of the unit without reducing the COP by more than 10%. The above explained

process involves only mass transfer and hence the process is rapid. To obtain a ‘double effect’, mass recovery could be initiated followed by heat recovery. An ideal heat and mass recovery cycle is shown in Fig 2.9, in which the heat recovery state for a two bed system is shown by the state points $e - e'$.

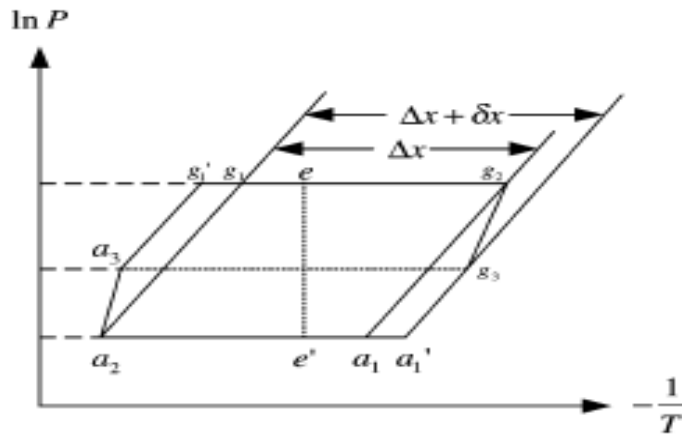


Figure (2.9): Diagram of heat and mass recovery cycle.

The mass recovery cycle ($a_2 - a_3 - g'_1 - g_2 - g_3 - a'_1 - a_1 - a_2$) is an extended form of a two bed-basic cycle or two bed heat recovery cycle ($a_2 - g_1 - g_2 - a_1 - a_2$), and the cycled mass is increased from Δx to $\Delta x + dx$, which causes the refrigeration effect to increase. The principle of these cycles—can be described using Fig.2.9[37]. The very first part of each half-cycle is the mass recovery process (path $g_2 - g_3$ and $a_2 - a_3$). Then the heat recovery process proceeds: heat is transferred from the hot adsorber to the cold one (path $g_3 - e'$). As a consequence, the hot adsorber is first depressurized (path $g_3 - a'_1$), it then adsorbs vapor from the evaporator (path $a' - e'$). Meanwhile, the cold adsorber is first pressurized (path $a_3 - g'_1$), and then vapor that is desorbed—passes into the condenser (path $g'_1 - e$). Theoretically, the heat recovery process develops until the adsorbents reach the-same temperature. Actually, there still remains a temperature difference

between the adsorbers at the end of this period. Then, for closing each half cycle, the adsorbers are, respectively, connected to the heat source and heat sink (path $e - g_2$ and $e' - a_2$). The second half-cycle is performed the same way except that the adsorbers now exchange their roles. Due to this process, about 35% of the total energy transmitted to each adsorber can be internally recovered, including part of the latent heat of sorption.

2.8.3 Thermal Wave Cycle

To further improve the heat regenerative ratio, Shelton [38] had proposed an attractive cycle called ‘thermal wave cycle’. In this process, it is assumed that a large temperature gradient exists along an adsorption bed.

The thermal wave cycle was proposed for the continuous system. Instead of only one adsorbent bed in the basic adsorption system, it consists of 2 adsorbent beds and 2 heat exchangers, which are connected in a series. Between this equipment, a working fluid (e.g. high temperature oil), flows in the closed cycle at a low flow rate. It is assumed that a large temperature gradient persists along the adsorption beds.

Schematic of the system is shown in Figure 2.10[1]. The operation of the cycle is divided into 2 phases. Sorption process occurs in one bed and desorption process occurs in another bed simultaneously [39,40]. These sorption and desorption processes swaps between the beds when the next operating phase occurs. In Phase 1, external heat is applied to heat exchanger 1. Bed 2 adsorbs the refrigerant from the evaporator, thereby releasing heat from the adsorbent to the oil. The oil is then pumped into heat exchanger 1, absorbing more heat and continues to bed 1. Bed 1 is heated up by the oil; the refrigerant is desorbed and flows to the condenser. The process continues until bed 2 reaches saturation.

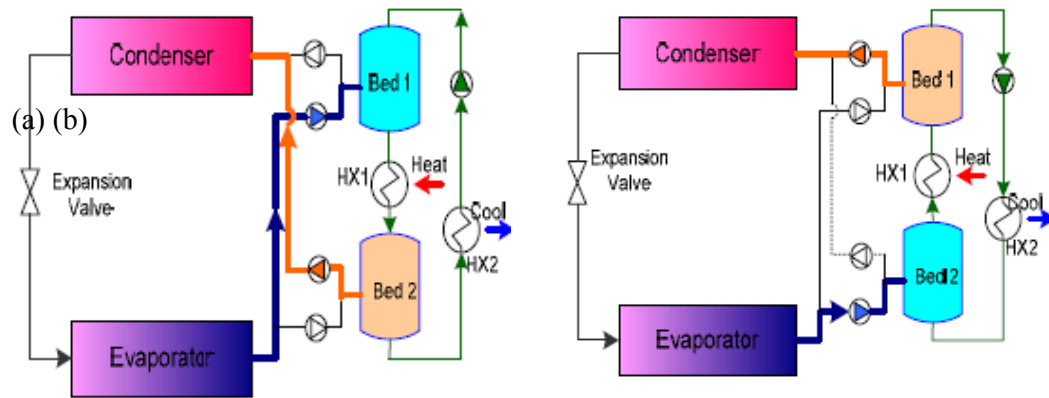


Figure (2.10): Thermal Wave Cycle, (a) Phase 1 and (b) Phase 2[1]

In Phase 2 the pumps and the processes in both beds are reversed. Bed 1 adsorbs the refrigerant from the evaporator and releases heat to the oil. The oil then absorbs heat from bed 1 and from heat exchanger 1. The heat is released to bed 2; the refrigerant is then desorbed to the condenser. Adsorption and desorption in both adsorbent beds are repeated, indicating that the thermal wave cycle can run continuously [1].

Though the procedure is simple, significant heat recovery can be achieved. Further, the system would achieve much better performance due to the combination of the special nature of the internal bed heat exchangers and the low flow rate.

Although many researchers have studied the cycle, up to now, there is no report of a successful prototype adopting thermal wave cycle. Also, some experimental reports had shown that the performance of the thermal wave cycle is not very good. The efficiency of the thermal wave regenerative system depends on a relatively large number of parameters: for example, rates of various heat transfer processes, the flow rate of the circulating fluid, the cycle time, the adsorber configuration, etc.

2.8.4 Multi-Stage and Cascading Cycle

The adsorption cycles discussed in previous sections are applicable only to a single stage cycle. The single stage cycle systems have certain limitations, that is, they cannot effectively utilize high temperature heat source, as well as do not perform well at very low temperatures. Hence, to improve the system performance under such situations, adsorptive processes may be adapted for advanced cycles such as, multi-stage and cascading cycle. The basic idea of a multi-stage cycle is to perform the desorption–condensation processes and evaporation– adsorption processes at different temperature/pressure levels by using the ‘same working pair’. The internal re-use of heat of condensation or adsorption can increase the system performance significantly. Another practical cycle that can make good use of high temperature heat source is the ‘cascading cycle’, which operates with ‘different working pairs’ (either liquid/liquid or solid/liquid), such as zeolite– water/activated carbon–methanol, or zeolite–water/silica gel–water, etc. These cascading cycles are applied to situations especially, when there exists a large temperature difference between the heat source/ambient and the temperature in the evaporator/refrigeration space. For such situations, it may not be practical to use single stage cycle. Hence, one way of dealing with such situations is to perform the evaporation/refrigeration process in stages, that is, to have two or more cycles that operate in series at different temperature levels (cascading) Fig.2.11. A high temperature heat source (e.g. boiler) is used to drive the high temperature stage adsorption refrigeration cycle.

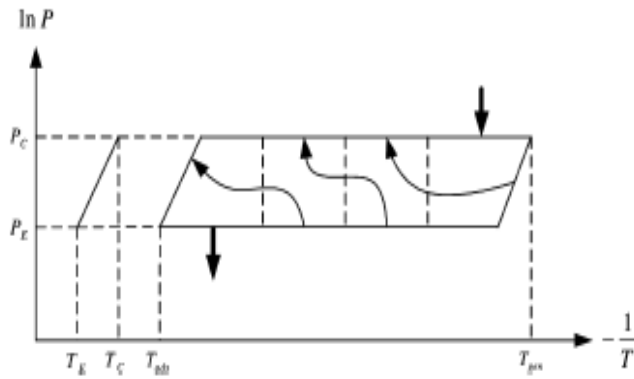


Figure (2.11): n-Adsorber cascading cycle

The low temperature stage adsorption refrigeration is driven by sensible heat and heat of adsorption obtained from high temperature stage. To minimize the contribution of sensible heat, special care has been attached to the heat management of the adsorbers; n-adsorber cycles operating with a single evaporator and a single condenser have been proposed with sequences of heat recovery between adsorbers. Such cycles offer some advantages: for example, a single condenser is used and pressure in the n-adsorber unit is not higher than that in the unit operating an intermittent cycle; moreover, adsorption heat at high temperature is used as desorption heat at low temperature. Counteracting heat transfer fluid circuits between adsorbers reduces entropy generation in comparison with what happens in intermittent cycles. The driving heat supplied to the cycle is at high temperature level (Fig.2.11) so that the entropy generation—due to the in adaptation between the temperature levels of the source and of the adsorber is much less in an n-adsorber cycle than in an intermittent cycle. The same thing happens for the rejected heat: the rejection temperature is much closer from the utility temperature with an n-adsorber cycle than with an intermittent cycle[37].

2.8.5 A combined Solar Adsorption Heating and Cooling System

In order to make a solar-powered adsorption system more efficient and useful in practice, a new hybrid system capable of both heating and cooling effects was tested by Wang et al. (2000)[41]. To ensure good heating and cooling of the adsorber, it was immersed into a water bath powered by a solar collector. It was shown that this simple design was effective but a comprehensive analysis of the system was lacking. As one would expect, the collected solar irradiance was used to heat up the water and adsorbent bed inside the water tank. Therefore, the collector area, amount of water and adsorbent must be considered simultaneously in obtaining an optimum design for such solar hybrid system. Figure (2.12) shows the schematic of the hybrid solar powered water heater and ice-maker. The system consists of the following components: an evacuated vacuum tube type solar collector, water tank, adsorbers, water storage tank, fin-type condenser/heat exchanger, an evaporator which acts as a refrigerator and several valves.

During the daytime, the solar energy gained through the collector is accumulated in the water tank and the hot water in the tank raises the temperature in the adsorbent bed. In an ideal process, the adsorbent temperature can reach a level very close to the water temperature in the tank[42].

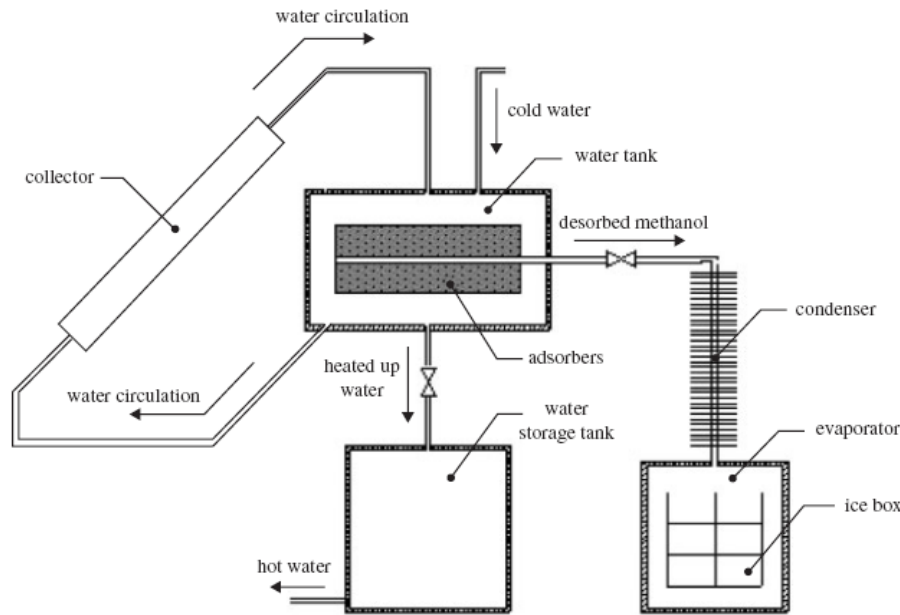


Figure (2.12): Schematic of the solar hybrid system[42]

When the temperature of adsorbent increase to temperature (T_B), desorption and evaporation of the refrigerant is initiated. With the progressive heating of the adsorbent, the refrigerant continues to desorb until the adsorbent reaches its maximum temperature (T_D). At this temperature, desorption ceases and the evaporated adsorbate is then cooled by the condenser and the liquid adsorbate finally is transferred and stored in the evaporator to complete the regeneration of the activated carbon fibre. During the night time, the hot water is drained and stored in the water storage tank temporarily or used directly for domestic purposes and the cold water is filled in the water tank. The cold water cools down the adsorber quickly, and the cooling–adsorption–evaporation process can thereby be initialized so that the sensible heat of the adsorber and heat of adsorption will preheat the cold water in the tank. This heat recovery process is important since the solar energy gained from the collector can be effectively utilized. The adsorber temperature decreases rapidly from (T_D to

T_F), lowering down the system pressure to the evaporation pressure (P_E). During this period of adsorption, the liquid refrigerant in the evaporator begins to evaporate by absorbing heat energy from water stored in the evaporator and gets absorbed by the adsorbent in adsorber. During this process, the water in the evaporator cools and ice is produced.

In the Clapeyron diagram shown in Figure 2.13, A-B-D-F-A represents an idealized combined cycle of both heating and cooling process along with heat recovery. A-B-D-F-A represents the path of activated carbon fibre and the adsorbed adsorbate while A-B-C-E-A represents path of desorbed methanol. Let the cycle begin at a point A, where the adsorbent is at a low temperature T_A and at low-pressure P_E (evaporating pressure); A-B represents the heating of adsorbent along with adsorbate with the increase in pressure. The progressive heating of the adsorbent from B to D causes some adsorbate to be desorbed and its vapor to be condensed. When the adsorbent reaches its maximum temperature T_D ; desorption ceases. Then the liquid methanol is transferred into the evaporator. Refilling the water tank with cold water, decreases the temperature of the adsorbent bed from T_D to T_F ; which induces the system pressure to decrease from P_C to P_E : As the adsorbent is continued to be cooled down from T_F to T_A both evaporation as well as adsorption of methanol is initiated.

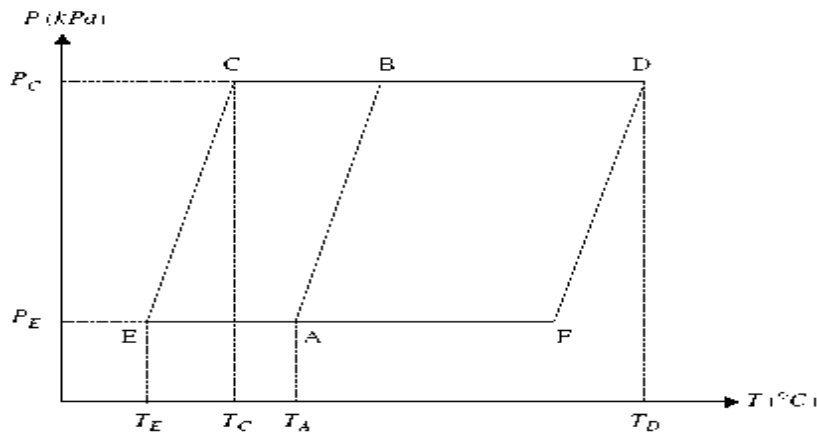


Figure (2.13): Clapeyron diagram ($\ln P$ Vs $-1/T$) of ideal adsorption cycle

During this cooling period, heat is rejected both to decrease the temperature of the adsorbent and to withdraw adsorption heat. The adsorption bed is the heart of a solid adsorption refrigeration system. Its characteristics play an important factor in the successful operation of such systems. To make sure an adsorption system is more efficient, it requires adsorbents with both good heat collecting and heat releasing. Hence, by using the above described hybrid water heating and ice-making system, it is possible to recover the heat rejected during the adsorption process and make the system be effective in two ways. But, such design has one main disadvantage; the heat transfer inside the adsorbent bed is low which leads to a decrease in the system performance. It is because the encapsulation thickness of adsorbent is so large that the temperature difference of adsorbent between surface layer and bottom of the bed becomes too high for adsorbent to either adsorb or desorb evenly. Also, the heat conduction ability of an adsorbent bed is not very good. To overcome these shortcomings of the adsorbent bed, instead of using traditionally used single bed adsorber, more adsorbents can be used to increase the heat transfer area. This adsorbent bed is generally known as ‘adsorber manifolds’ (Figure 2.14)[42].

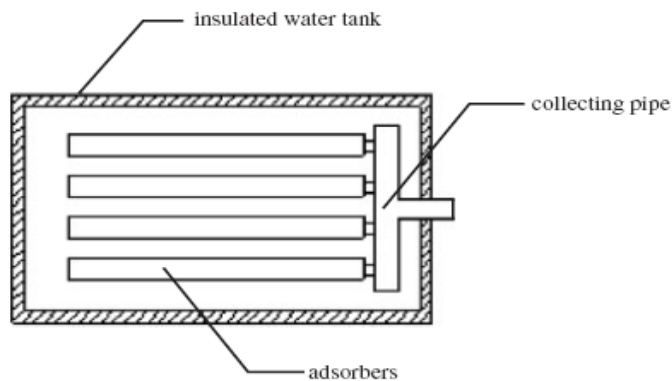


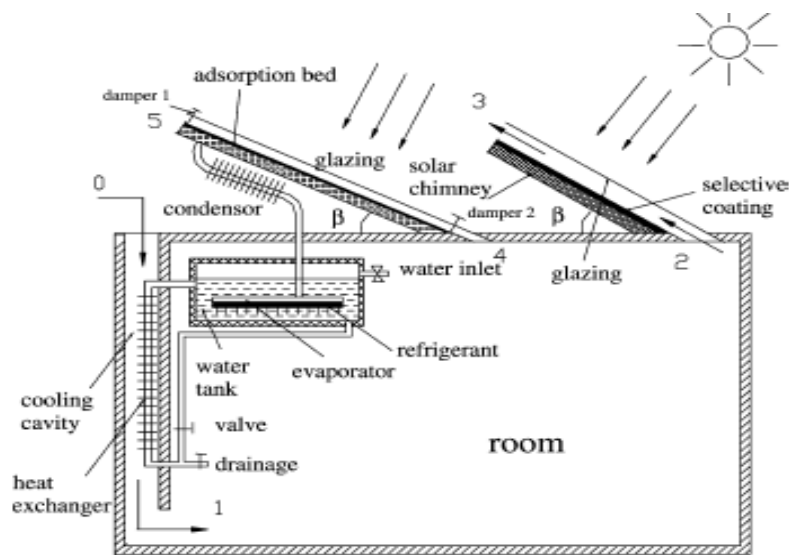
Figure (2.14): Section of the adsorbent bed

By this method, the contact area between adsorbent bed and water can be increased as well could obtain uniform heating compared to the traditional single adsorbent bed.

2.8.6 Solar House

The proposed solar house consists of two subsystems, i.e. the solar chimney and the solar adsorption cooling cavity [43]. Both subsystems contribute to inducing outdoor air into the room space. The components of a solar chimney include glazing, air channel, selective coating, and a thermal storage wall figure 2.15. It works on the principle of thermal buoyancy induced by solar heating. Similarly, the solar adsorption cooling system is configured by a flat plate adsorber, a condenser, and an evaporator, etc. The adsorber is regenerated during daytime when solar irradiation heats the adsorption bed and desorption process begins; during night time cooling effect is produced when the adsorber cools down and adsorption process is initiated. A water tank is provided to store the chilled water from the evaporator, which is circulated (thermosyphoning) through a heat exchanger in the cooling cavity. During this period, the ambient air is captured through the cavity inlet (0), gets cooled by the chilled water

through the heat exchanger, and further descends downwards into the room. The air motion is mainly due to the density difference of the air at the inlet and outlet of the system. Hence, during daytime, both solar chimney and cooling cavity induce ventilation, while at night, ventilation is induced mainly by the heat storage in solar chimney, the heat released during adsorption process, and by a chilled water circulation in the cooling cavity.



Figure(2.15): solar house with enhanced natural ventilation driven by solar chimney and adsorption cooling cavity [43]

In order to enhance the adsorption process, two dampers that enclose the space between the glass cover and the adsorption bed are released apart which facilitates the adsorption bed to be cooled more efficiently. The chimney effect can thus be realized in the air channel between the glass cover and the adsorption bed.

2.8.7 Solar-Driven Combined Ejector and Adsorption Refrigeration Systems

This system can be considered as 2 split cycles which work separately at different periods: an ejector cycle and an adsorption cycle. The system was proposed by Zhang, X. J. and Wang, R. Z. (2002b) [44].

The theoretical analysis of a solar-driven continuous combined solar adsorption – ejector refrigeration and heating system was presented by Zhang and Wang, 2002b[44]. A schematic of this system is shown in Figure 2-16. Zeolite – water were used as a working pair. The work principle of this system is explained in page (26,27). In the afternoon, when the temperature in the adsorber is high enough; the adsorber is used as a thermal collector for heating up tap water. The cooling capacity is 0.15 MJ/kg Zeolite during day-time and 0.34 MJ/kg Zeolite in the evening. This system can also heat up 290 kg of water to 45°C. A combined COP of about 0.33 was reached.

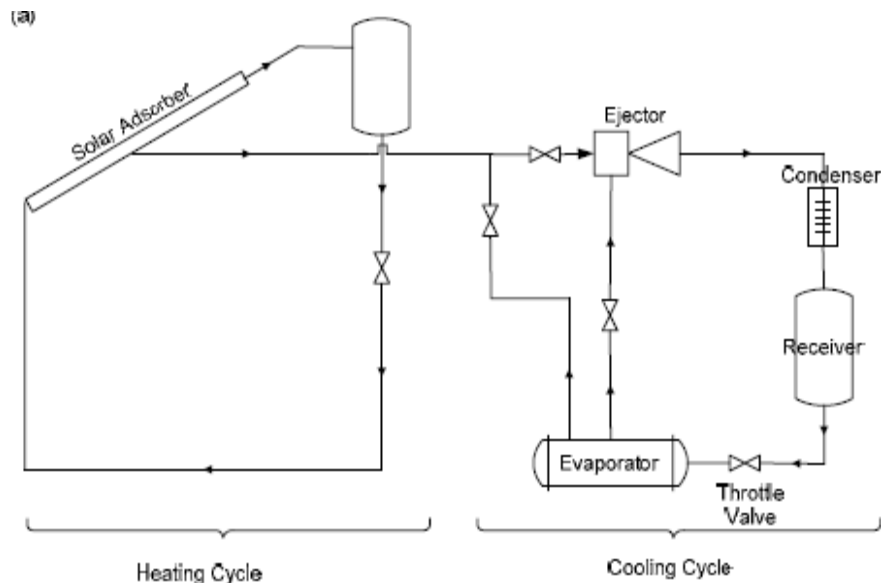


Figure (2.16): Solar Driven Ejector-Adsorption System and an Concentrating Adsorber Proposed by Zhang and Wang, 2002b [44]

Chapter Three

Potential of Solar Energy in Palestine

3.1 Solar Energy

The basic resource for all solar energy systems is the sun. Knowledge of the quantity and quality of solar energy available at a specific location is of prime importance for the design of any solar energy system. Although the solar radiation (insolation) is relatively constant outside the earth's atmosphere, local climate influences can cause wide variations in available insolation on the earth's surface from site to site. In addition, the relative motion of the sun with respect to the earth will allow surfaces with different orientations to intercept different amounts of solar energy. Figure 3.1 shows regions of high insolation where solar energy conversion systems will produce the maximum amount of energy from a specific collector field size[45].

In Palestine also we have very good potential of solar radiation and it could be used for many purposes, however, solar energy is available over the entire globe, and only the size of the solar system needs to be increased to provide the same amount of heat or electricity as in the shaded areas. It is the primary task of the solar energy system designer to determine the amount, quality and timing of the solar energy available at the site selected for installing a solar energy conversion system.

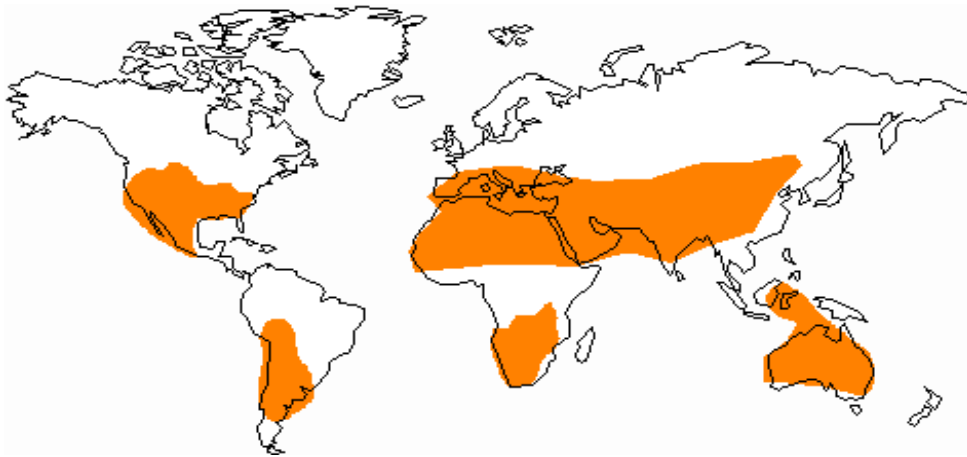


Figure (3.1): Areas of the world with high insolation

Just outside the earth's atmosphere, the sun's energy is continuously available at the rate of 1,367 Watts on every square meter facing the sun. Due to the earth's rotation, asymmetric orbit about the sun, and the contents of its atmosphere, a large fraction of this energy does not reach the ground. The effects of the atmospheric processes that modify the incoming solar energy, how it is measured, and techniques used by designers to predict the amount of solar energy available at a particular location, both instantaneously and over a long term must be discussed.

The peak rate of incident solar energy in Palestine occurs around 12:00 noon and is about 1,030 Watts per square meter[46].

3.1.1 Solar Radiation Components

Through the atmosphere the solar irradiance decreases and the spectral distribution changes. Ozone absorbs the ultraviolet radiation while water vapor, carbon dioxide and other greenhouse gases absorb some of the infrared radiation. In the visible spectrum, the shortest wavelengths (i.e. the blue light) is scattered by air molecules and dust. Therefore only part of this radiation reaches the surface, and in the form of diffuse radiation

(figure 3.2)[47]. The sum of the diffuse and direct radiation (that travels uninterrupted through the atmosphere, often called beam radiation) is referred to as the global irradiance. The direct normal irradiance is the radiation at a surface normal to the direct radiation. This component is used to define the angle of incidence, θ , as the angle between the direct normal radiation and the normal to the surface of interest.

The irradiance on a surface varies with the cosine of the incident angle:

$$E_g = E_d + E_r + E_n * \cos\theta, \quad (3-1)$$

Where, E_d is the diffuse irradiance, E_r is the ground reflected irradiance and E_n is the direct normal.

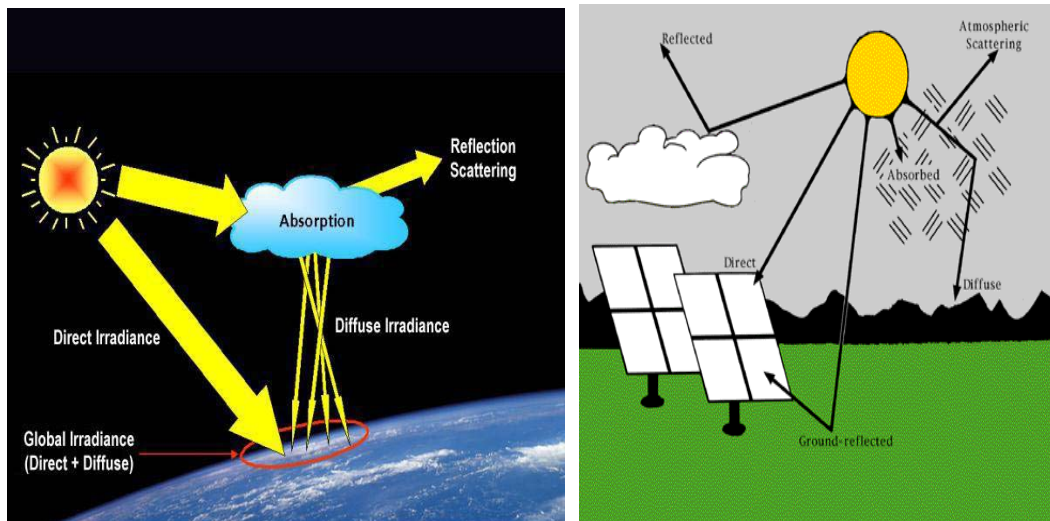


Figure (3.2): Sketches of the solar radiation through the atmosphere

3.1.2 Measurement of Solar Radiation - Pyranometer

A pyranometer is an instrument used to measure the global radiation (figure 3.3). The instrument has a hemispherical view of the surroundings. By adding a shading ring, the direct radiation is excluded by which the

pyranometer measures only the diffuse radiation. A pyranometer uses thermal sensors. One sensor is exposed to the solar radiation, while the other is shaded. The temperature difference registered by the sensors is used as a measurement of the solar radiation, [46].



Figure (3. 3): Pyranometers used for measuring the global radiation (left) and diffuse radiation (right)

3.2 Climate and Potential of Solar Radiation in Palestine

3.2.1 Climate in Palestine

As the characteristics of the cooling demand are different at various locations, depends on solar radiation , temperature level and other climate conditions therefore we need to analyze our local country climate.

Palestine is located between $34^{\circ} 20' - 35^{\circ} 30'E$ and $31^{\circ} 10' - 32^{\circ} 30'N$. It consists of two areas geographically separated from one another; the Gaza Strip is located on the western side of Palestine adjacent to the Mediterranean Sea and the West Bank which extends from the Jordan River in the east to center Palestine. Palestine's elevation ranges from 350m below sea level in the Jordan Valley, to sea level along the Gaza Strip seashore, exceeding 1000 m above sea level in some locations in the West Bank.

Climate conditions in Palestine vary widely. The coastal climate in Gaza Strip is humid and hot during summer and mild during winter. These areas have low heating loads, while cooling is required during summer. The daily average temperature and relative humidity vary in the ranges: 13.3 - 25.4 °C and 67 - 75% respectively. In the hilly areas of the West Bank, cold winter conditions and mild summer weather are prevalent. Daily average temperature and relative humidity vary in the ranges: 8 - 23 °C and 51 - 83% respectively. In some areas the temperature decline below 0°C. Hence, high heating loads are required, while little cooling is needed during summer. In Jericho and the Jordan Valley, almost no heating is needed during winter while high cooling during summer is needed[48].

3.2.2 Potential of Solar Energy in Palestine

Palestine has high solar energy potential, it has about 3000 sunshine hours per year and high annual average of solar radiation amounting to 5.4 kWh/m² – day (19.44MJ) on horizontal surface, which classified as a high solar energy potential. The lowest solar energy average is in December, it amounts to 2.63 kWh/ m² - day. The solar radiation on horizontal surface varies from 2.63 kWh/m²-day in December to 8.4 kWh/m² - day in June[46]. Table 3.1 and figure 3.4 shows the average total solar radiation per day for each month during 2006 at Jenin city as an example of West Bank region.

Table(3.1): The average total solar radiation per day for each month during 2006 at Jenin[46]

| Jenin-2006 | | |
|------------|---|------------------|
| Months | Solar Energy (Kwh/m ² - day) | Wind Speed (m/s) |
| 1 | 2.82 | 4.74 |
| 2 | 3.58 | 3.66 |
| 3 | 4.82 | 4.16 |
| 4 | 6.36 | 3.83 |
| 5 | 7.67 | 4.42 |
| 6 | 8.19 | 5.26 |
| 7 | 7.75 | 5.48 |
| 8 | 6.7 | 4.94 |
| 9 | 5.83 | 4.57 |
| 10 | 3.99 | 3.82 |
| 11 | 3.99 | 2.86 |
| 12 | 2.724 | 3.76 |

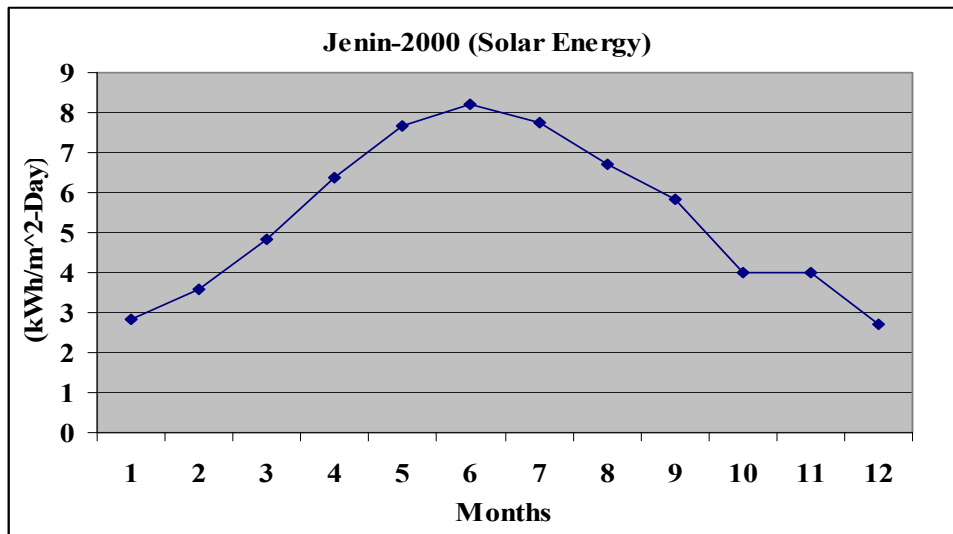


Figure (3.4): The average total solar radiation per day for each month during 2006 at Jenin[46]

These figures are encouraging to exploit the solar energy for different applications such as water heating, drying of crops, vegetables and fruits, water desalination, water pumping and electrification of remote locations isolated from the electrical networks, and we hope for cooling.

The Energy Research Centre at An-Najah National University (ERC) is carrying out, since Feb 2000, measurements on solar radiation intensity

using modern meteorological stations equipped with automatic data loggers as shown in Figure 3.5, and in the Fig 3.6 illustrate a sample of measurements in different cities in Palestine .

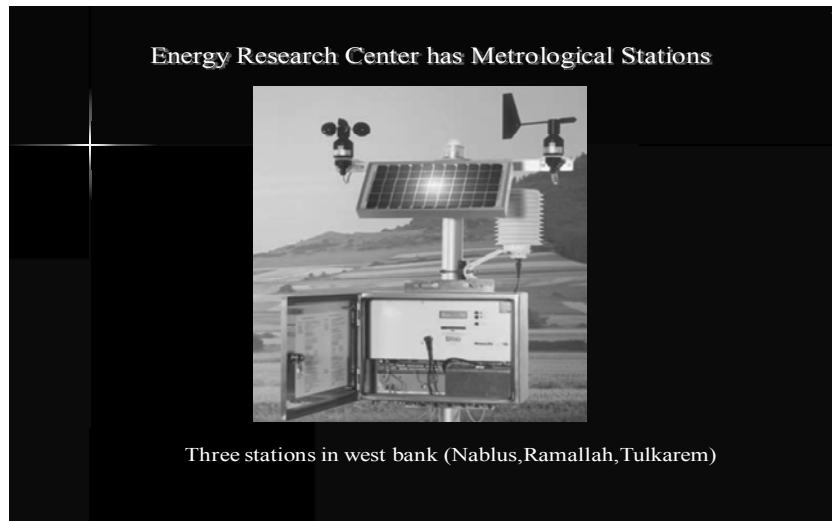


Figure (3.5): Meteorological station used by The Energy Research Centre At An-Najah National University

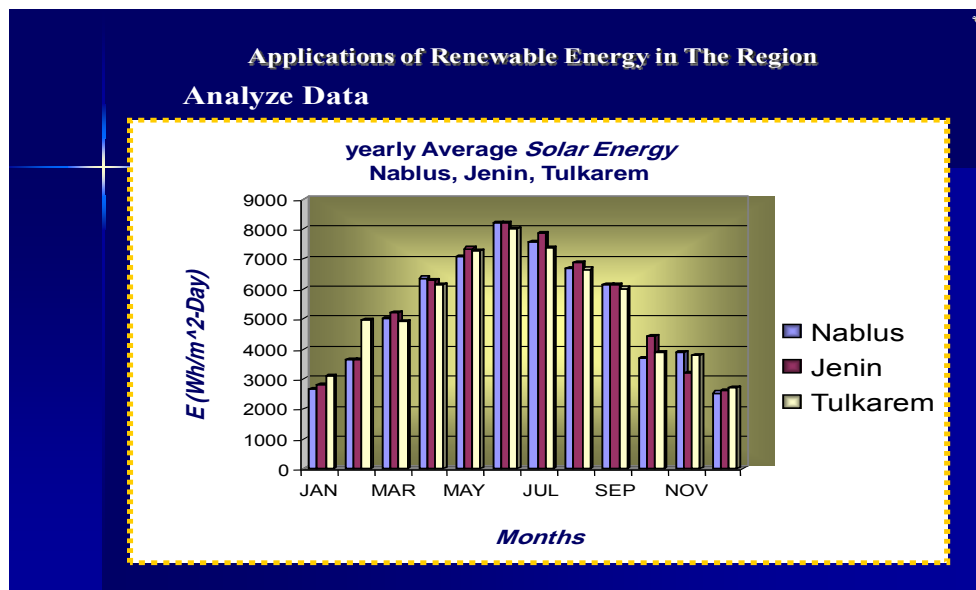


Figure (3.6): Yearly Average Solar Radiation in Different Cities in Palestine

The solar energy in Palestine has been utilized for crop and vegetable drying, also the solar water heaters are extensively used in the households in Palestine, about 70% of households using such systems [48].

Till now, the solar energy for cooling systems is not used in Palestine, and we have no studies about the feasibility of applications like this technology in Palestine.

Since Palestine have widely climate conditions and possesses high average annual daily solar radiation as we mentioned above, especially in summer's months where is a high demand cooling, we will try in this theses to evaluate the solar cooling systems taking into account our existing conditions shown in Appendix A.

3.3 Solar Energy Conversion System Design

3.3.1 Solar Collectors

Solar collectors capture incident solar radiation energy and either convert it to heat (thermal energy) or directly to electricity (photovoltaic cells). The solar collector is the key element in a solar energy system. It is also the novel technology area that requires new understandings in order to make captured solar energy a viable energy source for the future. The function of a solar collector is simple; it intercepts incoming insolation and changes it into a useable form of energy that can be applied to meet a specific demand. There are three major types of a thermal solar collector: Flat Plate Solar Collector, Evacuated Solar Collector and a Concentrating (Optical) Solar Collector. A flat plate solar collector allows both direct and diffuse solar radiation.

Flat-plate collectors will absorb energy coming from all directions above the absorber (both beam and diffuse solar irradiance). Because of this characteristic, flat-plate collectors do not need to track the sun. They

receive more solar energy than a similarly oriented concentrating collector, but when not tracked, have greater cosine losses [49].

Since tracking is not required, flat-plate collectors may be firmly fixed to a mounting structure, and rigid plumbing may be used to connect the collectors to the remainder of the system. Also the flat-plate collector absorbs both the direct and the diffuse components of solar radiation. This partially compensates for the fact that fixed surfaces receive less energy because of the cosine effect. Although the diffuse solar irradiance is only about 10 percent of the direct normal solar irradiance on a clear day, on a cloudy day almost all of the available solar irradiance is diffuse.

Currently, flat-plate collectors cost less than concentrating collectors. Part of reason is the lack of need for a complex tracking system.

3.3.2 Collector Performance

1. Orientation

The orientation of a flat-plate collector is a concern in system design. The designer must decide on both the collector azimuth and tilt angles or to install the collectors horizontally.

2. Economic and Environmental Considerations

The most important factor driving the solar energy system design process is whether the energy it produces is economical. Although there are factors other than economics that enter into a decision of when to use solar energy; i.e. no pollution, no greenhouse gas generation, security of the energy resource etc., design decisions are almost exclusively dominated by

the ‘levelized energy cost’. This or some similar economic parameter, gives the expected cost of the energy produced by the solar energy system averaged over the lifetime of the system.

3. Efficiency Measurement

The energy collection efficiency is normally determined by testing. Collector performance test data are correlated with a parameter comprised of the collector temperature rise above ambient divided by the solar irradiance[49]. For flat-plate collector performance, the collector temperature and the solar irradiance used in this correlation are different from those used for concentrating collectors.

The energy balance on a solar collector absorber or receiver can be written as;

$$Q_{\text{useful}} = E_{\text{opt}} - Q_{\text{loss}} \quad (3.2)$$

where: Q_{useful} - rate of ‘useful’ energy leaving the absorber

E_{opt} - rate of optical (short wavelength) radiation incident on absorber

Q_{loss} - rate of thermal energy loss from the absorber

The ‘useful’ energy for a solar thermal collector is the rate of thermal energy leaving the collector, usually described in terms of the rate of energy being added to a heat transfer fluid passing through the receiver or absorber, i.e.:

$$Q_{\text{useful}} = mc_p (T_{\text{out}} - T_{\text{in}}) \quad (3.3)$$

Where:

m - mass flow rate of heat transfer fluid (kg/s)

C_p - specific heat of heat transfer fluid (J/kg.K)

T_{out} - temperature of heat transfer fluid leaving the absorber (K)

T_{in} - temperature of heat transfer fluid entering the absorber (K)

Heat loss from the collector follows three paths: convection, radiation, and conduction. These losses are shown schematically in Figure 3.7[49].

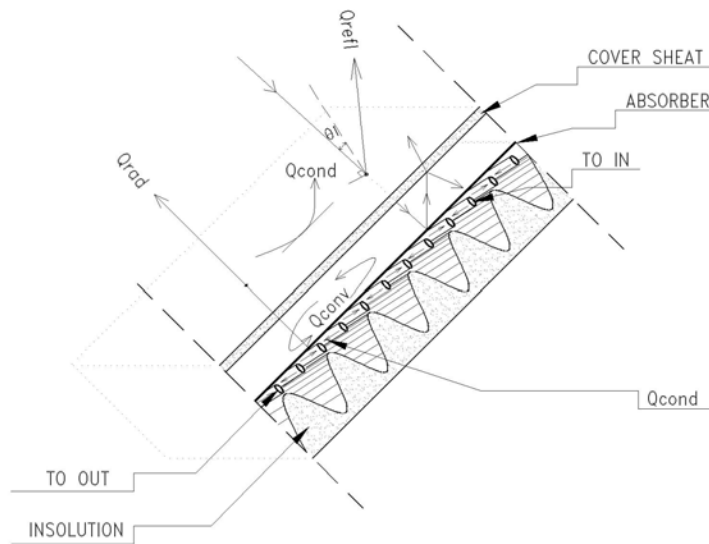


Figure (3. 7): Energy balance on a solar collector absorber / receiver

4. Collector Efficiency

The solar energy collection efficiency, η_{coll} of both thermal collectors and photovoltaic collectors is defined as the ratio of the rate of useful thermal energy leaving the collector, to the useable solar irradiance falling on the aperture area. Simply stated, collector efficiency is:

$$\eta_{\text{coll}} = Q_{\text{useful}} / A_a I_a \quad (3.4)$$

where:

Q_{useful} = rate of (useful) energy output (W)

A_a = aperture area of the collector (m^2)

I_a = solar irradiance falling on collector aperture (W/m^2)

This general definition of collector efficiency differs depending on the type of collector. The rate of useful energy output from thermal collectors is the heat addition to a heat transfer fluid as defined by Equation (3.2). Since flat-plate collectors (both thermal and photovoltaic) are capable of absorbing both direct (beam) and diffuse solar irradiance, the appropriate aperture irradiance is the global (total) irradiance falling on the collector aperture.

$$I_a = I_{t,a} \quad (3.5)$$

where $I_{t,a}$ is the global irradiance on a collector aperture.

The collector efficiency of the thermal and photovoltaic flat-plate collectors, then has the following definitions:

Flat-plate thermal collectors:

$$\eta_{\text{col}} = mc_p (T_{\text{out}} - T_{\text{in}}) / I_{t,a} A_a \quad (3.6)$$

Flat-plate photovoltaic collectors:

$$\eta_{\text{coll}} = i.v / I_{t,a} A_a \quad (3.7)$$

Where:

i – Electric current through the cell (amps)

v – Voltage across the cell (volts)

Figure 3.8 illustrate Typical solar collector efficiency curves [34].

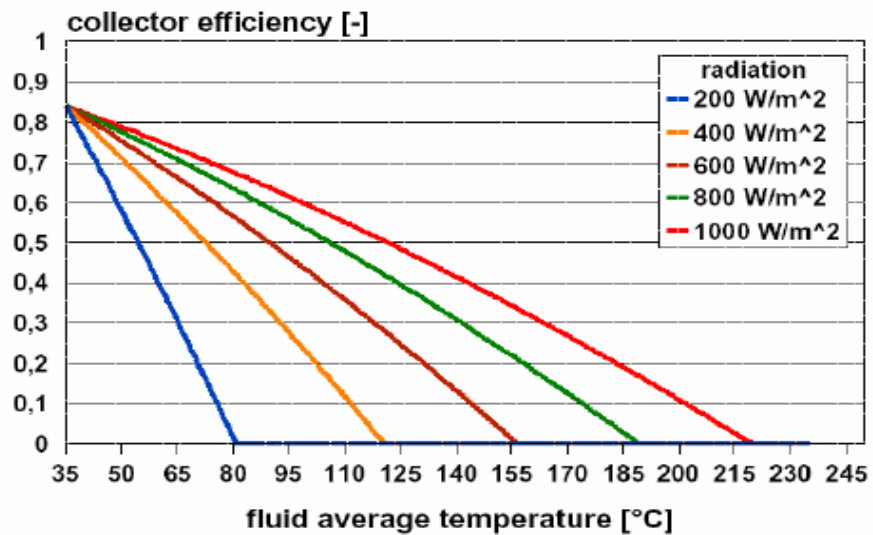


Figure (3.8): Typical solar collector efficiency curves [34]

In the experimental chapter the influence of solar radiation and the relationship between it and the cooling effect studied and discussed.

Chapter Four

Experimental Work, Results and Discussion

4.1 Working Principle of the No Valve Solar Cooler

A no valve, flat plate solar cooler is designed to meet the objective of this thesis by doing a large number of experiments and theory analysis. There are no valves and measure gauges installed on this advanced device except for experimental purposes, also there are no moving parts on this device. Activated carbon and methanol are used as working pair for this no valve solar cooler. Fig. 4.1 shows schematic layout of a no valve solar flat plate cooler. The solar cooler consists of a adsorbent bed (2), a condenser (8), an evaporator (9), water tank (11), insulation box (12) as well as connecting pipes. For this system, there are no reservoirs, connecting valves and throttling valve, the structure of the system is very simple.

The working principle of this no valve solar cooler is described as follows: On a sunny day, the adsorbent bed absorbs solar radiation energy, which raises the temperature of adsorbent bed as well as the pressure of refrigerant in adsorbent bed. When the temperature of adsorbent reaches the desorption temperature, the refrigerant begins to evaporate and desorbs from the bed. The desorbed refrigerant vapor condenses into liquid via the condenser and flows into the evaporator directly; this desorption process lasts until the temperature of adsorbent reaches the maximum desorption temperature. During night, when the temperature of the adsorbent bed decreases, the refrigerant vapor from the evaporator gets adsorbent back in the bed.

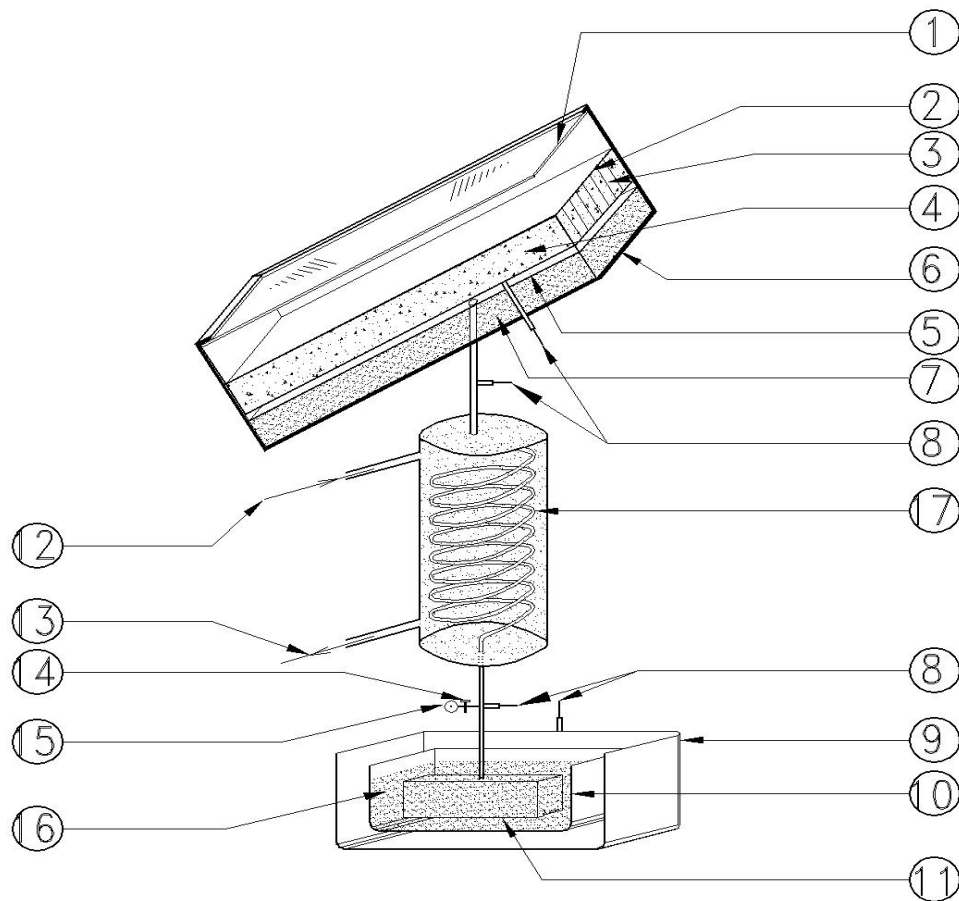


Figure (4.1): The sketch structure of the no valve cooler

(1) cover plate, (2) adsorbent bed, (3) stainless steel fins (4) granular activated carbon, (5) false bottom, (6) the collector, adsorbent bed case, (7) insulation materials, (8) thermocouple sensors, (9) insulation box, (10) cooler box, (11) evaporator, (12), (13) water condenser filling and drain, (14) charging and discharging valve, (15) pressure guage, (16) water to be cooled or iced, (17) condenser

During this adsorption process, the cooling effect is released from refrigerant evaporation, and the ice is expected to form in the water tank placed inside thermal insulated water box.

In general, the performance of solar ice maker are represented in terms of Q_{ref} (or ice mass gotten in water tank) and the performance efficiency COP_{solar} . They can be expressed as follows [50] :

$$Q_{ref} = \Delta x M_a L \quad (4.1)$$

$$\Delta x = x_{conc} - x_{dil} \quad (4.2)$$

where x_{conc} is the adsorption capacity before desorption, x_{dil} is the adsorption capacity after desorption, M_a is the mass of adsorbent inside adsorbent bed, L is the latent heat of vaporization.

$$COP_{solar} = (Q_{ref} - Q_{cc}) / \int i_{(t)} dt \quad (4.3)$$

where $Q_{cc} = \int M_a \Delta x C_{p_l} dT$ is the energy used to cool down the refrigerant liquid from condensing temperature T_c to evaporation temperature T_e , c_p ; specific heat of refrigerant, $\int i_{(t)} dt$, is the total radiant energy absorbed by the collector during one day operation[50].

4.2 Construction of No Valve Solar cooler

4.2.1 Adsorbent Bed

Adsorbent bed is the most important part of the solar cooler, it is the heart of solid adsorption refrigeration, and the characteristics of the adsorbent bed are the most obvious factors which directly affect solid adsorption systems. For the flat-plate solar cooler, the collector and adsorbent bed are often designed into an integrated shape to enhance heat transfer.

At the same time, several fins are also necessary to enhance heat transfer, so that the heat received by the adsorbent bed top surface can be quickly transferred inside the bed. Usually, this type of adsorbent bed possesses good heat transfer ability [51]. Generally speaking, a good adsorbent bed must have good heat and mass transfer. Recent research showed that the aluminum alloy have a stronger catalytic effect on the decomposition reaction under the solar adsorption refrigeration, therefore stainless steel are used as adsorbent heat transfer metal instead of aluminum alloy although stainless steel has poor heat transfer ability than that of aluminum alloy[50].

The adsorbent bed is made of flat plate stainless steel box, having surface area of nearly 1 m^2 , also about 20 kg adsorbent (activated carbon) is charged and sealed inside the steel plate box, then selective coating is covered on top surface of the steel plate box to enhance receiving solar flux radiation. Except for the top surface, every side of the adsorbent bed is covered in insulation material (insulated case).

On the top of the adsorbent bed, a glass cover is necessary to form a “greenhouse” for the adsorbent bed, the sketch of the cross section of the adsorbent bed shown in figure 4.2. However, in the evening, a moveable damper may be installed to effectively cool the adsorbent bed by air. As mentioned previously, in order to guarantee better heat transfer between the front side and the adsorbent, many fins (also made of stainless steel) are placed inside the adsorbent bed box in contact with the front side and the activated carbon. The distance between these fins is approximately 0.05 m.

The thickness of the adsorbent layer is about 0.04 m, those parameters mentioned above are obtained according to Ref. [50].

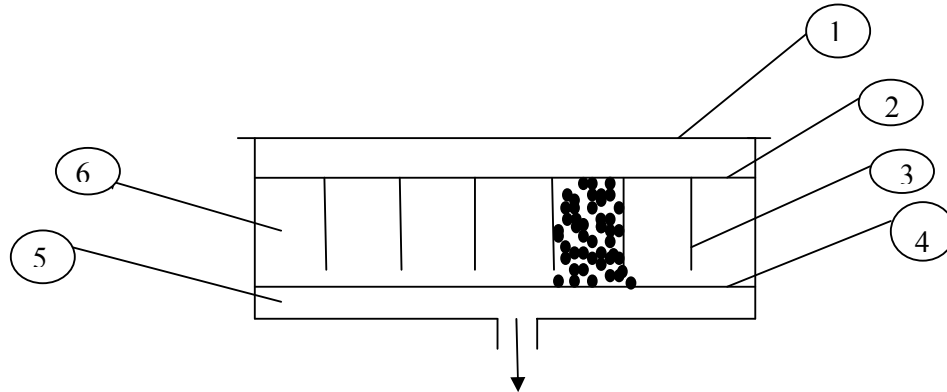


Figure (4.2): Cross section of the adsorbent bed

(1) glass cover, (2) adsorbing heating surface, (3) fin, (4) metallic mesh, (5) false bottom, (6) activated carbon

In order to improve the transfer of methanol vapor through the activated carbon layer, a false bottom (0.01 m thick in the radial distance) is included in the rear side of the adsorbent bed as mentioned by [16]. As this “false bottom” is completely open to the circulation of vapors, it permits uniform distribution of methanol in the adsorbent.

4.2.2 Condenser and Evaporator

During the process of desorption of methanol, a well designed condenser is needed to reject the desorption heat. A helical copper tubes condenser immersed in a water tank, or a stainless steel tube with fins were designed to make a test, and optimize one of them. The evaporator must have sufficient volume to collect the entire condensed methanol. In order to enhance the heat transfer effect, the heat exchange surface is designed as a

series of four trapezoidal cells shown in Fig.4.3 the dimension of the evaporator is $220 \times 320 \times 100$ mm and the heat exchange area is about 0.28 m^2 .

The evaporator is partially immersed in a water tank, which is made of stainless steel, and both the evaporator and water tank are placed in insulated box covered with insulation. In this way, it is very simple to remove the ice if be formed during adsorption cooling in the night.

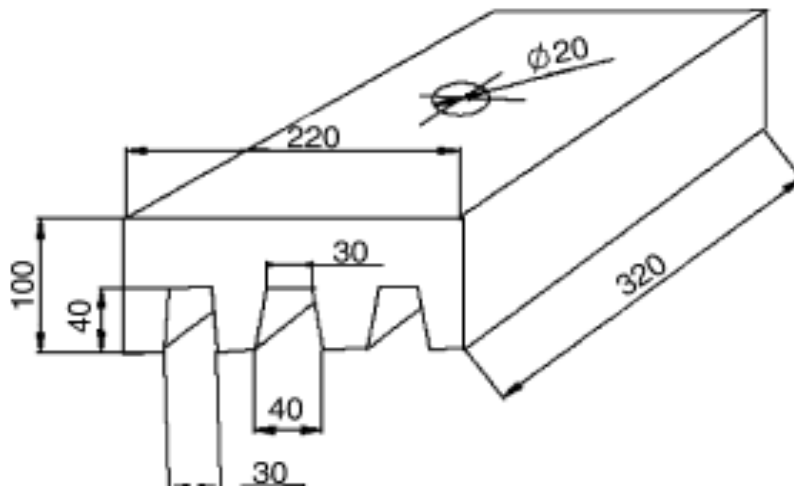


Figure (4.3): Sketch of the evaporator (mm)

4.2.3. Integration of the Subsystem

The adsorbent bed, condenser, evaporator were checked for vacuum proof and then were connected with each other using stainless steel pipe of 3/4 inch, and later with another pipe of 1/2 inch. The whole system was mounted on a frame bracket installed with wheels, so that it can be moved easily when necessary. Only one valve is installed beside condenser, which helps to vacuum the whole system as well as to charge the system with refrigerant. A pressure gauge is installed behind adsorbent bed to check for the pressure conditions in the system. Besides, no any other valves or

measuring instruments are used in the system. A thermocouple is used for monitoring the temperature only. (The photograph of the system is shown in Fig. 4.4). In order to ensure that the system can work normally, it is essential that the whole system should be vacuum proof.



Figure (4.4): Photograph of the system

4.3 The experimental method

The design, construction and test run of a solid adsorption solar cooler are presented to see if a cooling process or an ice accumulation will be achieved or not. Different heat fluxes, different temperature levels and different volumes of methanol were examined for comparative and for optimizing the characteristics of the adsorption refrigeration by solar energy.

Experiments for two types of condensers were made as mentioned previously, the first one was made by using a helical copper pipe immersed in a water tank, and the other was made by using an air-finned condenser. The affinity of different particle size of activated carbon to methanol was tested in the laboratory scale experiment.

After the construction of the system with water condenser, several tests were performed to ensure good sealing, since any kind of air leakage inside the system will lead to failure in the process, since such system work under vacuum. The total pressure may increase due to leaks or desorption of air from activated carbon, then the adsorption of methanol is reduced. Furthermore, the boiling temperature of the methanol increases and the rate of evaporation decreases, and as a result the cooling effect decreases. The first experimental setup was designed with movable lids. But due to difficulties in controlling the leakage, the system was completely sealed by special stainless steel welding.

4.3.1 Methanol Charging and Heating Process

After the system was sealed, it was evacuated side by side with heating to flush out entrapped air and moisture using a vacuum pump until the pressure in the system decreased to 30 kPa. This was also used to test the system for any leakage. Many attempts were done to overcome the leakage problem, and the system was left for sufficient time for leakage monitoring. These experiments divided to two steps :

Step 1:

The first experiment was done on the 23rd of July in 2007, at 11:30 o'clock. The system was evacuated to 50kPa, then the system was charged with 2L of methanol, and the condenser tank was filled with 17 liter of water and the cooler box with 5 liter of water.

As the solar heat flux density is taken from the solar source in Palestine, and the total radiant energy to the collector is assumed to be $f_{G(t)dt} = 20 \text{ MJ/m}^2 \text{ /day}$ which is about $5.4 \text{ kWh/m}^2\text{/day}$, electrical heater with regulator was used to simulate solar heating. For the solar collector, an average accepted radiation power of 770 W/m^2 during 7 hours is assumed, thus; a 770 W electrical heater can simulate a squared meter flat plate solar collector. This done by a potential regulator. Many parameters such as the temperature of the adsorbent inside the generator, the temperature of methanol at different points, condenser water temperature, room temperature, water temperature inside the cooling box and the standing pressure were monitored and recorded. The temperatures were measured by thermocouples placed in the system, (point 6 in Figure 4.1).

In the electric heating case, many experiments done to make sure that the system operated normally without significant problems such as leakage. The output data indicated as shown in Tables (4. 1) and (4.2).

Where:

T_1 : the temperature inside the adsorbent bed.

T_2 : the temperature at the inlet of the condenser.

T_3 : the temperature at the outlet of the condenser.

T_4 : the temperature inside the evaporator.

$T_{w,ev}$: Temperature of the water inside the cooler box.

T_{amb} : Ambient temperature .

$T_{w,cond}$: temperature of the condenser water .

P_{ev} : the pressure at the inlet of evaporator .

P_{cond} : the pressure at the inlet of condenser .

Table (4.1): Results of 4 hours heating by electrical heater at 770 W with 2 L of methanol and 30kPa starting pressure

| Date | Time | State | T ₁ (°C) | T ₂ (°C) | T ₃ (°C) | T ₄ (°C) | T _{amb.} (°C) | T _{w cond.} (°C) | T _{w ev.} (°C) | P _{cond} (kPa) | P _{ev.} (kPa) | Conclusion |
|----------|-------|-------------------|------------------------|------------------------|------------------------|------------------------|---------------------------|------------------------------|----------------------------|----------------------------|---------------------------|--------------------------------------|
| 1.8.2007 | 9:45 | Before heating | 29.6 | 28.5 | 28.5 | 28.7 | 28.8 | 27.7 | 28.2 | 70 | 70 | There was no cooling on the next day |
| | 13:00 | Through heating | 66.0 | 29.9 | 28.8 | 32.0 | 29.4 | 27.7 | 28.2 | 96 | 96 | |
| | 14:00 | End of heating | 94.5 | 30.2 | 28.9 | 28.7 | 32.0 | 30.0 | 30.0 | 111 | 111 | |
| | 15:30 | Adsorbing process | 53.4 | 30.0 | 29.0 | 28.8 | 31.0 | 27.8 | 28.2 | 25 | 25 | |

Table (4.2): Results of 770 W heating and 92.5 kPa starting pressure with 2L of methal

| Date | Time | State | T ₁ (°C) | T ₂ (°C) | T ₃ (°C) | T ₄ (°C) | T _{amb.} (°C) | T _{w cond.} (°C) | T _{w ev.} (°C) | P _{cond} (kp) | P _{ev.} (kp) | Conclusion |
|----------|-------|--------------------|------------------------|------------------------|------------------------|------------------------|---------------------------|------------------------------|----------------------------|---------------------------|--------------------------|---|
| 4.8.2007 | 8:50 | Before heating | 29.5 | 28.9 | 28.2 | 28.4 | 30.3 | 27.2 | 28.1 | 87 | 92 | 1) high pressure without variation of temperature. except adsorbent bed temperature. 2) no cooling was observed. |
| | 9:50 | Through heating | 63.3 | 29.6 | 28.3 | 28.3 | | | | 97 | 105 | |
| | 10:50 | Through heating | 75.2 | 30.2 | 28.6 | 28.4 | 30.6 | 27.4 | 27.9 | 113 | 116 | |
| | 11:22 | End of heating | 71.0 | 30.3 | 26.6 | 37.5 | | 27.6 | 28.0 | 111 | 111 | |
| | 13:52 | adsorbin g process | 42.4 | 29.8 | 31.4 | 28.5 | 29.4 | 27.8 | 28.0 | 95 | 109 | |
| | 15:40 | | 34.3 | 29.6 | 29.9 | 30.8 | 32.0 | 28.0 | 28.0 | 95 | 103 | |

On Monday, the 6th of August in 2007 at 9:10 A.M, the system was heated and evacuated to get rid of any air or water content. The regenerator was heated several times to higher temperature, and the air was evacuated to ensure methanol impurity. The system was charged with more 2L of methanol, and the output data are indicated as shown in Table (4.3).

Table (4.3): Results of heating and charging with 4L of methanol.

| Date | Time | State | T ₁ (°C) | T ₂ (°C) | T ₃ (°C) | T ₄ (°C) | T _{amb.} (°C) | T _{w,con} (°C) | T _{w,ev} (°C) | P _{cond} (kPa) | P _{ev.} (kPa) | Conclusion |
|----------|-------|---|------------------------|------------------------|------------------------|------------------------|---------------------------|----------------------------|---------------------------|----------------------------|---------------------------|----------------------------|
| 6.8.2007 | 12:00 | heating | 30.0 | 29.0 | 29.0 | 28.5 | 31.0 | 17.0 | 28.1 | 104 | 104 | No cooling on the next day |
| | 13:00 | | 113.1 | 30.6 | 26.5 | 26.4 | 31.0 | 25.1 | 27.0 | 102 | 101 | |
| | 14:00 | | 119.5 | 33.4 | 26.9 | 27.4 | 31.0 | 25.6 | 26.7 | 103 | 103 | |
| | 15:00 | | 123.0 | 31.7 | 27.3 | 27.3 | 27.5 | 25.9 | 26.2 | 103 | 103 | |
| 7.8.2007 | 9:12 | Evacuated, and charged with another 2000mL methanol | 26.6 | 28.2 | 26.1 | 25.8 | | 22.6 | 24.5 | 65 | 68 | |
| | 10:00 | | 27.4 | 27.8 | 24.7 | 24.7 | | | | 70 | 75 | |
| | 11:10 | | 90.9 | 29.8 | 30.3 | 25.5 | | | | 101 | 101 | |
| | 12:11 | | 111.6 | 26.5 | 30.7 | 25.8 | | | | 101 | 104 | |

On Wednesday 8.8.2007 at 1 P.M o'clock the system was charged with another 2L of methanol, as a result of no cooling on the previous day experiments. The pressure was $P_{cond} = 91\text{kPa}$, and $P_{ev.} = 98.5\text{kPa}$.

On Monday, August 13,2007, the pressures reading was $P_{cond} = 96\text{kPa}$ and $P_{ev} = 106\text{kPa}$. In the morning a solar heating process applied to ensure good distribution of heating in the regenerator. The results are listed in Table (4.4).

4.3.2 Lab Scale Experiments

In order to examine the ability of activated carbon to adsorb methanol, many experiments were carried out in lab scale setup. A simulation system was designed by the use of two glass flasks to represent the generator (adsorption bed) and the evaporator. Moreover, a double glass condenser was used to condensate the methanol vapor. An oil bath was used to heat the generator, with the evaporator was immersed in water bath. A sketch of the setup is given in Figure (4.5).

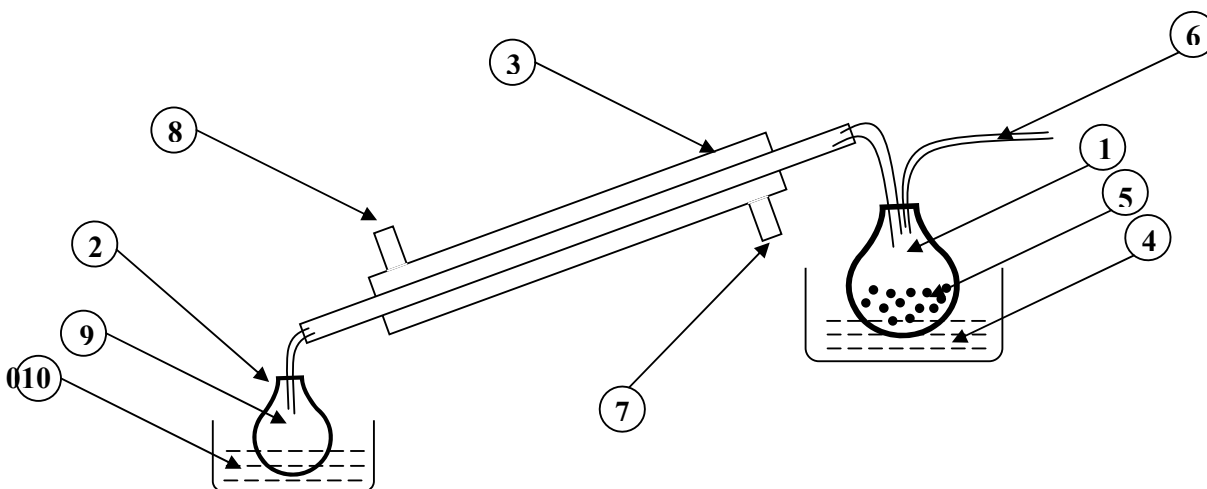


Figure (4.5): Lab scale setup

(1) generator flask, (2) evaporator flask, (3) glass condenser, (4) oil path, (5) granular activated carbon, (6) charging and vacuum valve, (7,8) water inlet, outlet, (9) condensed methanol, (10) water to be cooled.

240 mL of methanol was charged in the generator, and mixed with 175g of activated carbon. Within few hours the activated carbon adsorbed most of the methanol and the generator temperature increased by 2 °C.

By this result, we became sure of the affinity of the used activated carbon toward methanol. On the next step 175g fresh activated carbon was placed in the generator, and 240 mL of the methanol placed in the evaporator, but only 4mL of the methanol was adsorbed. We guess the reason was due to the higher operating pressure, or to the air leakage.

On August 14th, 2007, 250mL of methanol was added directly to 250g activated carbon in the generator, the generator was heated to 82 °C by the mean of the oil bath. At 52 °C the methanol started to evaporate and condensed. The system left to cool to the next day, and about 150 mL of the methanol was adsorbed by activated carbon in the generator. This experiment removed any suspensions toward the ability of the used pairs for the cooling process.

The high affinity of AC toward methanol in the previous experiment encouraged us to charge the pilot system of another 2L of methanol to have a sum of 8L of methanol in the evaporator, while the system was evacuated to 26 kPa, and the results of this experiment is listed in table (4.5).

Table (4.5): Experimental results of pilot setup charged with 8L of methanol, and heated by solar energy at 26kPa.

| Date | Time | State | T ₁ (°C) | T ₂ (°C) | T ₃ (°C) | T ₄ (°C) | T _{amb.} (°C) | T _{wcon} (°C) | T _{w ev} (°C) | P _{cond} (kpa) | P _{ev.} (kpa) | Conclusion |
|-----------------------|-------|--------------------|------------------------|------------------------|------------------------|------------------------|---------------------------|---------------------------|---------------------------|----------------------------|---------------------------|----------------------|
| 14.8. 2007 | 9:50 | Before charging | 29.5 | 26.1 | 24.6 | 25.8 | 27.0 | 25.6 | 25.7 | 66.0 | 69.0 | |
| | 10:40 | Heating& vacuum | 60.9 | 31.3 | 25.8 | 26.8 | | 23.7 | 25.7 | 36 | 36 | |
| | 14:15 | After charging | 95.3 | 44.4 | 32.0 | 28.7 | | 30.5 | 28.3 | 101 | 101 | |
| | 15:25 | | 96.3 | 58.0 | 33.2 | 29.4 | 29.0 | | | | | |
| Wed. 15.8. 2007 | 9:15 | | 26.0 | 26.0 | 25.0 | 24.0 | 26.0 | | | 46 | 48 | No cooling effect |
| | 13:00 | | 87.2 | 37.5 | 30.5 | 36.6 | 28.0 | 28.8 | 36.4 | 96 | 102 | |
| | 14:30 | | 91.8 | 40.1 | 33.9 | 33.2 | | 32.0 | 32.9 | 106 | 109 | |

On Wednesday 15.8.2007, small quantity of methanol was found in the evaporator, which means that the desorption process had occurred and the charged quantity of methanol is larger than that of AC capacity of adsorption. The evaporator was heated in hot water bath in order to evaporate the methanol, the pressure increased to $P_{\text{cond}} = 49\text{kPa}$, and $P_{\text{ev}} = 53.5\text{kPa}$. Despite this heating process a quantity of methanol remained in the evaporator, and this can be explained by the fact that activated carbon had reached its saturation capacity.

Another experiment was done with the Lab scale setup where 150mL of methanol was mixed with 220g of activated carbon in the flask representing the generator. The generator was heated with water bath, and the desorption process started when the temperature of hot water reached 52°C. The condensing process started 20 minute later. When the temperature of hot water reached 85°C, the heating process was stopped but the methanol in the evaporator didn't adsorbed back by AC in the generator and no significant cooling was observed.

To study the influence of the operating pressure at the performance of the system another experiment was done with the lab scale setup, where 80 ml of methanol was charged into the evaporator flask and a heating process at atmospheric pressure was applied to the generator flask to get rid of any methanol within the activated carbon. The desorption process started also at 52 °C. When the temperature of hot water reached 95 °C the heating process was stopped. The highest desorption quantity was occurred when the temperature of heating water was 80 °C to 90 °C. The system left to cool gradually, and the result was neither adsorption process nor cooling.

According to the previous results, the study was focused on the vacuum pressure, consequently on the same day at 1P.M. the pilot system was shadowed and evacuated to 26kPa. in order to see if there is any adsorption process occurred from evaporator at this pressure, since there was a quantity of methanol in the evaporator as a result of solar heating and the desorption process. Within 50 minute the methanol evaporated form the evaporator completely and the temperature of the of the evaporator slightly decreased. The pilot system reheated for another period, and evacuated to 26kPa, and the results are shown in table (4.6).

Table (4.6): Results of solar heating of pilot system at 26kPa.

| Date | Time | State | T ₁ (°C) | T ₂ (°C) | T ₃ (°C) | T ₄ (°C) | T _{amb.} (°C) | T _{w,co} nd. (°C) | T _{w ev} (°C) | P _{cond} (kpa) | P _{ev.} (kpa) |
|---------------------|-------|------------------------|------------------------|------------------------|------------------------|------------------------|---------------------------|----------------------------------|---------------------------|----------------------------|---------------------------|
| Sunday 19.8.2007 | 14:00 | Vacuum & heating | 38.0 | 31.2 | 27.6 | 25.0 | 27.0 | 26.2 | 26.0 | 36 | 38 |
| | 15:25 | | 85.5 | 37.2 | 30.6 | 26.8 | | 29.0 | 27.1 | 76 | 77 |
| | 16:00 | heating | 95.0 | 44.4 | 32.0 | 28.7 | | 30.5 | 28.3 | 101 | 101 |

On Monday 20.8. 2007 morning there was no methanol adsorbed, consequently neither cooling effect in the pilot system nor in the Lab scale system.

On the next day -Tuesday 21 .8 .2007- at 10 A.M: The influence of high temperature was investigated using corn oil bath instead of water to heat the generator of lab scale system, the temperature obtained was higher than 120 °C. 170mL of methanol was mixed with 220g AC in the generator flask, then the flask was heated until the oil temperature reached 120 °C on which the highest desorption process occurred. The quantity of methanol desorbed was 144mL, but the methanol was not adsorbed back by the activated carbon.

In order to examine the ability of activated carbon for methanol adsorption under a deep evacuation process, a volume of 50mL of methanol was placed in the flask representing evaporator and a quantity of 100g of AC was placed in the flask representing the generator. The adsorption process occurred resulting in a temperature drop of 16 °C.

Another experiment was done to examine the adsorption ability of two particle size (granular and powder) of activated carbon. 10g of each size was placed in a beaker, and placed near another beaker contains 80mL of methanol in a vacuum oven. The oven was evacuated to 10kPa. On the next day, the granular activated carbon weight increased by 2.8g, while the powder increased by 1.9g, on the other hand the methanol volume decreased by 12.8mL.

Another experiment was done in order to examine the ability of activated carbon for methanol adsorption. In this experiment 20g of fresh AC was charged in the flask representing the generator, while 15mL of methanol poured in the flask representing the evaporator. The system was evacuated to the boiling pressure of methanol at room temperature (30°C). After the evacuation process, the methanol started to evaporate and was adsorbed by the activated carbon resulting a cooling effect at the surface of the evaporator, while the temperature was increased at the surface of the generator, but after a while the process was slow down due to the increasing of pressure inside the system as a result of none perfect sealing. This experiment is a good indicator of the importance of keeping the system sealed and at low pressure as possible.

In order to examine the effect of evaporator volume, another experiment was performed using the lab scale setup. In this experiment the condenser was shortened and smaller volume of evaporator was used.

45g of fresh activated carbon was placed in the generator flask, while 20mL of methanol was placed in the evaporator flask. After making the required evacuation process, the methanol evaporation was observed, and adsorbed by the activated carbon. The temperature of the evaporator decreased from 29.6 °C to 27.8 °C within 2 hours. The cooling process was observed during 3 hours and all the time the cooling effect existed.

On the next day the volume of methanol in the evaporator decreased by 8mL while the weight of AC increased by 11.6 g.

These results encouraged examining the influence of the quantity of activated carbon on the adsorption process, therefore, 60g of granular activated carbon and 22mL of methanol were placed in the generator flask and the evaporator flask respectively. After evacuation process, a low temperature was obtained on the surface of the evaporator. The temperatures were: $T_{ev.} = 15.5^{\circ}\text{C}$, $T_{gen} = 34^{\circ}\text{C}$ and $T_{amb.} = 30.4^{\circ}\text{C}$, and after 5 minutes the temperatures were 15.7, 35.2 and 31 °C respectively.

The cooling effect continued for four hours, and evaporating process was still occurring.

According to these results one can calculate the adsorption capacity of the used activated carbon as:

$$\text{AC adsorption capacity} = \frac{\text{mass of methanol adsorbed}}{\text{mass of activated carbon used}}$$

Mass of methanol = volume \times density = 0.787×22 g/ mL

Mass of AC = 60g

Then, the adsorption capacity of AC is :

$$22 \times 0.787 / 60 = 0.29 \text{ kg methanol/kg AC}$$

This value is less than the value that some researchers indicated [27].

From the previous experiments we could conclude that the adsorption – desorption cycle had been achieved.

4.3.3 Conclusions

After the previous experiments, some conclusions were reached:

- 1) The adsorption bed has the greatest effect on the performance and the characteristics of the solar cooler. It must be well manufactured, well sealed and well controlled; as a result, another type of generator may be used such as two coaxial pipes.
- 2) In low pressure systems, the condenser and the evaporator must be close to each other and to the collector. Thus, they should be located directly under the generator such that the refrigerant flows into them by gravity. As a result the condenser in the pilot scale setup should be replaced by a pipe condenser.
- 3) Both of the size and shape of the evaporator must be optimized, it have to be sized to suit the amount of the methanol, as a result of lab scale experiments.

- 4) The generator (adsorbent bed) must be positioned not far from the evaporator in order to ensure high pressure of methanol vapor and good distribution of vapor.
- 5) The size and the shape of condenser must be optimized, as a result of lab scale experiments.
- 6) Desorption process started from **52 to 58°C**. when the operating pressure was the boiling pressure of methanol at room temperature (30 °C).
- 7) The system must manufactured in an integrated manner.
- 8) The activated carbon must be heated over 80 °C under a deep vacuum pressure, in order to enhance the desorption of methanol.
- 9) The vacuum pressure has the greatest effect on the system operation. The pressure must be less than 20kPa. Therefore to modify pressure in the solar pilot system the following modifications are proposed:
 - a) A new type of pipe condenser must be used, pressure resistant collector frame can be used, and high quality and larger size connecting pipe should be used.
 - b) Design of another collector/ generator consist of several coaxial pipes in which the inner tubes were perforated axially and circumferential. Each annular space between the inner and outer tube charged with activated carbon. The schematic diagram of this design is shown in figure (4.6).

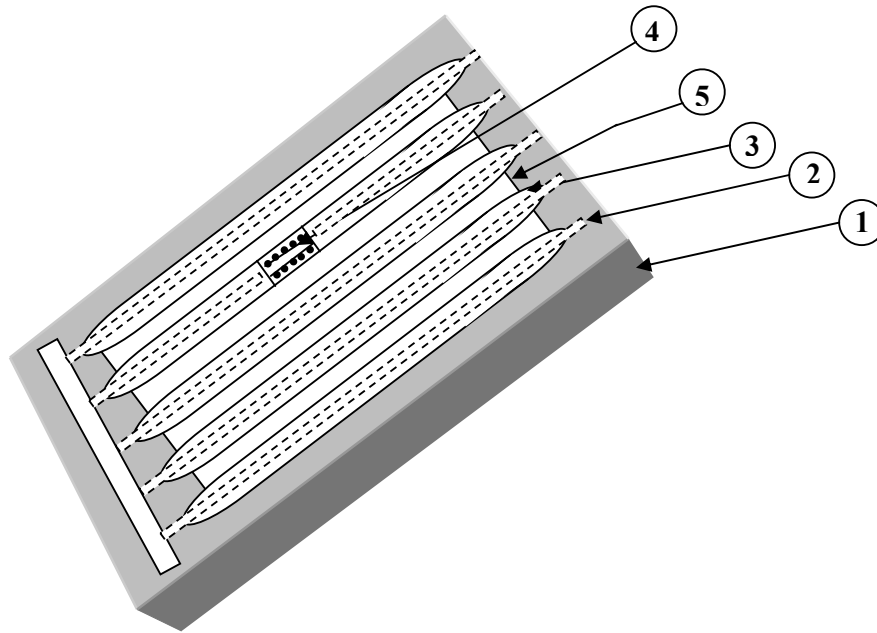


Figure (4.6): The sketch of the suggested coaxial pipes generator/collector

(1) The insulation collector box, (2) perforated inner tube, (3) outer tube, (4) granular activated carbon, (5) solar absorption plate.

4.3.4 Experimental Work on the Modified Solar Pilot Setup

The solar pilot system was modified according to the previous finding and recommendations. The main frame of the generator was modified by adding a new high strength metallic mesh and support beams, at the same time; the helical water condenser was replaced by finned tube condenser. An additional return tube was replaced between the evaporator and the generator in order to increase the flux of evaporated methanol and to keep higher vapor pressure of methanol surrounding the activated carbon without any pressure drop that can be caused by the condenser.

The schematic diagram of the modified system and condenser is shown in figure (4.7).

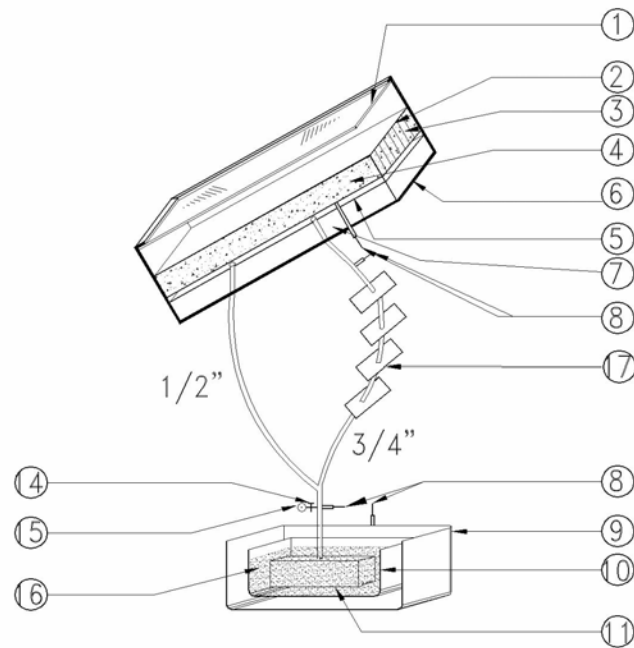


Figure (4-7): The schematic diagram of the modified solar system

(1) cover plate, (2) adsorbent bed, (3) stainless steel fins (4) granular activated carbon, (5) false bottom, (6) the collector, adsorbed bed case, (7) insulation materials, (8) thermocouple sensors, (9) insulation box, (10) cooler box, (11) evaporator, (12), (13) water condenser filling and drain, (14) charging and discharging valve, (15) pressure guage, (16) water to be cooled or iced, (17) condenser

The system was charged with 23kg of granular activated carbon, and well sealed. The system was checked several times to ensure good sealing, and for leakage.

As a preliminary experiment, the system was evacuated to 39 kPa using the vacuum pump. Then the system was heated by the special heating

element connected to a voltage regulator. More evacuation process was carried out with special traps to decrease the pressure of the system to 20 kPa. The system was monitored for 50 hours and the pressure inside the system increased to 53.5 kPa, thus the evacuation and heating process repeated again after fixing the problem. The results of this experiment are shown in table (4.7).

Table (4.7). Results of heating and evacuations process of the modified system

| Time | Process | T1 °C | T2 °C | T3 °C | T4 °C | Troom °C | Tw,ev) °C | P kpa |
|-------|----------------------|----------|----------|----------|----------|-------------|--------------|----------|
| 9.30 | Leakage test | 15.0 | 16.0 | 15.6 | 14.0 | 15.9 | | 54 |
| 10.00 | Heating & evacuation | 44.0 | | | | | | 30 |
| 11.00 | evacuation | 47.0 | | | | | | 25 |
| 12.00 | evacuation | 58.8 | 48.0 | 36.0 | 14.7 | | | 25 |
| 14.00 | Cooling | 33.9 | 20.0 | 18.7 | 14.7 | | | 20 |
| 14.30 | | 30.7 | 19.2 | 18.6 | 14.3 | | | 18 |

After the system became well sealed, the evaporator was charged with 2L of methanol under a suitable heating rate, and evacuation process. In this preliminary experiment the cooling effect was seen as indicated in table (4.8).

Table (4-8): Preliminary results of evacuated pilot solar setup charged with 2L of methanol

| Time | process | T1 (°C) | T2 (°C) | T3 (°C) | T4 (°C) | Troom (°C) | Tw,ev (°C) | P kPa | Conclusion |
|-------|--|---------|---------|---------|---------|------------|------------|-------|--------------------------------|
| 9.00 | | | | | | | | 19 | Remains sealed |
| 10.00 | Heating | 14.0 | 13.8 | 15.6 | 13.3 | 13.4 | 12.3 | 23 | |
| 11.00 | | 45.7 | 21.1 | 15.1 | 15.7 | 14.0 | 12.5 | 64 | |
| 11.15 | | | | | | | | 70 | |
| 11.20 | Evacuation | | | | | | | 36 | |
| 11.24 | The end of evacuation | 65.0 | 45.2 | 43.5 | 23.0 | | | 33 | |
| 11.50 | | 74.3 | 52.2 | 28.0 | 25.8 | | | 50 | |
| 12.08 | Stop heating and charging with 2 L of methanol | 80.9 | 55.1 | 26.9 | 28.0 | 14.5 | 12.8 | 60 | |
| 12.45 | Cooling | 75.0 | 36.0 | 22.8 | 22.6 | | | 36 | |
| 14.00 | | 54.0 | 19.0 | 14.5 | 13.9 | 13.8 | 12.5 | 25 | |
| 15.20 | | 39.1 | 14.7 | 12.2 | 8.8 | 13.0 | 8.7 | 30 | Adsorption & cooling succeeded |
| 9.15 | Monitoring the process next day morning | 14.3 | 14.0 | 13.5 | 11.9 | 14.5 | 9.6 | 20 | Still cooling effect |

An experiment was done to examine the effect of the cooling time of the generator on the performance of the pilot solar system. a rapid cooling method was applied to the generator after the heating process. The result was no cooling as can be seen in table (4.9).

Table (4-9): Effect of rapid cooling

| Time | Process | T1 (°C) | T2 (°C) | T3 (°C) | T4 (°C) | Troom (°C) | Tw(ev) (°C) | P kPa | Conclusion |
|-------|---------------|---------|---------|---------|---------|------------|-------------|-------|-------------------|
| 9.40 | Heating | 15.3 | | 16.3 | 14.8 | 16.0 | 13.5 | 36 | |
| 10.30 | | 36.8 | 19.2 | 16.9 | 18.9 | 16.5 | 13.6 | 65 | Steady pressure |
| 11.30 | | 52.5 | 26.2 | 18.6 | 18.2 | 16.5 | | 65 | |
| 12.30 | | 77.7 | 53.0 | 28.0 | 25.0 | 17.4 | 14.1 | 113 | |
| 12.37 | | 84.1 | 54.0 | 28.1 | 25.0 | 17.4 | | 119 | |
| 13.00 | Rapid cooling | 89.0 | 48.8 | 26.9 | 23.9 | 17.0 | 14.2 | 98 | |
| 14.00 | | 66.6 | 29.9 | 20.2 | 19.9 | | 14.4 | 65 | |
| 15.07 | | 44.4 | 91.7 | 18.4 | 17.8 | | 14.7 | 60 | |
| 9.00 | | 15.8 | 16.0 | 16.0 | 15.6 | 15.4 | 14.7 | 45 | No cooling effect |

Since the pressure increased to 76 kPa again, it was concluded that the solar system must be evacuated from time to time as needed .

In another preliminary experiment, the system was heated to 79 °C and then evacuated to 41 kPa, and recharge with 2.5 L of methanol. The system was re-evacuated again, when the temperature reached 96 °C.

The system recharged with another 1.25 L of methanol, and the results of this experiment is given in table (4.10).

Table (4.10): Successive heating, evacuation, and heating for several days

| Date | Time | Process | T1 (°C) | T2 (°C) | T3 (°C) | T4 (°C) | T _{room} (°C) | T _{w(ev)} (°C) | P kPa | conclusions |
|---------------|-------|--|------------|------------|------------|------------|---------------------------|----------------------------|-------------------|--|
| Sun.3.2.2008 | 13.15 | Heating | 96.2 | 48.2 | 37.5 | 25.8 | 17.0 | 14.5 | 46 | |
| | 14.00 | | 114.0 | 56.7 | 28.8 | 25.7 | | | 68 | |
| | 15.00 | | 112.0 | | | | | | 75 | |
| Mon.4.2.008 | 9.00 | | 17.0 | 16.8 | 13.2 | 15.5 | 17.0 | 20 | No cooling effect | |
| Sun.10.2.2008 | 8.09 | After 7 days | 16.4 | 17.0 | 17.0 | 16.3 | 16.5 | 15.4 | 65 | |
| | 8.37 | Heating | 33.7 | 18.1 | 18.0 | 16.7 | 16.5 | | 101 | |
| | 8.44 | Evacuation | | | | | | | 36 | |
| | 9.13 | | 72.0 | | | | | | 45 | Desorption occur at this temp. |
| | 9.15 | | | | | | | | 36 | Pressure suddenly fall |
| | 9.38 | | | | | | | | 36 | |
| | 9.50 | Charge the system with 1250mL methanol | 104.0 | 36.0 | 28.0 | 23.0 | 19.0 | | 45 | |
| | 10.00 | Evacuation | 116.6 | 39.6 | 24.3 | 23.8 | 20.6 | 15.6 | 45 | |
| | 10.15 | Stop heating | 120.0 | | | | | | 65 | |
| | 10.20 | | 117.6 | 32.7 | 23.0 | 21.7 | | | 55 | |
| | 11.15 | | 67.6 | 32.3 | 21.2 | 19.7 | 17.2 | 15.7 | 36 | Temperature falls quickly |
| | 12.00 | | 19.0 | 19.2 | 17.0 | 17.0 | | 15.8 | 16 | No cooling, perhaps for quick cooling of the generator |
| | 13.15 | Heating & continuous vacuu | 52.0 | 36.7 | 22.7 | 22.5 | 20.8 | | 36 | |
| | 13.55 | Stop vacuum | 67.9 | 40.5 | 35.0 | 24.0 | | | 36-40 | |
| | 14.18 | | 106.0 | 53.4 | 44.7 | 27.0 | | | 70-75 | |
| | 14.44 | | 108.7 | 45.8 | 30.7 | 25.6 | | | 70 | |
| Mon.11.2.2008 | 9.30 | | 17.2 | 17.0 | 15.0 | 14.5 | 17.5 | 14.0 | 18 | Cooling effect recorded but not much |

As shown in table (4.10), the temperatures in the cooler box and in the evaporator, after a day, were about 2 to 3 below room temperature, this means that there was a cooling effect consequently an adsorption process occurred at the previous night and day . The pressure in the system stayed at 18kPa . The system was charged with 0.5 L of methanol .

On the next day the system was charged with another 0.5L of methanol to improve the cooling effect obtained in the previous experiment. The heating process was carried out side by side with a continuous evacuation process .

The pressure stayed at 28 kPa, while the evaporator was empty of any methanol which gives an indication that all methanol was adsorbed by the activated carbon. The results are indicated in table (4.11).

On the next day, the evaporator was checked to ensure that activated carbon adsorbed all the methanol. Small quantity of methanol was found inside the evaporator, and this means that activated carbon reached the saturation capacity. The pressure decreased to 20 kPa to discharge any methanol. The residual discharged methanol was 0.35 L, and the remaining quantity (the suitable charging quantity) of methanol was fixed at (7.4 L), consequently the maximum adsorbing capacity equals to : $(7.4 \times 0.787)/23 = 0.254$ kg methanol / kg AC.

The final results of this experiment are given in table (4.12).

Table (4.12): Results pilot scale setup charged with optimum volume of methanol(7.4L)

| Date | Time | Process | T1 (°C) | T2 (°C) | T3 (°C) | T4 (°C) | T _{room} (°C) | T _{w ev} (°C) | P kPa | conclusions |
|----------------|-------|---------------------------|------------|------------|------------|------------|---------------------------|---------------------------|----------|-------------------------------------|
| Sunday2/3/2008 | 8.30 | heating | 26.4 | 21.0 | 17.8 | 17.8 | 17.0 | 17.0 | 20 | |
| | 9.10 | Heating with vacuum | 49.5 | 27.7 | 22.7 | 17.5 | 17.0 | 17.0 | 18 | |
| | 9.18 | | 54.5 | 29.2 | 23.7 | 17.4 | 17.4 | | 17 | |
| | 9.20 | | 60.0 | | | | | | 20 | |
| | 10.10 | | 97.7 | 50.2 | 20.1 | 18.6 | | | 51 | |
| | 11.00 | Stop heating | 111.3 | 61.6 | 23.7 | 20.0 | | | 70 | Adsorption started |
| | 14.00 | | 36.7 | 20.9 | 12.6 | 13.5 | 17.6 | | 13 | |
| | 14.35 | | 36.4 | 21.9 | 13.0 | 11.3 | 18.0 | | 13 | Cooling effect started |
| | 14.55 | | 35.7 | 22.2 | 13.3 | 10.8 | 18.0 | | 13 | |
| | | | 33.7 | 16.5 | | 9.3 | 18.0 | 10.0 | 12 | |
| | 14.50 | | 31.0 | | | 8.4 | 19.0 | 9.5 | 15 | |
| | | | 28.0 | | | 7.9 | 19.0 | 8.8 | 15 | Good cooling effect |
| Monday3/3/2008 | 10.00 | | | | | 12.5 | 17.0 | 12.0 | 18 | Cooling effect still standing |

In the previous experiment, a good cooling effect was achieved and such cooling results may be used for air conditioning purposes and fruit, vegetables and vaccine conservations.

4.3.5 Experiments on the Optimized Pilot Scale Setup

To study the exact performance of the solar cooler and to see a continuous data, the thermocouples which measure the temperature at different points in the system, was connected to a computer with special data acquisition software for 24 hours.

Many experiments were performed to study the influence of temperature levels and different heat fluxes on the solar cooler performance in order to optimize the best conditions.

4.3.5.1 Effect of Generator Temperature

This experiment was done to see the influence of temperature level only without taking into account the heat flux quantity. The adsorbent temperature in the adsorbed bed, the condensing methanol temperature, the room temperature, and the methanol temperature in the evaporator variations with time are illustrated in Fig. (4.8).

The experiment was started at 9.00 a.m. local time and ended at 9.00 a.m on the next day after the refrigeration was completed. It can be seen from Fig.(4.8) that the variations in the adsorbent temperature in the adsorption bed followed the solar radiation pattern, consequently depends on the solar radiation level. The system was heated rapidly for 5 hours. During this heating process the pressure increased progressively due to methanol generation.

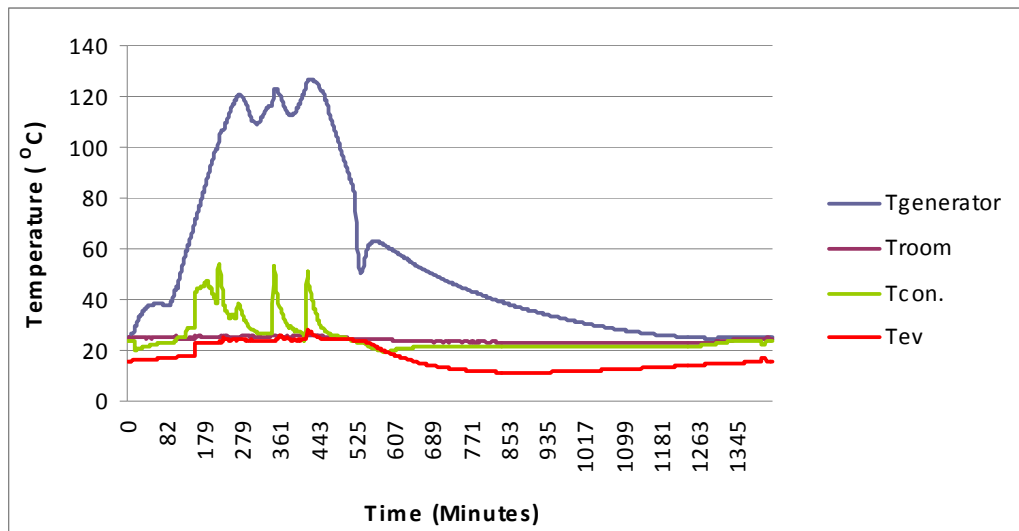


Figure (4.8): Continuous data from the pilot scale setup using variable heat flux

As the heating process ceased after 9 hours the temperature falls quickly by natural cooling, after a while the temperature re-increased slightly due to the heat of adsorption. After the progress of the adsorption process side by side with methanol evaporation in the evaporator, the temperature started to fall down reaching a minimum value after 16.30 hour from the start of heating process, producing a good cooling effect, and the lowest temperature obtained was 11.2 C°. The generation time lasts about 9 hours through the day while the cooling period lasts about 12 hours during night.

4.3.5.2 Effect of heating behavior

This experiment was done to see the cooling effect under the average daily solar radiation at Palestine. The heating /desorption process and the cooling/adsorption process parameters are indicated in Fig.(4.9). In this experiment the highest temperature of the adsorbent obtained was 118 °C after (5) hours of heat, while the minimum evaporator temperature was (12.8 °C), and after (12) hours from the starting of heating process. The

generation time lasts about (5) hours while the cooling period lasts about (12) hours.

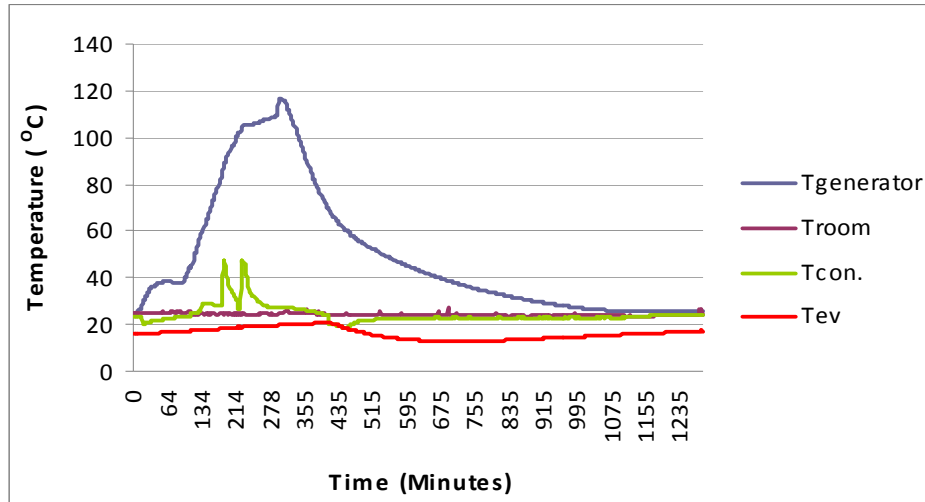


Figure (4-9): The temperature variations with time under the average daily solar radiation at Palestine ($5.4 \text{ kWh/m}^2/\text{day}$)

4.3.5.3 Effect of fixed flux heating

This experiment done with increasing the heat flux around $7.25 \text{ kWh/m}^2/\text{day}$. The heating /desorption process and the cooling/adsorption process parameters are indicated in Fig.(4.10).

In this experiment the highest temperature of the adsorbent obtained was (144°C) after (7.45) hours of heating, while the minimum evaporator temperature was (10.6°C), and after (15) hours from the starting of heating. The generation time lasts for (7.45) hours while the cooling period lasts for (12) hours.

This experiment shows that the higher the generating temperature will lead to lower the evaporator temperature, and this due to the increasing of desorbed methanol from activated carbon. Also the longer heating duration time has a positive effect on the cooling process.

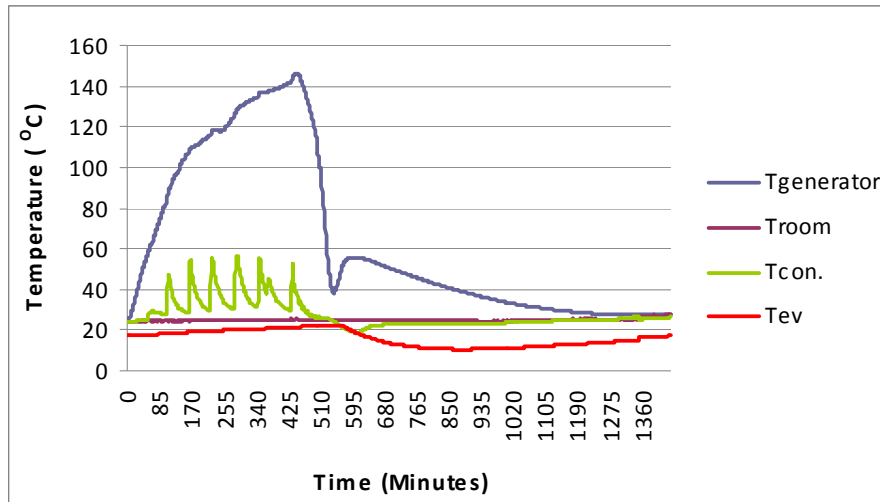


Figure (4.10): The temperature variations with time under constant heat flux of $7.25\text{kWh/m}^2/\text{day}$

4.3.5.4 Effect of heating time

This experiment was done partially under solar heating at low generating temperature. The heating /desorption process and the cooling/adsorption process parameters are indicated in Fig.(4.11). In this experiment it is obvious that the heating duration time is short, and the generation temperature is relatively low, therefore no cooling effect was observed.

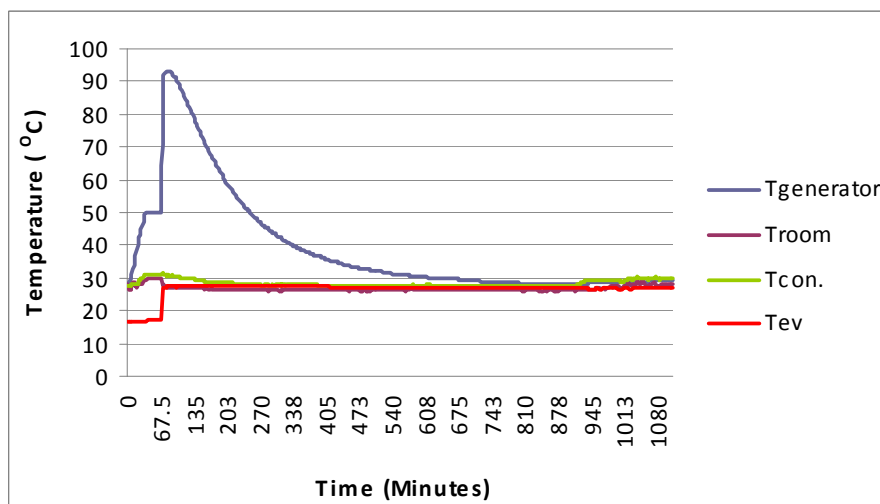


Figure (4.11): The temperature variations with time under partially solar heating, at low generation temperature

4.3.6 Experimental data summery

- The total incident global solar energy Q_{it} is determined from the product of incident solar flux over the whole day G_i and the collector exposed surface area :

$$Q_{it} = G_i A_{coll} (4.4)$$

$$\times 0.95m^2 = 6.88 \text{ kWh/day} = 7.25 \text{ kWh/ m}^2 \text{ day}$$

$$= 6.88 \times 3600 = 24795 \text{ kJ}$$

- The actual useful cooling produced was the heat extracted from water in the cooler box to lower its temperature.

$$Q_c = C_{p_w} m_w \Delta T_w (4.5)$$

$$= 4.187 \times 5 \times 14 = 293 \text{ kJ}$$

-The actual or useful overall coefficient of performance, COP_{act}

$$COP_{act} = Q_c / Q_{it} (4.6)$$

$$= 293 / 24795 = 0.01182$$

Chapter Five

Conclusions and Recommendations

The performance of the adsorption system depends highly on the adsorption pairs, processes involved, and on the well manufacturing of the all parts of the system. Generally speaking, enhancing the heat transfer between metallic plate and adsorbent, increasing the thermal conductivity of adsorbent are two obvious methods for improving performance of solar cooler. Simultaneously, choosing a suitable environmental condition may improve the performance of solar cooler. So long as we choose the optimization parameters on design of solar system, the practical use of solar cooler will become more reasonable.

From this study, one can conclude that the possibility of using non-polluting materials and to save the energy involved in this sector are obviously the most important characteristics but simplicity, low maintenance, and the absence of noisy components are also very important features that make this type of system suitable for numerous other applications such as air-conditioning in cars or food transportations or solar cooling. However, the main disadvantage is the long adsorption/desorption time.

5.1 Conclusions

The following conclusions may be drawn from the foregoing solar powered solid adsorption cooler studies:-

- 1- A solar powered solid adsorption cooler using an activated carbon/methanol adsorbent pair has been successfully designed, constructed and tested.

2-The condenser and evaporator must necessarily be close to each other and to the collector since the system operates at low pressure, thus they are located directly under the collector such that the refrigerant flows into them by gravity.

3- The adsorption bed (generator) is the heart of the system and it has the greatest effect on the performance of the system. A good design of the generator leads to smooth operation and better results, so more attention must be go to the design influence on the performance of the system .

4- The type of the generator such as packed bed or hollow tubes should be selected according to the manufacturing opportunity.

5- Chilled water was only produced at temperature around 10°C. Fruit, vegetables and vaccines with preservations temperatures over 13°C can be preserved .

6-The cooling load of the system is direct proportional to the adsorbed quantity and to the latent heat of methanol, the higher volume of methanol adsorbed, the high cooling capacity of the system.

7- The adsorption /desorption tests for activated carbon/methanol pair showed that there must be sufficient time to get the highest desorption of methanol, and the optimum time for that was found to be 5-10 hours.

8- The generation temperature must be over 100°C in order to generate higher volume of methanol from activated carbon.

9- It was found experimentally that the activated carbon which was used in our study has low methanol adsorption capacity and it was about 0.25 kg to 0.29 kg methanol/kg activated carbon, while some researchers [27] indicate that activated carbon with adsorption capacity of 0.45kg methanol/kg activated carbon is available commercially.

5.2 Recommendations:

- It is recommended to construct a system with hollow tubes generator, since it was found that in this type of generator it is easier to control the leakage and the pressure inside the system.
- A multi generator bed are recommended with the same activated carbon quantity in order to get higher solar radiation absorption area.
- A high performance vacuum pump can be used with special liquid Nitrogen cold trap, with such instruments it is easier to decrease the pressure to the lowest value without losing any methanol vapor.
- A monitoring devices, such as sight glasses, and scaled receivers may be essential to build in the suitable places in order to indicate the more correct readings i.e. the volume of the desorption methanol.
- Different types of activated carbon such as activated carbon fiber, or consolidate activated carbon, which have higher adsorption capacity may be used to get better results.
- Adopting double glass covers, and using a high quality selective coating material are two ways to increase properties of solar cooler.

References

- [1] Wimolsiri Pridasawas, (2006) . **Solar-Driven Refrigeration Systems with Focus on the Ejector Cycle**, Doctoral Thesis, Royal Institute of Technology, KTH, Denmark.
- [2] Althous, A., Turnquist, C., and Branciano, A.(1988). **Modern Refrigeration and Airconditioning, 5th edition**, Goodheart-Willcox, INC., USA.
- [3] Wimolsiri Pridasawas, and Teclemariam Nemariam. (2003), **solar cooling**, Assignment for Ph.D. Course: Solar Heating, Technical University of Denmark (DTU).
- [4] Gengel, Y., and Boles, M., (2006), **Thermodynamics an Engineering Approach**, 5th edition,McGraww Hill, NY, USA.
- [5] <http://www.powerfromthesun.net/index.htm>, chapter six. April, (2007).
- [6] Rabl, A. (1985). **Active Solar Collectors and Their Applications**. USA, Oxford University Press Inc.
- [7] Twidell, J. and Weir, T. (1998). **Renewable Energy Resources**. Great Britain, E&FN Spon.
- [8] <http://www.eere.energy.gov/de/thermally-activated/tech-basics.html> Absorption chillers, Technology basics, Energy Efficiency and Renewable Energy Program, US Department of energy. June, (2007).
- [9] Granryd, E. (1998). **Introduction to Refrigerating Engineering**. **Stockholm**, Dept. of Energy Technology, KTH.

- [10] Foley, Gerald (1993). **Photovoltaics in Primary Health Care**, Working Papers on Solar Energy and Health for the World Solar Summit, WHO/EPI/LHIS/93.3, Paris.
- [11] Zigler F. (1999). **Recent developments and future prospects of sorption heat pump systems**. International Journal of Thermals;38:191–208.
- [12] Miller EB. (1929). **The Development of SilicaGel, Refrigerating Engineering**, The American Society of Refrigerating Engineers.
- [13] A.O. Dieng, R.Z. Wang, (2001) **Literature review on solar adsorption technologies for ice-making and air conditioning purposes and recent developments in solar technology**, Renewable and Sustainable Energy Reviews 5313–342
- [14] Stephan K, Krauss R. (1992).**Regulated CFCs and their alternatives**. In: Meunier F, editor. **Proceedings: Solid Refrigeration Symposium**. Paris: Ministere de la Recherche et de L’Espace,;32–43.
- [15] Suzuki M, (1980).**Adsorption for energy transport**. In: **Adsorption Engineering**. Japan;
- [16] M. Pons, J.J. Guilleminot, (1986).**Design of an experimental solar-powered, solid-adsorption ice maker**, Transactions of the ASME, Journal of Solar Energy Engineering 108 (November) 332–337.
- [17] F. Lemmini, J. Buret-Bahraoui, (1990)**Performance of an adsorptive solar refrigerator using two types of activated carbon**, Energy and Environment 2 774–779, World Renewable Energy Congress.

- [18] N.M. Khattab, (2004), **A novel solar-powered adsorption refrigeration module**, Applied Thermal Engineering 24, 2747–2760
- [19] R.E. Critoph, (1994). **An ammonia carbon solar refrigeration for vaccine cooling**, Renewable Energy 5 (Part I) 502–508
- [20] F. Meunier, (1994). **Sorption solar cooling**, Renewable Energy 5 (Part I) 422–429.
- [21] Leite, Antonio Pralon Ferreira, Michel Dagueneb. (2000) **Performance of a new solid adsorption ice maker with solar energy regeneration**. Energy Conversion & Management 41 1625-1647
- [22] Leite, APF. (1998). **Thermodynamic analysis and modeling of an adsorption-cycle system for refrigeration from low- grade energy sources**. Journal of the Brazilian Society of Mechanical Sciences;20(3):301-24.
- [23] Meunier F, Douss N. (1990). **Performance of adsorption heat pumps: active-carbon-methanol and zeolite-water pairs**. In: Trans. ASHRAE Meeting, Saint Louis, USA.. p. 491-8.
- [24] Dubinin MM, Astakhov VA. (1971) **Development of the concept of volume filling of micropores in the adsorption of gases and vapors by microporous adsorbents**. Washington, DC, USA: American Chemical Society,
- [25] E.E. Anyanwu, (2004). **Review of solid adsorption solar refrigeration II :An overview of the principles and theory**, Energy Conversion and Management 45 (2004) 1279–1295

[26] R. E. Critoph, **activated carbon adsorption cycles for refrigeration and heat pumping**. Engineering Department, University of Warwick, Coventry, CV4 7AL. U.K.

[27] L.W. Wang, R.Z. Wang, Z.S.Lu, C.J. Chen, K. Wang, Wang, J.Y. Wu. (2006). **The performance of two adsorption ice making test units using activated carbon and a carbon composite as adsorbent**, Carbon 44 2671-2680.

[28] Meunier F, Douss N. **Performance of adsorption heat pumps: activated carbon-methanol and Zeolite-water pairs**. In: Trans. ASHRAE Meeting, Saint Louis, USA. 1990.p.491-8.

[29] Grenier Ph, Pons M. (1984). **Experimental and theoretical results on the use of an activated carbon/methanol intermittent cycle for the application to a solar powered ice maker**. In: Szokolay SV, editor. **Solar World Congress**, vol. 1. Pergamon Press; p. 500–6.

[30] A. Boubakri, (2006). **Performance of an adsorptive solar ice maker operating with a single double function heat exchanger (evaporator/condenser)**, Renewable Energy 31 1799–1812.

[31] M. Li, R.Z. Wang. (2002) **A study of the effects of collector and environment parameters on the performance of a solar powered solid adsorption refrigerator**, Renewable Energy, 27 369–382.

[32] Gacciola G, Restuccia G. (1994) **Progress on adsorption heat pump**, Heat Recovery System & CHP; 14(4):409–20.

- [33] Pons M.(1987) **Experimental data on a solar-powered ice maker using activated carbon and methanol adsorption pair.** Trans ASME, J Sol Energy Eng 1987;109(4):303–10.
- [34] Nadim Samen,(2006) **Active Solar Cooling: Processes & Performance Workshop**, Session 1.2 Istanbul, 15+16
- [35] Wang RZ. (2001).**Adsorption refrigeration research in Shanghai JiaoTong University.** *Renewable Sustainable Energy Rev*; 5(1):1–37.
- [36] Wang RZ. (2001).**Performance improvement of adsorption cooling by heat and mass recovery operation.** *Int J Refrigeration* 2001;24:602–11.
- [37] K. Sumathy, K.H. Yeung, Li Yong. (2003). **Technology development in the solar adsorption refrigeration systems**, *Progress in Energy and Combustion Science* 29 301–327.
- [38] Shelton SV, Wepfer WJ. (1990).**Solid–vapor heat pump technology.** In: *Proceedings of the IEA Heat Pump Conference*, Japan: Tokyo;. p. 525–35.
- [39] Sun, L. M., Feng, Y. and Pons, M. (1997). "**Numerical Investigation of Adsorptive Heat Pump Systems with Thermal Wave Heat Regeneration under Uniform-Pressure Conditions.**" *International Journal of Heat and Mass Transfer* 40(2): 281-293.
- [40] Ben Amar, N., Sun, L. M. and Meunier, F. (1996). "**Numerical Analysis of Adsorptive Temperature Wave Regenerative Heat Pump.**" *Applied Thermal Engineering* 16(5): 405-418.

[41] Wang RZ, Li M, Xu YX, Wu JY. (2000). **An energy efficient hybrid system of solar powered water heater and adsorption ice maker.** Solar Energy 68(2):189–195.

[42] Yeung K.H. and Sumathy K. (2003). **Thermodynamic analysis and optimization of a combined adsorption heating and cooling system** INTERNATIONAL JOURNAL OF ENERGY RESEARCH Int. J. Energy Res.; 27:1299–1315 (DOI: 10.1002/er.944)

[43] Dai YJ, Sumathy K, Wang RZ, Li YG. (2003). **Enhancement of natural ventelation in a solar house with a solar chimney and a solid adsorption cooling cavity.** Solar Energy.

[44] Zhang, X. J. and Wang, R. Z. (2002). **"A New Combined Adsorption– Ejector Refrigeration and Heating Hybrid System Powered by Solar Energy."** Applied Thermal Engineering 22: 1245-1258.

[45] <http://www.powerfromthesun.net/index.htm>, chapters(1), June (2007).

[46] Energy Research Centre At An- Najah National University, Solar measurements, Nablus, Palestine.

[47] <http://www.powerfromthesun.net/index.htm>, chapters(2), June (2007).

[48] Dr. Afif Hasan, Dr. Marwan Mahmoud, and Dr. Rateb Shabaneh, **Renewable Energy Assessment for Palestine**, Palestinian Energy and Environment Research Center (PEC) Jerusalem, July 1996.

[49] <http://www.powerfromthesun.net/index.htm>, chapters(5), June (2007).

[50] M. Li, C.J. Sun, R.Z. Wang, W.D. Cai, (2004). **Development of no valve solar ice maker**, Applied Thermal Engineering 24 865– 872

[51] Li M., R.Z. Wang, Y.X. Xu, J.Y. Wu, A.O. Dieng, (2005). **Experimental study on dynamic performance analysis of a flat-plate solar solid-adsorption refrigeration for ice maker**, Applied Thermal Engineering 25 1614–1622.

Appendix

Zone B Hilly Regions

(Palestine Energy and Environment Research Center)

The following tables show the climatologically averages of temperature (c°), relative humidity (%) ,heating degree days (°c day) , and global radiation (W.hr/m2.day) for the middle heights region , taken at the Jerusalem airport station .

Palestine (Hilly Regions) monthly Temperature (°c)

| Month | 1 | 2 | 3 | 4 | 5 | 6 | 7 | 8 | 9 | 10 | 11 | 12 |
|----------------------|------|------|------|------|------|------|------|------|------|------|------|------|
| Average daily max. | 11.8 | 13.5 | 16.2 | 20.9 | 25.4 | 27.9 | 28.9 | 28.9 | 27.9 | 25.2 | 18.9 | 13.4 |
| Daily average . | 8 | 9.2 | 11.5 | 15.2 | 19 | 21.6 | 23 | 23 | 22.1 | 19.6 | 14.2 | 9.6 |
| Average daily min. | 4.3 | 4.9 | 6.8 | 6.9 | 12.6 | 15.4 | 17.2 | 17.2 | 16.3 | 13.9 | 9.5 | 5.8 |
| Average daily range. | 7.5 | 8.6 | 9.4 | 11.3 | 12.8 | 12.5 | 11.7 | 11.7 | 11.6 | 11.3 | 9.4 | 7.6 |
| Average monthly max. | 17.1 | 20.9 | 25.5 | 30.4 | 34.2 | 34.6 | 34.1 | 33.4 | 33.8 | 31.4 | 24.9 | 19.8 |
| Absolute max. | 21.8 | 26 | 29 | 33.8 | 39.3 | 38.2 | 37.7 | 38.9 | 37.1 | 33.4 | 28.2 | 26.7 |
| Average monthly min. | 0.3 | 0.6 | 1.4 | 3.8 | 6.3 | 11.3 | 14.6 | 14.4 | 12.7 | 9.2 | 4.7 | 1.7 |
| Absolute min . | -1.5 | -2.9 | -2 | 1.9 | 4.1 | 9.2 | 13 | 13 | 10.1 | 6.9 | 1.7 | -1.6 |

Palestine (Hilly Regions) monthly Relative Humidity (%)

| Month | 1 | 2 | 3 | 4 | 5 | 6 | 7 | 8 | 9 | 10 | 11 | 12 |
|--------------------|----|----|----|----|----|----|----|----|----|----|----|----|
| Daily average . | 76 | 73 | 70 | 59 | 51 | 52 | 59 | 83 | 66 | 59 | 62 | 74 |
| Average at hour | 81 | 7 | 72 | 57 | 44 | 45 | 55 | 62 | 65 | 58 | 65 | 79 |
| Average at hour | 63 | 60 | 55 | 44 | 36 | 37 | 42 | 43 | 42 | 40 | 46 | 60 |
| Average at hour | 80 | 78 | 77 | 68 | 62 | 64 | 71 | 77 | 78 | 70 | 70 | 79 |
| Average daily max. | | | | | | | | | | | | |
| Average daily min. | | | | | | | | | | | | |

Palestine (Hilly Regions) monthly Heating Degree-Days (°c day)

| Annual Month | 1 | 2 | 3 | 4 | 5 | 6 | 7 | 8 | 9 | 10 | 11 | 12 |
|--------------|-----|-----|-----|-----|----|---|---|---|---|----|-----|-----|
| 1354 | 322 | 260 | 215 | 114 | 32 | 2 | | | | 19 | 122 | 268 |

جامعة النجاح الوطنية
كلية الدراسات العليا

التبريد بواسطة الطاقة الشمسية باستخدام تقنية الادمصاص

إعداد

وائق خليل سعيد حسين

إشراف

د. عبد الرحيم أبو صفا

د. عماد بريك

قدمت هذه الأطروحة استكمالاً لمتطلبات نيل درجة الماجستير في هندسة الطاقة النظيفة
وإستراتيجية الترشيد بكلية الدراسات العليا في جامعة النجاح الوطنية في نابلس، فلسطين.

2008

ب

التبريد بواسطة الطاقة الشمسية باستخدام تقنية الامصاص

إعداد

وائق خليل سعيد حسين

إشراف

د. عبد الرحيم أبو صفا

د. عماد بريك

الملخص

إن لارتفاع المتزايد لأسعار الوقود والخوف من نفاذه وتلوث البيئة الناتج عن استخدام هذا الوقود، وما آلت إليه أسعار الغذاء نتيجة الاستخدام المفرط للمواد الزراعية في استخراج الوقود الحيوي، ألزم الباحثين لإيجاد مصادر جديدة طبيعية ونظيفة للطاقة.

إن التبريد والتكييف ضرورة من ضرورات الحياة العصرية، وتعتبر مستهلكا رئيسا للطاقة، وعليه فقد تم التركيز في هذا البحث على استغلال الطاقة الشمسية المباشرة في عملية التبريد والتكييف.

يعتمد نظام التبريد الشمسي قيد البحث على تقنية ادمصاص الميثانول على الكربون المنشط لتحويل الطاقة الشمسية إلى تبريد حيث تتميز هذه التقنية ببساطة التصنيع ومن مواد متوفرة محليا، ويعمل بدون ضجيج أو أجزاء متحركة، ويتميز بعدم وجود أي نوع من الملوثات للبيئة، ولا يتطلب أي مصدر للطاقة غير الشمس.

تم التطرق في هذا البحث إلى شرح مفصل لعمليات التبريد المختلفة التي تستخدم الطاقة الشمسية ومقارنتها معا، إضافة إلى دراسة خصائص المواد الماصة ودرجة موائمتها مع المواد الممتصة. لقد تم اختيار عملية التبريد التي تستخدم تقنية ادمصاص الميثانول على الكربون المنشط، ومن أجل ذلك تم بناء وتصميم نظام تبريد يستخدم هذه التقنية ويعمل بالطاقة الشمسية.

يتكون نظام التبريد الشمسي والذي يعمل بتقنية الامصاص من الأجزاء التالية:

1- المولد أو الممتص أو المجمع الشمسي والذي يقوم بامتصاص الطاقة الشمسية وإيصالها إلى الكربون المنشط الحبيبي (المادة الماصة) حيث توضع بداخله.

2- المكثف والذي يعمل على تبريد المادة الممتصة وتحويلها من غاز إلى سائل.

3- المبخر والذي يستقبل السائل ومن ثم يكون الفعل التبريدي.

4- صندوق الماء البارد، والذي يصنع من مادة ستانلس ستيل ، حيث يوضع المبخر بداخله.

5- الصندوق المعزول حراريا، يوضع بداخله صندوق الماء البارد والمبخر.

إن أهم جزء في هذا النظام هو المجمع الشمسي (المولد) حيث يعتبر قلب هذا النظام ، وتقاس فاعلية النظام ومردوده بحسن تصنيع هذا القلب. وقد تم اختيار النوع المستوي بمساحة $0.95m^2$ تقريبا. لقد تم اختبار نوعين من المكثفات، يتكون الأول من أنبوب حلزوني مغمور في وعاء ماء، بينما الآخر يتكون من أنبوب ذي ريش ينحدر بشكل انسيابي لتسهيل جريان الميثانول.

لقد قمنا بإجراء عدة تجارب واختبارات لتقييم أداء هذا النظام وهي كما يلي :-

1 - تم اختبار قدرة الكربون المنشط الحبيبي على امتصاص الميثانول وعلى موائمة كمية الميثانول مع كمية الكربون المنشط الحبيبي.

2- تأثير درجة حرارة المولد أو درجة حرارة الكربون المنشط وتأثير شدة الإشعاع الشمسي على أداء النظام الشمسي. وجد إن درجة حرارة الكربون المنشط في المولد يجب أن تزيد عن 100 درجة مئوية لكي تحصل عملية المج، وكلما زادت درجة الحرارة زادت عملية تبخر الميثانول وبالتالي يزداد الفعل التبريدي.

3- تحديد الضغط العامل حيث وجد أن الضغط العامل عنصر مهم جدا من أجل تحقيق عملية التبريد حيث وجد أن هذا النظام لا يعمل إلا بضغط تخطي كبير يصل إلى اقل من 20 kPa

4- تم اختيار نوع المكثف حيث وجد أن المكثف يجب أن يكون انسيابي وقليل المقاومة لجريان الميثانول وقريب ما أمكن بين المولد والمبخر وبالتالي تم تصنيع مكثف يتكون من انبوسون ذي ريش ينساب ما بين المولد والمبخر وذلك لتجنب حصول هبوط ضغط عالي.

5- في معظم الاختبارات استطعنا الحصول على ماء في المبخر بدرجة حرارة حوالي 10 درجات مئوية حيث أن درجة الحرارة هذه تتأثر بشكل مباشر بشدة الإشعاع الشمسي المطبق وبطول فترة الامتزاز والمج حيث وجد أن الفترة الزمنية الأفضل لعملية التسخين يجب أن لا تقل عن 5 ساعات بينما الفترة الزمنية اللازمة للحصول على التبريد تمتد إلى أكثر من 10 ساعات. إن درجة الحرارة التي حصلنا عليها تتناسب مع استخدام هذا النظام في عمليات التكييف وحفظ الأطعمة والأدوية واللقاحات وماء الشرب، وخاصة في المناطق النائية.

6- تم بناء نظام تبريد شمسي في المختبر يحاكي نظام التبريد المصنع وقد وجد إن حجم المبخر له تأثير مهم على أداء هذا النظام حيث وجد إن حجم المبخر يجب إن لا يزيد عن اكبر كمية من الميثانول يمكن شحنها في هذا النظام ووجد إن سعة الامصاص للكربون المنشط المستخدم تساوي 0.26 كغم ميثانول / كغم كربون منشط.

7- وجد أن المولد المستخدم في هذه الدراسة يتمتع بقدرة عالية على امتصاص الحرارة إلا انه يعاني من مشكلة عدم الحفاظ على الضغط العامل وبالتالي تم اقتراح تصميم آخر جاسئ يتكون من مجموعة من الأنابيب داخلي و خارجي حيث يتوضع كل أنبوبين بشكل تكون فيه متحدة المحاور ويكون الأنبوب الداخلي مثقب من اجل جريان الميثانول فيه و يتوضع الكربون المنشط بينهما.